



1996

## Nonsense Codon-Mediated Degradation of Immunoglobulin Heavy-Chain [Mu] Messenger RNA in B Cells

Tianhong Li  
*Loyola University Chicago*

Follow this and additional works at: [https://ecommons.luc.edu/luc\\_diss](https://ecommons.luc.edu/luc_diss)



Part of the [Microbiology Commons](#)

---

### Recommended Citation

Li, Tianhong, "Nonsense Codon-Mediated Degradation of Immunoglobulin Heavy-Chain [Mu] Messenger RNA in B Cells" (1996). *Dissertations*. 3405.  
[https://ecommons.luc.edu/luc\\_diss/3405](https://ecommons.luc.edu/luc_diss/3405)

This Dissertation is brought to you for free and open access by the Theses and Dissertations at Loyola eCommons. It has been accepted for inclusion in Dissertations by an authorized administrator of Loyola eCommons. For more information, please contact [ecommons@luc.edu](mailto:ecommons@luc.edu).



This work is licensed under a [Creative Commons Attribution-NonCommercial-No Derivative Works 3.0 License](#).  
Copyright © 1996 Tianhong Li

LOYOLA UNIVERSITY OF CHICAGO

NONSENSE CODON-MEDIATED DEGRADATION OF  
IMMUNOGLOBULIN HEAVY-CHAIN  $\mu$  MESSENGER RNA IN B CELLS

A DISSERTATION SUBMITTED TO  
THE FACULTY OF THE GRADUATE SCHOOL  
IN CANDIDACY FOR THE DEGREE OF  
DOCTOR OF PHILOSOPHY

DEPARTMENT OF MICROBIOLOGY AND IMMUNOLOGY

BY

TIANHONG LI

CHICAGO, ILLINOIS

JANUARY, 1996

LOYOLA UNIVERSITY MEDICAL CENTER LIBRARY

**Copyrights by Tianhong Li, 1996**

**All Rights Reserved.**

## ACKNOWLEDGEMENTS

I would like to express my appreciation to my advisor, Dr. Hans-Martin Jäck, for his guidance in the process of the experiments and the opportunity to finish my graduate education in his laboratory.

I would like to thank my committee members, Dr. Sally A. Amero (dissertation committee chairperson), Dr. Thomas M. Gallagher, Dr. Phong T. Le and Dr. Alan J. Wolfe for their advice, their time spent reviewing this dissertation and their valuable suggestions. Thanks are also extended to the other faculty members in the Graduate School and the Department, especially Dr. Katherine L. Knight and Dr. Charles F. Lange for their dedication and positive encouragement in finishing my graduate education.

Dr. Thomas M. Ellis and Ms. Pat Simmon are acknowledged for their generous help in the CD30 collaboration project; Dr. Amero and Dr. John McNulty for their help in attempting better approaches to my research; Qian Li for data processing; Dolph Ellefson, Laura Hartwell and Jeanette Paintsil for proof-reading this dissertation.

I would like thank all the people in the department and my fellow labmates for their help from time to time and their friendship. Especially, I would like to express my thanks to Ms. Gabrielle Beck-Engeser for her excellent assistance in my research.

I am also very thankful to my former advisor, Dr. Shutong Wang, for his

discovery of my potential, for his understanding and encouragement to pursue graduate education in the United States. I have been very fortunate to have personal and constructive attention from a great teacher who has had a profound influence in my life.

All my family members and friends are deeply appreciated for their understanding, support and confidence in me which enabled me to look forward, especially in the very difficult times. Too many names need to be mentioned: Mr. Surine Napaprucksachart and Mr. Charoen Charoensivakorn for their generous support to come to the United States; Howie Friedman, Zehan Chen and Martha Friedman for the early settlement in Chicago; Qian and Lianshen, the Lins, Xia and Wei, Yuyao and Junpeng, Mei and Jianyi for their long time friendship and generous help.

I owe special gratitude to my parents, Yichang Li and Biqian Ye, from whom I learned the meaning of love, care and generosity, and to whom I wish to dedicate this work. Your positive attitude to life is an invaluable treasure to me. I will always remember your advice: There are so many unpredictable things that could happen in your life. It does not matter what you will be, the most important thing is to be a nice person and to be yourself. And you do mean it, my sister (Chunhong) and I have gone into complete different careers. No matter whatever I have done and whoever I will be, I always want you to be proud of me.

# TABLE OF CONTENTS

ACKNOWLEDGMENTS	iii
LIST OF FIGURES	x
LIST OF TABLES	xii
LIST OF ABBREVIATIONS	xiii
ABSTRACT	1
Chapter	
I.	REVIEW OF THE RELATED LITERATURE
1.1	Nonsense Codon-Mediated RNA Degradation . . . . . 3
1.2	Mechanism of Nonsense Codon-Mediated mRNA Reduction in the Nucleus . . . . . 6
1.3	Ig Gene Expression During B Cell Development . . . . . 10
1.4	B Cells Have a Mechanism to Eliminate Ig mRNA Containing Nonsense Codons . . . . . 12
1.5	The Mechanism of Nonsense Codon-Mediated Reduction of $\mu$ mRNA in Plasma Cells . . . . . 14
II.	MATERIALS AND METHODS
2.1	Chemicals and Reagents . . . . . 16
2.1.1	General Chemicals and Reagents . . . . . 16
2.1.2	Radiochemicals . . . . . 17
2.1.3	Kits . . . . . 17
2.1.4	Antibodies . . . . . 18
2.1.4.1	Antibodies Used for Immunofluorescence Analysis . . . . . 18
2.1.4.2	Antibodies Used for Immunoprecipitations . . . . . 18
2.1.5	Molecular Weight Standards . . . . . 18
2.2	Oligonucleotides and Linkers . . . . . 19
2.2.1	Oligonucleotides . . . . . 19
2.2.1.1	Sequencing . . . . . 19
2.2.1.2	Site-Directed Mutagenesis . . . . . 19
2.2.1.3	Polymerase Chain Reaction (PCR) . . . . . 20
2.2.1.3.1	Sense Oligonucleotides . . . . . 20
2.2.1.3.2	Antisense Oligonucleotides . . . . . 20
2.2.2	Phosphorylated Linkers . . . . . 21
2.3	Enzymes . . . . . 21

Chapter		Page
2.4	Bacterial Stains . . . . .	22
2.4.1	Bacterial Stains . . . . .	22
2.4.2	Preparation of Competent Bacterial Cells . . . . .	22
2.4.2.1	Solutions and Reagents . . . . .	22
2.4.2.2	Procedure for the Preparation of Competent Bacterial Cells . .	24
2.5	Plasmids and DNA Probes . . . . .	25
2.5.1	Plasmids . . . . .	25
2.5.2	DNA Probes . . . . .	26
2.6	DNA Manipulations . . . . .	27
2.6.1	Plasmid DNA Preparation . . . . .	27
2.6.1.1	Solutions and Media . . . . .	27
2.6.1.2	Small Scale Preparation of Plasmid DNA (Miniprep) . . . . .	30
2.6.1.3	Large Scale Preparation of Plasmid DNA . . . . .	30
2.6.2	DNA Digestion . . . . .	32
2.6.3	DNA Agarose Gel Electrophoresis . . . . .	32
2.6.4	DNA Band Isolation from the Agarose Gel . . . . .	33
2.6.4.1	6 M Method of DNA Band Isolation . . . . .	33
2.6.5	Quantitation of DNA . . . . .	34
2.6.6	Dephosphorylation of DNA Fragment (CIP-treatment) . . . . .	34
2.6.7	DNA Ligation . . . . .	35
2.6.7.1	Solutions . . . . .	35
2.6.7.2	Sticky-End Ligation of DNA Fragment . . . . .	36
2.6.7.3	Blunt-End Ligation of DNA Fragment with Phosphorylated Linkers . . . . .	36
2.6.7.4	Two-Step Ligation of DNA Fragment . . . . .	36
2.6.8	DNA Transformation . . . . .	38
2.6.9	Screening of Recombinant DNA . . . . .	39
2.6.9.1	Blue/White Color Screening . . . . .	39
2.6.9.2	Colony Lift . . . . .	39
2.6.10	Labeling of DNA Probes . . . . .	40
2.6.10.1	Nick Translation . . . . .	40
2.6.10.2	Random Priming . . . . .	41
2.6.10.3	5' End Labeling . . . . .	41
2.7	Site-Directed Mutagenesis . . . . .	42
2.7.1	Solutions . . . . .	42
2.7.2	Preparation of Phagemid Single-Stranded DNA . . . . .	43
2.7.3	5' Phosphorylation of Oligonucleotides . . . . .	45
2.7.4	Site-Directed Mutagenesis . . . . .	46
2.8	Reverse Transcription Polymerase Chain Reaction . . . . .	46
2.8.1	Synthesis of cDNA Fragment by Reverse Transcriptase . . . . .	46
2.8.2	PCR Amplification . . . . .	48
2.9	DNA Sequencing . . . . .	49

2.10	Cell Culture Techniques and DNA-Mediated Cell Transfection . . . . .	50
2.10.1	Cell Maintenance . . . . .	50
2.10.2	Cell Lines That Were Used in the Dissertation . . . . .	50
2.10.3	Cell Harvesting . . . . .	51
2.10.4	Freezing and Thawing of Cells . . . . .	51
2.10.5	Cell Counting . . . . .	51
2.10.6	Subcloning . . . . .	52
2.10.7	Transfection . . . . .	52
2.11	DNA Isolation from Mammalian Cells and Analysis . . . . .	53
2.11.1	DNA Isolation by Guanidinium Thiocyanate/Cesium Chloride Method . . . . .	53
2.11.2	Quantitation of DNA . . . . .	53
2.11.3	Southern Blot Analysis . . . . .	54
2.12	RNA Isolation from Mammalian Cells and Analysis . . . . .	55
2.12.1	Total RNA Isolation . . . . .	55
2.12.1.1	Guanidinium Thiocyanate/Cesium Chloride Method . . . . .	55
2.12.1.2	Trizol or RNazol™ B Method . . . . .	56
2.12.2	Cytoplasmic RNA Isolation . . . . .	57
2.12.3	Nuclear RNA Isolation . . . . .	58
2.12.3.1	RNA Isolation for Crude Nuclei Fractions . . . . .	58
2.12.3.2	RNA Isolation for Purified Nuclei . . . . .	58
2.12.4	Quantitation of RNA . . . . .	62
2.12.5	Northern Blot Analysis . . . . .	64
2.12.6	mRNA Decay Rates Measured by the Actinomycin C1 or DRB Treatment . . . . .	69
2.12.7	DRB Titration Experiment . . . . .	70
2.13	Analysis of Proteins . . . . .	71
2.13.1	Immunofluorescence Analysis . . . . .	71
2.13.2	Metabolic Labeling and Immunoprecipitation . . . . .	71
2.13.3	Protein SDS Polyacrylamide Gel Electrophoresis . . . . .	74

### III. IMMUNOGLOBULIN mRNA WITH A NONSENSE CODON IS DECREASED IN BOTH THE NUCLEUS AND THE CYTOPLASM OF PLASMA CELLS

3.1	Characterization of the Cell Lines That Are Used in This Chapter . . . . .	77
3.2	Nonsense Codons Decrease the Level of $\mu$ RNA but Not Precursor $\mu$ RNA in Hybridomas . . . . .	86
3.3	Nonsense Codons Reduce the Steady-State Level of $\mu$ RNA in the Nucleus . . . . .	95



3.4	Cytoplasmic Decay Rates of $\mu$ mRNA With or Without a Nonsense Codon . . . . .	119
3.5	Nonsense Codons Affect the Size of $\mu$ mRNA . . . . .	134
3.6	Discussion . . . . .	141
3.6.1	Ig mRNA with a Nonsense Codon Starts to Decrease in the Nucleus of Plasma Cells . . . . .	141
3.6.2	$\mu$ mRNA With a Nonsense Codon is Degraded Faster Than $\mu$ mRNA Without a Nonsense Codon in the Cytoplasm of Plasma Cells . . . . .	144
3.6.3	DRB Does Not Influence the RNA Metabolism of H2b Gene . . . . .	146

#### IV. TEST OF A MODEL TO EXPLAIN THE MECHANISM BY WHICH IG $\mu$ mRNA WITH A NONSENSE CODON IS DECREASED IN THE NUCLEUS OF PLASMA CELLS

4.1	Introduction . . . . .	150
4.2	Results . . . . .	155
4.2.1	Construction of Plasmids . . . . .	155
4.2.1.1	Deletion of the Membrane Exons in the $p\mu^{\Delta}gpt\Delta M$ Plasmid . . . . .	155
4.2.1.2	cDNA Replacement and Deletion of Downstream Sequences of the Nonsense Linker in the $p\mu^{\Delta}gpt\Delta M$ Plasmid . . . . .	157
4.2.1.3	Introduction of a Nonsense Linker into Four Exons of Constant Region in the $p\mu^{\Delta}gpt\Delta M$ Plasmid . . . . .	158
4.2.1.4	Generation of a Pcmv- $\mu$ cDNA With or Without a Nonsense Linker . . . . .	158
4.2.1.5	Generation of Stable Transfectants Containing Modified $\mu$ Genes . . . . .	159
4.2.2	Positional Effect of a Nonsense Codon on the Steady-State Level of $\mu$ mRNA . . . . .	164
4.2.3	cDNA Replacement of Sequences Downstream of a Nonsense Linker Does Not Restore Its Steady-State Level of Ig $\mu$ mRNA to Its Wild-Type . . . . .	172
4.2.4	Removal of Intron Sequences from Ig $\mu$ Gene Does Not Protect Its mRNA from the Nonsense Codon-Mediated RNA Degradation . . . . .	180
4.3	Discussion . . . . .	183
4.3.1	A Nonsense Codon Does Not Affect the Steady-State Level of Ig mRNA by Preventing the Splicing of Its Downstream Sequences . . . . .	183
4.3.2	Introns Are Required for Effective Expression of $\mu$ Gene . . . . .	184
4.4	Proposed Further Experiments . . . . .	187
4.4.1	For the Result of Positional Effect of a Nonsense Codon . . . . .	187

Chapter		Page
4.4.2	For the Result of cDNA Replacement on $\mu$ mRNA Expression . . . . .	188
4.4.3	For the Effect of a Nonsense Codon in $\mu$ mRNA Derived from Pcmv- $\mu$ cDNA . . . . .	188
SUMMARY	. . . . .	190
REFERENCES	. . . . .	191
VITA	. . . . .	200

## LIST OF FIGURES

Figure	Page
1. Schematic Representations of DNA Structures, Hybridization Probes and $\mu$ Transcripts . . . . .	80
2A. PCR Analysis to Screen for the Presence of $C\mu$ Gene Segments in Hybridoma Subclones . . . . .	82
2B. Southern Blot Analysis to Identify the Deletion in the $J_H-C\mu$ Intron of $\mu$ Gene on the V2 Allele . . . . .	84
3A. Northern Blot Analysis of Total Cellular RNA Isolated from Various Subclones . . . . .	89
3B. Northern Blot Analysis of Total Cellular RNA Isolated from Various Subclones . . . . .	92
4. Comparison of Methods to Isolate Nuclear RNA from Hybridomas <i>FH</i> and <i>CH2XH</i> . . . . .	96
5A. A Flow Chart of Nuclear RNA Isolation Procedure . . . . .	102
5B. Quantitation of the Extent of Cytoplasmic mRNA Contamination in Purified Nuclei by Northern Blot Analysis . . . . .	103
6. Representative Photographs of Nuclei in the Nuclei Isolation Procedure . . . . .	106
7. A Flow Chart of RNA Isolation Procedures . . . . .	110
8. Northern Blot Analysis to Quantify the Steady-State Levels of RNAs in Subcellular Compartments of Hybridomas . . . . .	111
9A. Northern Blot Analysis of Cytoplasmic Decay Rates of $\mu$ mRNA in Hybridomas Using the Actinomycin C1 Method . . . . .	122
9B. Northern Blot Analysis of Cytoplasmic Decay Rates of $\mu$ mRNA in Hybridomas Using the DRB Method . . . . .	125

Figure	Page
10. Northern Blot Analysis to Determine the Effect of DRB Concentration on the Level of H2b mRNA . . . . .	132
11. Northern Blot Analysis to Test the Effect of RNA Loading on Mobility .	137
12. RT-PCR Assay to Compare the Length of Coding Region of $\mu$ mRNAs With or Without a Nonsense Codon . . . . .	139
13. A Schematic Representation of $\mu$ RNA Metabolism in Plasma Cells . . .	148
14. A Modified Translational Translocation Model . . . . .	153
15. A Schematic Representation of the $p\mu^{\Delta}gpt\Delta M$ Plasmid . . . . .	156
16. Restriction Analysis of DNA Constructs Containing Wild-Type and Modified $\mu$ Genes . . . . .	160
17. Restriction Analysis of DNA Constructs Containing Wild-Type and Modified $\mu$ Genes Containing a Nonsense Codon at Different Positions of the Constant Region of $\mu$ Gene . . . . .	162
18. Analysis of $\mu$ mRNA Expression in <i>J558L</i> Transfectants Containing a Nonsense Codon at Different Positions of the Constant Region of $\mu$ Gene (A and B) . . . . .	166
19. Analysis of Intracellular and Secreted $\mu$ Heavy Chain Expression in <i>J558L</i> Transfectants Containing a Nonsense Codon at Different Positions of the Constant Region of $\mu$ Gene . . . . .	170
20. Analysis of $\mu$ mRNA Expression in <i>J558L</i> Transfectants (A and B) . . .	174
21. Analysis of Intracellular $\mu$ Heavy Chain Expression in <i>J558L</i> Transfectants . . . . .	178
22. Expression of $\mu$ mRNA Transcribed from Pcmv- $\mu$ cDNA With or Without a Nonsense Codon in <i>J558L</i> Transfectants . . . . .	181

## LIST OF TABLES

Table	Page
1. Average Yield of RNA . . . . .	63
2A. Quantitation of Northern Blot Analysis in Figure 3A . . . . .	91
2B. Quantitation of Northern Blot Analysis in Figure 3B . . . . .	94
3. Quantitation of the Amount of Cytoplasmic RNA Contamination to the Purified Nuclei . . . . .	105
4. Steady-State Levels of RNA Transcripts . . . . .	114
5A. Cytoplasmic Decay Rates of RNAs (the Actinomycin C1 Method) . . . . .	124
5B. Cytoplasmic Decay Rates of RNAs (the DRB Method) . . . . .	127

## LIST OF ABBREVIATIONS

A	adenine
Act C1	actinomycin C1
APS	ammonium persulphate
b	base
bp	basepair(s)
BPB	bromophenol blue
BSA	bovine serum albumin
C	cytosine
C	constant
°C	degrees Celcius
CD	cluster of differentiation
cDNA	complementary DNA
Chisam	Chloroform:isoamyl alcohol = 24 + 1
Ci	Curie
CIF	cytoplasmic immunofluorescence
C $\mu$	constant region of $\mu$ gene
CMV	cytomegalovirus
cpm	counts per minute
DEPC	diethyl pyrocarbonate

dFA	deionized formamide
DMSO	dimethyl sulfoxide
DNA	deoxyribonucleic acid
DNase	deoxyribonuclease
dNTP	2'-deoxy nucleotides
DOC	deoxycholic acid
DRB	5,6-dichloro-1- $\beta$ -D-ribofuranosylbenzimidazole
DTT	dithiothreitol
EDTA	ethylenediaminetetraacetic acid
EM	electron microscopy
EtBr	ethidium bromide
FACS	fluorescence activated cell sorter
FBS	fetal bovine serum
FCS	fetal calf serum
FDA	fluorescein diacetate
FITC	fluorescein isothiocyanate
G	guanine
g	gram
GAPDH	glyceraldehyde-3-phosphate dehydrogenase
GIT	guanidine isothiocyanate
gpt	guanosyl-phosphoribosyl transferase
H	heavy chain of immunoglobulin

HCl	hydrochloric acid
hnRNA	heteronuclear RNA
hr	hour(s)
HEPES	N-[2-Hydroxyethylpiperazine-N']-[2-ethanesulfonic acid]
Ig	immunoglobulin
IL	interleukin
IPTG	isopropyl $\beta$ -D-thiogalactoside (isopropyl $\beta$ -D-thiogalactopyranoside)
J	joining
kb	kilobase
L	light chain of immunoglobulin
l	liter
LB	Luria broth
$\beta$ -ME	2-mercaptoethanol
mAb	monoclonal antibody
min	minute(s)
MOPS	3-[N-Morpholino]propanesulfonic acid
MPA	mycophenolic acid
mM	millimolar
M	molar
ml	milliliter
$\mu$ l	microliter



<b>mol</b>	<b>moles</b>
<b>MW</b>	<b>molecular weight</b>
<b>NaCl</b>	<b>sodium chloride</b>
<b>NEO</b>	<b>neomycin phosphotransferase gene</b>
<b>nt</b>	<b>nucleotide</b>
<b>P</b>	<b>promoter</b>
<b>PAGE</b>	<b>polyacrylamide gel</b>
<b>PBS</b>	<b>phosphate buffered saline</b>
<b>PBSF</b>	<b>phosphate buffered saline with BSA</b>
<b>PCR</b>	<b>polymerase chain reaction</b>
<b>PEG</b>	<b>polyethylene glycol</b>
<b>PMSF</b>	<b>phenylmethanesulfonyl fluoride</b>
<b>Poly(A)</b>	<b>polyadenylation</b>
<b>Prot K</b>	<b>proteinase K</b>
<b>RE</b>	<b>restriction endonuclease(s)</b>
<b>RNA</b>	<b>ribonucleic acid</b>
<b>mRNA</b>	<b>messenger RNA</b>
<b>RNase</b>	<b>ribonuclease</b>
<b>rpm</b>	<b>revolutions per minute</b>
<b>RT</b>	<b>room temperature</b>
<b>RT</b>	<b>reverse transcriptase</b>
<b>SE</b>	<b>standard error</b>

SDS	sodium dodecyl sulfate
sec	second(s)
SSC	standard saline citrate (15 mM sodium citrate, 0.15 M sodium chloride)
T	thymine
TAE	40 mM Tris, 1% glacial acetic acid, 1 mM EDTA
TBE	Tris-borate-EDTA (89 mM Tris, pH 7.5, 89 mM boric acid, 2 mM EDTA)
TE	Tris-EDTA
TEMED	N,N,N',N'-tetramethylethylenediamine
TCA	trichloroacetic acid
Tris	Trizma base (tris[hydroxymethyl]aminomethane)
TRITC	thiomethyl rhodamine
U	unit
5' UTR	5' untranslated region
V	variable
v	volume
vol	volume(s)
x g	times gravity
X-Gal	5-bromo-4-chloro-3-indolyl $\beta$ -D-galactopyranoside (5-bromo-4-chloro-3-indolyl $\beta$ -D-galactoside)

## ABSTRACT

Immunoglobulins (Igs) are expressed exclusively in B lymphocytes to protect vertebrates from invading pathogens. This dissertation is designed to better understand the mechanism by which B cells and plasma cells produce functional Ig proteins. An Ig molecule consists of two identical heavy and two identical polypeptide light chains. The genes encoding heavy and light chains are assembled from gene segments (V, D, and J) through DNA rearrangements during B cell development. If these rearrangements do not preserve the translational reading frame, the resulting Ig gene very likely contains a premature translational stop (a nonsense codon) and is, therefore, a nonproductive gene. Since both Ig alleles can be rearranged, a B cell might end up with a productive (i.e., a gene without a nonsense codon) and a nonproductive Ig gene. The  $\mu$  gene encodes the heavy chain of IgM, which is the main Ig isotype produced in a primary immune response. Our laboratory has previously shown in hybridomas and pre-B cell lines that a  $\mu$  gene with a nonsense codon is transcribed at the same rate as a  $\mu$  gene without a nonsense codon. In contrast, the cytoplasmic steady-state level of  $\mu$  mRNA with a nonsense codon is 30-100 times lower than the steady level of  $\mu$  mRNA without a nonsense codon. Based on these data we proposed that  $\mu$  mRNA with a nonsense codon is degraded faster than  $\mu$  mRNA without a nonsense codon in B cells.

To elucidate the mechanism of this nonsense codon-mediated reduction of Ig mRNA, I first determined in which subcellular compartment this reduction in Ig mRNA

level occurs. By using Northern blot analysis, I found that the level of mature  $\mu$  mRNA containing a nonsense codon is reduced in the nucleus by approximately seven fold when compared to the level of  $\mu$  mRNA without a nonsense codon. In contrast,  $\mu$  precursor RNA increases in the nucleus of hybridomas that contain nonsense codons in their  $\mu$  genes by at least 2 fold, suggesting that a nonsense codon decreases the splicing efficiency of  $\mu$  precursor RNA. I also showed that the presence of a nonsense codon correlates with an accelerated turnover rate of  $\mu$  mRNA in the cytoplasm, suggesting that in the cytoplasm the reduction of  $\mu$  mRNA level with a nonsense codon is, at least partially, due to the increased degradation rate. From these data, I conclude that the reduction of cytoplasmic level of  $\mu$  mRNA with a nonsense codon results from both a nuclear as well as a cytoplasmic event. These events may contribute to the potent efficiency of humoral immune response by preventing the translation of nonproductive Ig mRNAs in B cells.

I have also attempted to test a possible mechanism, the translational translocation model, which explains how a nonsense codon triggers the reduction of mRNA in the nucleus. From the results of three different approaches, I suggest that the translational translocation model is not the mechanism by which  $\mu$  mRNA with a nonsense codon is reduced in the nucleus of plasma cells.

# CHAPTER I

## REVIEW OF RELATED LITERATURE

### 1.1 Nonsense Codon-Mediated RNA Degradation

A nonsense codon is a premature translational termination signal that is in-frame with the translational initiation codon in a messenger RNA (mRNA). Nonsense codon-mediated RNA degradation refers to the phenomenon by which nonsense codons can trigger the rapid degradation of a mRNA. It is a unique phenomenon because there are many out-of-frame stop codons in a mRNA that have no effect on RNA metabolism. Only those stop codons that are in-frame with the translation initiation codon in a mRNA can trigger RNA degradation (Daar and Maquat, 1988; Belgrader and Maquat, 1994; Pulak and Anderson, 1993). In other words, a single nucleotide change may result in RNA degradation. This is a fascinating system for cell biology because it prevents the production of truncated proteins. Although not all truncated proteins are disruptive to a cell, a cell is protected from those that are deleterious by eliminating all mRNAs containing nonsense codons. Nonsense codons have been reported to be responsible for many human diseases, such as the  $\beta$ -globin gene of  $\beta$ -thalassemia (Humphries *et al.*, 1984; Takeshita *et al.*, 1984) and the human fibrillin (FBN1) gene of Marfan syndrome (Diatz *et al.*, 1993). Nonsense codons in the unc-54 myosin heavy chain gene of *Caenorhabditis elegans* have been reported to disrupt the body-wall muscle ultrastructure.

The affected *C. elegans* have reduced brood size (Pulak and Anderson, 1993).

The steady-state level of mRNA actually represents a balance between the rate of nuclear RNA synthesis (transcription), the rate of nuclear RNA precursor processing, the extent of intranuclear mRNA degradation, the rate of mRNA transport from the nucleus to the cytoplasm, the rate of cytoplasmic mRNA degradation, and the efficiency of protein translation (Ehretsmann *et al.*, 1992; Belasco and Brawerman, 1993). Among them, the regulation of mRNA stability has been shown to be a major control mechanism in gene expression in the last decade (Atwater *et al.*, 1990; Sachs, 1993; Decker and Parker, 1994). The decay rates of mRNAs can differ from each other by more than 50 fold in eukaryotic cells (Ross, 1989; Atwater *et al.*, 1990; Sachs, 1993). The high degree of stability of some mRNAs, such as the globin mRNAs, contributes to their accumulation to high steady-state levels (Aviv *et al.*, 1976). Highly unstable mRNAs with half-lives of about 10-15 minutes, such as the lymphokine and protooncogene mRNAs, are normally present at low steady-state levels (Kelly *et al.*, 1983; Greenberg and Ziff, 1984). Although low mRNA steady-state level could be achieved through a low rate of transcription, the time course of changing the mRNA level in response to a stimulus is determined solely by the turnover rate of the mRNA, which permits rapid cessation of the production of a protein and its more rapid induction (Ross, 1989). This is of particular importance in the case of proteins that play critical regulatory roles for brief periods during a development process or physiological transitions. Notably, shifts in mRNA stability (i.e., massive reorganization of the pattern of gene expression) contribute to *Xenopus* oocyte and early embryo development and erythroid differentiation

(Richter, 1991; Krowczynska *et al.*, 1985); the synthesis of histones, which takes place only during the S phase of the cell cycle (Gallwitz, 1975).

A nonsense codon might potentially influence the steady-state level of a mRNA by influencing any or all of the regulatory processes described above. Indeed, nonsense codons have been reported to have various effects on mRNA metabolism. Among them, the importance of translation to mRNA stability is particularly important for mRNAs with nonsense codons (see reviews in Atwater *et al.*, 1990; Belasco and Brawerman, 1993). Consistent with the assumption that nonsense codons are recognized during translation in the cytoplasm of eukaryotic cells, the lower steady-state level of most mRNAs that contain nonsense codons is attributed to their increased turnover rates in the cytoplasm. Some examples are the yeast URA3 mRNA (Losson and Lacroute, 1979) and HIS4 mRNA (Herrick *et al.*, 1990), Rous sarcoma virus *gag* mRNA (Barker and Beemon, 1991), human and mouse  $\beta$ -globin mRNA (Maquat *et al.*, 1981; Takeshita *et al.*, 1984; Lim *et al.*, 1992), and mouse histone mRNA (Graves *et al.*, 1987). However, several recent studies suggest that nonsense codons may decrease the steady-state level of their mRNAs by influencing of nuclear processing, and/or transport without affecting their cytoplasmic stability. Several examples are human  $\beta$ -globin mRNA (Humphries *et al.*, 1984), mouse Ig heavy chain  $\mu$  mRNA (Connor *et al.*, 1994), hamster dihydrofolate reductase mRNA (Urlaub *et al.*, 1989), human  $\beta$ -globin mRNA under the control of the simian virus 40 promoter in Syrian hamster cells (Baserga and Benz, 1992), nonstructural protein NS2 mRNA of the minute virus of mice (MVM) (Naeger *et al.*, 1992), human triosephosphate isomerase (TPI) mRNA (Cheng and Maquat, 1993), the T cell receptor

$\beta$  mRNA (Qian *et al.*, 1993), *v-src* mRNA of avian sarcoma virus (Simpson and Stoltzfus, 1994), and mouse Ig  $\kappa$  light chain mRNA (Lozano *et al.*, 1994). In all of these cases the exact degradation mechanism has not been elucidated; however, for nonstructural protein NS2 of the minute virus of mice (MVM) (Naeger *et al.*, 1992) and mouse Ig  $\kappa$  light chain (Lozano *et al.*, 1994), it has been suggested that nonsense mutations influence the nuclear RNA processing events by inhibiting splicing. It is puzzling, however, how nonsense codons can affect nuclear mRNA processing, since nonsense codons are recognized in a fully spliced transcript (mRNA) in the cytoplasm during protein synthesis. Possible mechanisms are discussed in section 1.2 in detail.

Many *cis*-acting elements have been reported to be involved in nonsense codon-mediated mRNA degradation, such as the coding regions (Cleveland, 1988; Parker and Jacobson, 1990; Peltz *et al.*, 1993), introns (Cheng *et al.*, 1994), and 3'-untranslated regions (Jackson, 1993). Genes encoding factors that specifically degrade certain mRNAs with nonsense codons, while having no effect on functional mRNA, have been cloned and characterized as up frameshift (*UPF*) genes in yeast *Saccharomyces cerevisiae* (Leeds *et al.*, 1991; Leeds *et al.*, 1992) and *smg* genes in *C. elegans* (*smg* denotes suppressor with morphogenetic defects on genitalia) (Pulak and Anderson, 1993). The mammalian gene encoding for the nonsense codon-specific degradation factor has not yet been cloned.

## 1.2 Mechanism of Nonsense Codon-Mediated mRNA Reduction in the Nucleus

Although little is known about the mechanism of nonsense codon-mediated



reduction of mRNA, several models have been proposed to explain nonsense codon-mediated RNA reduction in the nucleus. Since the only identified and accepted system that can recognize a nonsense codon is the translational machinery in the cytoplasm of eukaryotic cells, it has been reasoned that mRNA with a nonsense codon should be recognized and degraded in the cytoplasm. Based on this assumption, Urlaub *et al.* (1989) proposed an elegant model to link the cytoplasmic translation event to the nuclear RNA processing and nucleus-to-cytoplasmic transport events. The essence of Urlaub's model suggests that the initiation of cytoplasmic  $\mu$  protein translation starts before the completion of RNA processing in the nucleus and the nucleus-to-cytoplasm transport. Once the 5' end of the RNA transcript has been processed with a cap structure and spliced, the partially processed RNA begins transport to the cytoplasm via the nuclear pore. The binding of ribosome subunits and initiation factors to the free 5' end of the RNA transcript on the cytoplasmic side of nuclear membrane initiates  $\mu$  protein translation. The translation in the cytoplasm serves as a force to facilitate not only the splicing of the 3' part of the RNA transcript but also the export of fully spliced nuclear mRNA from the nucleus to the cytoplasm. This model requires that recognition of a nonsense codon occurs after splicing in the cytoplasm, and has been best studied by Maquat and colleagues with human TPI mRNA.

Maquat *et al.* showed that nonsense codons located within the first three-fourths of the coding region of TPI mRNA reduce the level of TPI mRNA to 20 to 30 % of normal (Cheng *et al.*, 1990; Cheng and Maquat, 1993). This reduction is not attributable to a decrease in the half-life of cytoplasmic TPI mRNA (Cheng *et al.*, 1990). Maquat *et*

*al.* further determined that this reduction of TPI mRNA is dependent on the translatability of mRNA with nonsense codons. They showed that nonsense codon-mediated reduction of TPI mRNA is at least partially inactivated by a stem-loop in the 5'-UTR (that acts in *cis* to inhibit translation initiation by the 40S ribosomal subunit), or by a suppressor tRNA (that acts in *trans* to suppress the nonsense codon (Belgrader *et al.*, 1993). Maquat *et al.* have further shown that deletion of a 5' splice site of the TPI gene results predominantly in the removal (by skipping) of the upstream exon (that contains the nonsense codon) as a part of the flanking introns (Belgrader *et al.*, 1994). Based on these data, Maquat *et al.* concluded that translation is required in the nonsense codon-mediated reduction of TPI mRNA in the nucleus, and that the recognition of a nonsense codon occurs after splicing. Since they did not separate the cytoplasmic compartment from the nuclear compartment in their studies, they did not distinguish whether the recognition of nonsense codons occurs in the cytoplasm or in the nucleus. They also did not rule out the possibility that the stem-loop in the 5'-UTR or a suppressor tRNA abrogated the effect of nonsense codons on TPI mRNA level by competitive binding to the translational machinery. Thus, I do not think they have tested the translational translocation model.

A variation of the translational translocation model proposes that the recognition of nonsense codons in the cytoplasm sends out a degradation signal to the nucleus via the continuous cellular network or tracks with which both nuclear and cytoplasmic mRNAs may associate (Maquat, 1991; Belgrader *et al.*, 1993). The mRNA localization pathway involved in processing and transport was reviewed by Wilhelm and Vale (1993); and the

relationship between mRNA and the cytoskeletal framework was reviewed by Pachter (1992). This model argues against the pulling effect of translation on RNA processing. I think there are two main requirements to validate this model. First, mRNA export from the nucleus into the cytoplasm travels in a locomotive track; and secondly, disruption of the transport track (such as the important components) abrogates the nonsense codon-mediated reduction of mRNA.

An alternative model, the nuclear scanning model, proposes that the recognition of a nonsense codon occurs in the nucleus and not in the cytoplasm before or at the time of RNA splicing (Urlaub *et al.*, 1989; Nagger *et al.*, 1992). The recognition of nonsense codons before RNA splicing is hard to imagine since it requires that the recognition system distinguish exons from introns and recognize the correct open reading frame in separate exons. There is as yet no convincing biochemical or structural data showing that the nucleus has translational machinery like that of the cytoplasm. Thus, no direct test for this model has been carried out. The best data supporting this model are that nonsense codons trigger exon skipping in mutated genes (Diatz *et al.*, 1993; Belgrader and Maquat, 1994). If these data are true, a nuclear process is clearly involved in the nonsense codon-mediated mRNA degradation because exon skipping has to occur at the time of splicing. Recently, Maquat *et al.* showed that TPI mRNA with nonsense codons is degraded in the nucleus (Belgrader *et al.*, 1994). This result suggests that the recognition of a nonsense codon occurs on the mature mRNA in the nucleus. This is a variation of the nuclear scanning model. In summary, to validate the nuclear scanning model, one needs to show that: 1) the recognition of stop codons that are in-frame with

the translational initiation codon on unspliced and spliced RNAs in the nucleus; and 2) there are, at least part of, the translational-like machinery (such as ribosomal subunit or tRNA) in the nucleus to perform the function of scanning.

### 1.3 Ig Gene Expression during B Cell Development

Immunoglobulins (Igs) are exclusively expressed in B lymphocytes of higher vertebrates. An Ig molecule consists of two identical heavy (H) and two identical light (L) polypeptide chains. In bone marrow stem cells, there are no complete genes for Ig chains, only gene segments. During differentiation of B cells from stem cells in the bone marrow, these gene segments are randomly shuffled by an ordered progression of DNA rearrangements that are capable of generating tremendous different specificities (Alt *et al.*, 1984; Okada and Alt, 1994). This tremendous diversity in Ig structure allows a vertebrate to respond to a vast number of potential antigens (Kuby, 1994).

For example, at the H chain locus of chromosome 12 in the mouse, there are about 300-1,000  $V_H$ , about 12 diversity ( $D_H$ ), and 4 joining ( $J_H$ ) gene segments. In the pre-B cells, a H chain gene is formed by assembling one gene segment of each type. Thus, there is a large combinatorial diversity for the H chains. Further diversity of Ig molecules is mainly generated by somatic mutations (Tonegawa, 1983; Honjo, 1983). The mutation rate in pre-B cell line is reported to be  $0.3-1 \times 10^{-4}$  per cell generation (Wabl *et al.*, 1985). B cells also rearrange light chain genes through a similar process, and express both heavy and light chains that are assembled into functional Ig molecules. These Ig molecules are expressed on the cell surface of B cells (Wall and Kuehl, 1983;

Tonegawa, 1983). Thus mature B cells are antigenically committed to specific epitope. When these cells encounter their corresponding antigen they become activated and differentiate into plasma cells that secrete more than 2,000 molecules of Ig per second (Tonegawa, 1985). This B cell differentiation process is accompanied by a 10-100 fold increase in the cytoplasmic steady-state level of Ig mRNA (Perry and Kelley, 1979; Jäck *et al.*, 1989), which is regulated by post-transcriptional mechanisms (Gerster *et al.*, 1986; Kelly and Perry, 1986), mainly at the level of mRNA stability (Mason *et al.*, 1988; Jäck *et al.*, 1989; Cox and Emtage, 1989; Genovese and Milcarek, 1990). The half-lives of Ig mRNA increase from 2 to 5.5 hr in B cell lines to 13-34 hr in plasma cell lines, depending on the cell lines and the methods used (Mason *et al.*, 1988; Cox and Emtage, 1989; Genovese and Milcarek, 1990).

$\mu$  mRNA encodes the heavy chain of IgM, which is the major Ig isotype produced during the primary response (Kuby, 1994). The  $\mu$  gene consists of a leader, a VDJ, four constant, and two membrane exons. Generation of a functional  $\mu$  gene requires first a D-to-J and then a V-to-DJ rearrangement event, which generates a VDJ exon. These rearrangements do not always preserve the correct reading frame and the resulting Ig mRNA transcribed from that gene may encounter premature termination codons (nonsense codons). A B cell contains two Ig alleles. If one allele rearranges nonproductively, the cell goes on to rearrange the other allele. In mouse, 40-80% of B cells rearrange the second allele of Ig genes. Thus a B cell may contain both productive and nonproductive Ig genes (Altenburger *et al.*, 1980; Reth and Alt, 1984; Alt *et al.*, 1984; Atkinson *et al.*, 1991). If both alleles fail to rearrange productively, B cell

differentiation will be terminated (Alt *et al.*, 1984).

#### 1.4 B Cells Have a Mechanism to Eliminate Ig mRNA Containing Nonsense Codons

Jäck *et al.* have shown by nuclear run-on assays that both productive and nonproductive  $\mu$  genes are transcribed at the same rate (Jäck *et al.*, 1989); therefore, one would expect to find a large amount of nonproductive Ig mRNAs in B cells. But by use of RNA dot blot analysis, they found that the cytoplasmic steady-state level of nonproductive  $\mu$  mRNAs is 60-100 fold lower than the level of the productive  $\mu$  mRNAs (Baumann *et al.*, 1985; Jäck *et al.*, 1989). A similar phenomenon was also observed in the pre-B cell lines (Jäck *et al.*, 1989). Based on these observations, I propose that B cells have a mechanism to eliminate immunoglobulin RNA containing nonsense codons. This is consistent with emerging data in the field of that almost all cytoplasmic Ig heavy chain mRNAs (approximately 99%) in peripheral B cells are productive as revealed by sequencing  $\mu$  cDNA clones obtained from the spleen cDNA libraries.

I reason that it is very important for B cells to have a mechanism to eliminate Ig mRNAs that contain nonsense codons. As discussed before, the tremendous diversity for antigens is a phenomenon unique to Igs. It is mainly generated by assembling variable regions from hundreds of gene segments of H and L chain genes and by somatic mutation. Thus the probability for B cells to generate nonsense codons in Ig genes is higher than for other genes. If  $\mu$  mRNA with nonsense codons could be translated at the same rate as  $\mu$  mRNA without nonsense codons, the resulting truncated  $\mu$  protein may assemble with a complete  $\mu$  protein and two functional light chains to form a chimeric

antibody. Heavy chains translated from productive and nonproductive  $\mu$  mRNAs very likely encode different antigen-binding specificities. The one expressed from nonproductive allele may be self-reactive. Thus, if B cells do not reduce the amount of  $\mu$  mRNA with nonsense codons, they would express bi-specific antibodies on the surface, which may result in autoimmunity.

It is also important for plasma cells to have a mechanism to eliminate Ig mRNAs that contain nonsense codons. Plasma cells are terminally differentiated B lymphocytes, in which more than 2,000 molecules of Igs are produced per second (Tonegawa, 1985). In plasma cells, Ig mRNA comprises about 10% of poly (A)+ mRNAs in the cytoplasm (Schibler *et al.*, 1978), and accounts for 20-30% of the total protein synthesis in plasma cells. In the case of heavy chain  $\mu$  mRNA, if both  $\mu$  mRNAs with or without a nonsense codon could be translated into  $\mu$  chains,  $\mu$  mRNA with a nonsense codon (nonproductive) will compete with the  $\mu$  mRNA without a nonsense codon (productive) for the translational machinery. In addition, the truncated  $\mu$  heavy chains will compete with the functional heavy chains for the binding with the light chains. Thus, the amount of functional antibody molecule will be decreased. Since the amount of Ig protein has been shown to be crucial for the success of an effective humoral immune response, the production of large amounts of truncated  $\mu$  chains would interfere with an efficient humoral immune response. That is, the production of antibodies would not be large enough to eliminate the pathogen. The efficiency of the humoral immune response could also be decreased because the truncated proteins would lack the carboxyl-terminal ends that mediate important functions of Igs, such as binding to the Fc receptor, binding to

the heavy chain binding protein Bip (a chaperone) within the endoplasmic reticulum, or binding and activating complements (Kuby, 1994). In addition, the truncated  $\mu$  proteins could not be secreted into the extracellular environment, presumably they would be trapped in the endoplasmic reticulum (Li and Jäck, see Chapter IV). The accumulation of truncated  $\mu$  proteins in the endoplasmic reticulum of plasma cells might destroy the architecture of cells, as it has been shown in *C. elegans* (Pulak and Anderson, 1993).

### 1.5 The Mechanism of Nonsense Codon-Mediated Reduction of $\mu$ mRNA in Plasma Cells

The main observation leading to this dissertation is that the amount of cytoplasmic  $\mu$  mRNA with a nonsense codon is 60-100 fold lower than the amount of  $\mu$  mRNA without a nonsense codon, although their transcriptional rates are the same (Jäck *et al.*, 1989). The objective of this dissertation is to understand the mechanism of nonsense codon-mediated  $\mu$  mRNA reduction in plasma cells.

The lower cytoplasmic steady-state level of  $\mu$  mRNA with a nonsense codon might result from either a cytoplasmic or a nuclear event, or both. These events include nuclear RNA processing (capping, splicing, or polyadenylation), nuclear RNA degradation, nucleus-cytoplasm export of RNA, cytoplasmic RNA degradation. To determine whether a cytoplasmic or a nuclear event is involved in the reduction of  $\mu$  mRNA with nonsense codons, I will isolate RNA from the nuclear and cytoplasmic fractions of plasma cells, and quantify the levels of  $\mu$  RNA in the two cellular compartments by Northern blot analysis. If  $\mu$  mRNA with a nonsense codon is reduced only in the cytoplasm and there is no blocking of RNA export from the nucleus to the



cytoplasm, I would expect to find that the nuclear RNA level is the same for  $\mu$  mRNA with or without a nonsense codon. In contrast, if  $\mu$  mRNA with a nonsense codon is reduced in the nucleus, I would expect to find that the nuclear  $\mu$  RNA level with a nonsense codon is lower than that of  $\mu$  mRNA without a nonsense codon. Additionally, the cytoplasmic degradation could be an independent event from the nuclear degradation. Therefore, I will further determine whether  $\mu$  mRNA with a nonsense codon is also degraded in the cytoplasm by measuring the cytoplasmic decay rates of endogenous  $\mu$  genes using two well established inhibitors of RNA synthesis, Actinomycin D and DRB. If  $\mu$  mRNA with a nonsense codon is degraded faster in the cytoplasm than  $\mu$  mRNA without a nonsense codon, I would expect to find  $\mu$  mRNA without a nonsense codon has a decreased half-life. The results of these experiments are presented in Chapter III.

Knowing that  $\mu$  mRNA with a nonsense codon is degraded in both the nucleus and the cytoplasm of plasma cells, I modified the testable translational translocation model (Urlaub *et al.*, 1989) to explain the mechanism of how a nonsense codon triggers the reduction of  $\mu$  mRNA in the nucleus. The preliminary results of three different approaches to test the model are summarized in Chapter IV.

## CHAPTER II

### MATERIALS AND METHODS

#### 2.1 Chemicals and Reagents

##### 2.1.1 General Chemicals and Reagents

All general chemicals were molecular biology grade and were purchased from Fisher Scientific (Pittsburgh, PA), Sigma Chemical Co. (St. Louis, MO) and Boehringer Mannheim (Indianapolis, IN). DRB and hygromycin B were purchased from CalBiochem (San Diego/La Jolla, CA); Actinomycin C1, ampicillin (sodium salt) and potassium acetate from Boehringer Mannheim (Mannheim, Germany); polyacrylamide, AG<sup>R</sup>501-X8 (D) (Mix bead resin), APS, gelatine, glycerol, TEMED, BIS and Tween 20 from Bio-Rad (Richmond, VA); antibiotic medium, tryptone, yeast extract and Bacto-agar from Difco (Detroit, MI); mycophenicol acid (MPA), Geneticin (G-418 Sulfate), cesium chloride (ultra pure), DTT, LB base, Penicillin-Streptomycin (500 units/ml) and RPMI 1640 powder from Gibco BRL Life Technologies, Inc. (Gaithersburg, MD); dextran sulfate from Pharmacia (Uppsala, Sweden); ethyl alcohol (absolute) from Aaper Co (Shelbyville, Kentucky); FCS from HyClone (Logan, Utah); universal autoradiography enhancer (Intensify Part A and B) from DuPont NEN (Boston, MA); iodoacetamide and Triton X-100 (pure) from Serva (Heidelberg, Germany); Non-fat dry milk from Real (Los Angeles, CA); sodium hydroxide from Mallinckrodt (St. Louise, MO); scintillation

liquid (Econo-Safe) from RPI (Mount Prospect, IL). All solutions were prepared in deionized water unless otherwise indicated.

### 2.1.2 Radiochemicals

$[\alpha\text{-}^{32}\text{P}]$ dCTP (PB.165/10165/10385)	Amersham, Arlington Heights, IL
Redivue $[\alpha\text{-}^{32}\text{P}]$ dCTP (AA0075)	Amersham, Arlington Heights, IL
$[\alpha\text{-}^{35}\text{S}]$ dATP (SJ.264/1304)	Amersham, Arlington Heights, IL
L- $[\text{}^{35}\text{S}]$ Methionine (SJ. 204)	Amersham, Arlington Heights, IL
$[\text{}^{14}\text{C}]$ methylated proteins (CFA.626)	Amersham, Arlington Heights, IL
Trans $^{35}\text{S}$ -label (Cat# 51006)	ICN Biomedicals, Irvine, CA
$[\gamma\text{-}^{32}\text{P}]$ dATP (Cat# 35020)	ICN Biomedicals, Irvine, CA

### 2.1.3 Kits

Cytoplasmic RNA isolation kit	5 Prime $\rightarrow$ 3 Prime, Inc. <sup>®</sup> , West Chester, PA
DNA 5'-end labeling kit	Boehringer Mannheim, Germany
Magic mini prep kit	Promega, Madison, WI
Nick-translation kit	Gibco BRL, Gaithersburg, MD
pGEM-T vector system I	Promega, Madison, WI
Sequenase kit (version 2.0)	United States Biochemical, Cleveland, OH
Site-directed mutagenesis kit	Promega, Madison, WI

Superscript cDNA library kit	GIBCO BRL, Gaithersburg, MD
RNAzol™ B	Tel-Test, Inc., Friendswood, TX
TRIzol™ Reagent (Total RNA Isolation Reagent)	GIBCO BRL, Gaithersburg, MD

#### 2.1.4 Antibodies

##### 2.1.4.1 Antibodies Used for Immunofluorescence Analysis

Goat anti-mouse $\mu$ -FITC	Fisher Biotech, Pittsburgh, PA
Goat anti-mouse $\kappa$ -Tex Red	Fisher Biotech, Pittsburgh, PA

##### 2.1.4.2 Antibodies Used for Immunoprecipitations

Goat anti-mouse IgM	Southern Biotech, Birmingham, AL
---------------------	----------------------------------

#### 2.1.5 Molecular Weight Standards

Bacteriophage $\phi$ X174 DNA markers	Gibco BRL, Gaithersburg, MD
1Kb DNA Ladder	Gibco BRL, Gaithersburg, MD
$\lambda$ DNA/ <i>Hind</i> III fragments	Gibco BRL, Gaithersburg, MD
0.24-9.7 Kb RNA Ladder	Gibco BRL, Gaithersburg, MD
Rainbow protein marker	Amersham, Buckinghamshire, England
[ <sup>14</sup> C] methylated proteins (CFA.626)	Amersham, Arlington Heights, IL

## 2.2 Oligonucleotides and Linkers

### 2.2.1 Oligonucleotides

All oligonucleotide primers for the polymerase chain reaction (PCR) and site-directed mutagenesis were designed with the aid of an oligonucleotide software analysis program (Oligo™, National Bioscience, Plymouth, MN) and synthesized by National Biosciences (Plymouth, MN).

#### 2.2.1.1 Sequencing

V<sub>H</sub>17.2.25.2: 17 bases; T<sub>m</sub>=61.1°C

5'-CATAAGGACATTCCAGC-3'

SP6 primer: 19 mer;

5'-d(GATTTAGGTGACACTATAG)-3'

T7 primer: 20 mer;

5'-d(TAATACGACTCACTATAGGG)-3'

M13 primer (-40): 17 mer;

5'-d(GTTTTCCCAGTCACGAC)-3'

#### 2.2.1.2 Site-Directed Mutagenesis

Leader mutated primer: 57 bases; T<sub>m</sub>=92.7°C

5'GCCCCTTCCCTGTATCCTCTTCCTCCCGGGAGTAGGTACTCG  
*Sma*I  
 AGCTGCATTTTCATTG-3'

(Italized nucleotides represent the mutated sequences.)

3'Ck.ClaI: 26 bases;  $T_m=77.6^\circ\text{C}$

5'-AAGATAGGATCGATCTGGGGAGCTGG-3'  
*ClaI*

### 2.2.1.3 Polymerase Chain Reaction (PCR)

#### 2.2.1.3.1 Sense Oligonucleotides

$V_{H81X}$ .Forward: 34 mer;  $T_m=81.6^\circ\text{C}$ ;

5'-AGCGGCCGCACCATGGACTTCGGGCTCAGCTTGG-3'  
*NotI*

5' $C_{\mu 1}$ .Forward: 27 mer;  $T_m=92.0^\circ\text{C}$

5'-TGGCCATGGGCTGCCTAGCCCGGGACT-3'

991 $\mu 3$ .Forward: 22 mer;  $T_m=51.6^\circ\text{C}$

5'-ACTGACTCAAACCATGGAATGG-3'

991k3.Forward: 28 mer;

5'-TTGGTACCATCAGCATGAGGGTCCTTGC-3'  
*BamHI*

#### 2.2.1.3.2 Antisense Oligonucleotides

$C_{\mu 2}$ Bam.Backward: 27 mer;  $T_m=65.0^\circ\text{C}$ ;

5'-GGGGTGTGGATCCTTTCTTCTCGATGG-3'

3' $C_{\mu 4}$ .Backward: 28 mer;  $T_m=86.0^\circ\text{C}$

5'-GCCTGACTGAGTTCACACACAAGGAGGA-3'

3'UT. $\mu 1$ : 20 mer;

5'-GGATTTTTTTTATTTCTAAT-3'

3'UT. $\mu$ 2: 20 mer;

5'-TATGCAACATCTCACTCTGAC-3'

3'UT. $\mu$ 3: 21 mer;

5'-A(c)GACACCCAG(a)GGCCTGCCTGG-3'

991 $\mu$ 3.Backward: 24 mer;

5'-ATCGATTCATGACCTGAAATTCAG-3'  
*Cl*I

991k3.Backward: 28 mer;

5'-ATATCGATTAGGTAGACAATTATCCCTC-3'  
*Cl*I

## 2.2.2 Phosphorylated Linkers

*Cl*I linker [d(pGATCGATC)] and *Spe*I linker [d(pGACTAGTCTC)] were purchased from New England Biolabs (Beverly, MA). *Cl*I linker [d(pATCGAT)] was purchased from National Biosciences (Plymouth, MN). *Eco*RI linker [d(pCGGAATTCCG)] was purchased from Amersham (Arlington Heights, IL). *Nhe*I amber stop linker with nonsense codons in all three reading frames [5'-pd(CTAGCTAGCTAG)-3'] was purchased from Pharmacia (Piscataway, NJ).

## 2.3 Enzymes

Restriction endonucleases were obtained from either Boehringer Mannheim (Mannheim, Germany) or Gibco BRL Life Technologies, Inc. (Gaithersburg, MD); AmpliTaq™ DNA polymerase from Perkin Elmer Cetus (Norwalk, CT); T4 DNA ligase

and Klenow fragment from Pharmacia (Piscataway, NJ) or Promega (Madison, WI); DNase I, RNasin (40u/ $\mu$ l), S1 nuclease and Mung bean nuclease from Promega (Madison, WI); RNase A (bovine pancreas) and lysozyme from Sigma Chemical Company (St. Louis, MO); DNA sequenase version 2.0 from United States Biochemical (USB, Cleveland, OH); Proteinase K from Boehringer Mannheim (Indianapolis, IN); Superscript reverse transcriptase from Gibco BRL (Gaithersburg, MD).

## 2.4 Bacterial Strains

### 2.4.1 Bacterial Strains

*Escherichia coli* (*E. coli*) strain HB101 or JM109 or DH5 $\alpha$  from Bethesda Research Laboratories (BRL) and BMH 71-18 mut S from Promega were made competent using a calcium chloride procedure (Sambrook *et al.*, 1989). For some vectors (such as pGEM-Zf series and pSELECT<sup>TM</sup>-1) that contain a sequence coding for the *E. coli*  $\beta$ -galactosidase (*lac Z*)  $\alpha$ -peptide, interrupted by a multiple cloning site, blue/white color selection was used for insert selection. Colonies containing plasmids with no inserts were blue, while those containing inserts were white when grown on Luria Broth agar plates (1.5% Bacto-agar in LB medium, pH 7.0) containing 100  $\mu$ g/ml ampicillin, 40  $\mu$ g/ml X-Gal, and 5 mM IPTG.

### 2.4.2 Preparation of Competent Bacterial Cells

#### 2.4.2.1 Solutions and Reagents

y-a plate (per liter)

20 g

Bacto-tryptone



5 g Bacto-yeast extract

5 g MgSO<sub>4</sub>

(Adjust pH to 7.6 with KOH)

14 g Bacto-agar

y-b medium (per liter)

20 g Bacto-tryptone

5 g Bacto-yeast extract

5 g MgSO<sub>4</sub>

Adjust pH to 7.6 with KOH.

Tbf1

30 mM KAc

100 mM KCl

10 mM CaCl<sub>2</sub>

50 mM MnCl<sub>2</sub>

15 % Glycerol

Adjust pH to 5.8 with 0.2 M acetic acid.

Tbf2

10 mM MOPS

75 mM CaCl<sub>2</sub>

10 mM KCl

15 % Glycerol

Adjust pH to 6.5 with KOH.

\* All solutions were filter-sterilized through a 45- $\mu$ m filter and stored at 4°C.

#### 2.4.2.2 Procedure for the Preparation of Competent Bacterial Cells

Bacteria of interest were streaked from a frozen storage onto a y-a plate. (JM stains must be streaked onto a minimal plate that contains no proline to maintain the F' episome. HB 101 might start from a fresh LB plate.) A single colony of the bacteria was inoculated into 5 ml of y-b media and shaken at 300 rpm overnight at 37°C (Gyrotory® Shaker, Model G10, New Brunswick Scientific Co., Inc., Edison, NJ). A secondary culture was prepared by inoculating 500  $\mu$ l of the overnight culture into 50 ml of pre-warmed y-b media, and aerating at 300 rpm and 37°C for 2 to 4 hours until the OD<sub>550</sub> has reached 0.48. The culture was chilled on ice for 5 min and centrifuged at 3000 rpm for 5 min at 4°C (Beckman tabletop centrifuge, Model GPR, Palo Alto, CA). Bacteria pellet was resuspended in 40 ml of ice-cold Tbf1 and incubated on ice for 5 min. After pelleting, the bacteria was resuspended in 4 ml of ice-cold Tbf2 and further incubated on ice for 15 min. The competent bacteria were pipetted in aliquot (e.g. 250  $\mu$ l) into pre-chilled microcentrifuge tubes placed in an ethanol-dry ice bath, and stored at -70°C. Efficiency of transformation was determined by transforming 50  $\mu$ l of competent bacteria with 20 ng of a plasmid DNA as described in section 2.6.8. Efficiency should approach  $1 \times 10^8$  cfu/ $\mu$ g supercoiled DNA.

## 2.5 Plasmids and DNA Probes

### 2.5.1 Plasmids

pAB $\mu$ -11	From Dr. I. Haas (Bothwell <i>et al.</i> , 1981)
pBluescript II KS +/-	Stratagene, San Diego, CA
pBR-H4	Dr. R. Grossschedl, UCSF, San Francisco, CA (Grossschedl and Baltimore, 1985a; Grossschedl <i>et al.</i> , 1985b)
pBR-V <sub>H</sub> 17.2.25	Dr. R. Grossschedl, UCSF, San Francisco, CA (Grossschedl and Baltimore, 1985a; Grossschedl <i>et al.</i> , 1985b)
pBS-myc	Dr. Jeff Ross, University of Wisconsin, Madison
pCR <sup>TM</sup> II	Invitrogen Corp., San Diego, CA
pCEP4	Invitrogen Corp., San Diego, CA
p5.1	From Dr. I. Haas (Reth <i>et al.</i> , 1984)
p $\gamma$ 2b(11) <sup>7</sup>	Dr. P. Tucker (Tucker <i>et al.</i> , 1979)
pGEM-zfs	Promega, Madison, WI
pGEM <sup>TM</sup> -T Vector System	Promega, Madison, WI
pGm $\beta$ -actin	From Dr. Joel Pachter (Tokunaga <i>et al.</i> , 1986)
pP2-5'	Dr. Nahum Sonenberg, McGill University, Montreal, PQ, Canada (Pelletier <i>et al.</i> ,

	1988)
pRGAPDH	Dr. K. Marcus (Fort <i>et al.</i> , 1985)
pUHD10-1	Dr. H. Bujard (Deuschle <i>et al.</i> , 1989)
pSV2gpt	Dr. J. Murnane (Mulligan <i>et al.</i> , 1981)
pSV2neo	Dr. J. Murnane (Southern <i>et al.</i> , 1982)
pT1gpt	Dr. Falkner (Altenburberg <i>et al.</i> , 1980)
pu <sup>a</sup>	Dr. R. Grossschedl, UCSF, San Francisco, CA (Grossschedl and Baltimore, 1985a; Grossschedl <i>et al.</i> , 1985b)
pu <sup>a</sup> gpt	Jäck <i>et al.</i> , 1992
pu <sup>a</sup> gptΔM	Li and Jäck (unpublished, see section 4.2.1.1 in Chapter IV)

## 2.5.2 DNA Probes

mouse β-actin	1.9 kb <i>HindIII/BamHI</i> fragment from pGmβ-actin
human c-myc	1 kb <i>ClaI/SmaI</i> fragment from pBS-myc
mouse cDNA (Cμ1-4)	1.1 kb <i>SmaI/ApaI</i> fragment from pABμ-11
enhancer probe of mouse μ gene	1.0 kb <i>XbaI</i> fragment from pu <sup>a</sup> gpt
γ 2b	1.0 kb <i>Asp718/BamHI</i> or 320 bp <i>SstI</i> fragment from pBγ2b
rat GAPDH	1.3 kb <i>BamHI/EcoRI</i> fragment from

	pRGAPDH
gpt	1.9 kb <i>Bam</i> HI/ <i>Hind</i> III fragment from pSV2gpt.2 <i>Xho</i> I
Histone 2b	Oncor. Inc. (Gaithersburg, MD) (Grandy <i>et al.</i> 1982)
neo probe	2.4 kb <i>Bam</i> HI/ <i>Hind</i> III fragment from pSV2neo
5'-UTR of poliovirus	0.7 kb <i>Hind</i> III/ <i>Eco</i> RV fragment from pP2-5'
V $\lambda$ 1	1.0 kb <i>Hind</i> III/ <i>Xba</i> I fragment

## 2.6 DNA Manipulations

### 2.6.1 Plasmid DNA Preparation

Plasmids used for cloning and transfection were prepared by the alkaline lysis method for small and large scale plasmid preparation as described by Sambrook (Sambrook *et al.*, 1989). A rapid, small-scale plasmid preparation method (Magic minipreps kit, Promega Corporation, Madison, Wisconsin) was used for restriction enzyme analysis of recombinant plasmids or small-scale DNA probe isolation (see section 2.6.4.2 below).

#### 2.6.1.1 Solutions and Media

1 X M9CA media	2 mM	MgSO <sub>4</sub>
	2%	Glucose

	0.1 mM	CaCl <sub>2</sub>
	0.0025%	Nicotinic Acid
	0.005%	Thiamine
	100 µg/ml	Ampicillin
LB-Amp medium	2.5%	LB
	0.2%	maltose
	5 mM	glucose
	100 µg/ml	ampicillin
Lysis buffer	1%	glucose
	10 mM	EDTA (pH 8.0)
	25 mM	Tris (pH 8.0)
Lysozyme solution	30 mg/ml	in lysis buffer
Alkali solution	1%	SDS
	0.2 N	NaOH
	(prepare fresh)	
Potassium acetate (pH 4.8)	60 ml	of 5M KAc
(per 100ml)	11.5 ml	of glacial acetic acid

	28.5 ml of H <sub>2</sub> O
Proteinase K buffer	50 mM Tris, pH 8.0 10 mM CaCl <sub>2</sub>
Proteinase K stock	10 mg/ml in proteinase K buffer (store at -20°C)
RNase A stock	10 mM Tris-HCl, pH 7.5 15 mM NaCl (store at -20°C)
Sodium acetate (3 M, pH 5.2)	Dissolve 12.3 g NaAc (MW 82.03) in about 40 ml deionized water (0.1% DEPC water in the case of RNA solution). Adjust with glacial acetic acid to pH 5.2. Bring the volume to 50 ml with water.
TE buffer	10 mM Tris-HCl, pH 8.0 1 mM EDTA
TE-saturated phenol/chisam	Thaw phenol at RT before melting at 65°C

for about 30 min. Add 8-Hydroxy Quinoline to final concentration of 1 mg/ml phenol. Extract the phenol with equal volume of 1 M Tris-HCl (pH 8.0) for 3 to 5 times until the pH in TE reaches pH 7-8. Then mix 1 part of the lower, phenol phase with 1 part of chisam (chloroform+isoamyl alcohol = 24+1).

#### 2.6.1.2 Small Scale Preparation of Plasmid DNA (Miniprep)

A fresh, single colony was inoculated into 5 ml of LB medium (containing antibiotics). The cultures were aerated at 300 rpm overnight at 37°C in a shaker (Gyrotory® Shaker, Model G10, New Brunswick Scientific Co., Inc., Edison, NJ). Next morning, 1.5-3 ml of the overnight culture was centrifuged in an Eppendorf tube for 30 seconds at room temperature and the plasmids were isolated using a magic mini prep kit from Promega (Madison, Wisconsin) according to manufacturer's instructions.

#### 2.6.1.3 Large Scale Preparation of Plasmid DNA

2.5 ml of a fresh overnight culture was inoculated into 250 ml of M9CA medium in a 1 liter flask. The bacteria culture was grown at 300 rpm and 37°C to an OD<sub>550</sub> of 0.5-0.6 (about 4 hours) before adding 25 mg of Chloramphenicol (final concentration is 100 µg/ml, Sigma), and further aerated overnight. The next morning, the bacteria was



pelleted by centrifugation in a swinging bucket rotor in a Beckman centrifuge (Model GPR) at 3,500 rpm for 20 minutes at 3°C. The supernatant was discarded and the bacterial pellet was resuspended in 5 ml of ice-cold lysis buffer on ice. 1 ml of freshly prepared lysozyme solution (30 mg/ml in lysis buffer) was added to the suspension, and incubated at room temperature for 5 min, followed by incubation on ice for 5 min. The bacteria were completely lysed by incubating with 12 ml of freshly prepared alkali solution on ice for 10 min. Proteins and chromosomal DNA were precipitated with 9 ml of ice-cold potassium acetate solution for 20 minutes on ice and centrifuged in a Sorvall SS34 rotor at 18,000 rpm and 3°C for 30 min (Sorvall® RC-5B Refrigerated Superspeed Centrifuge, Du Pont Instruments, Wilmington, DE). Plasmid DNA was precipitated from the supernatant with 1 volume of ice-cold isopropanol on ice for 20 minutes and then centrifuged in a Sorvall SS34 rotor at 12,000 rpm and 3°C for 30 min. DNA pellet was air-dried at room temperature for approximately 20 min. RNA in the sample was digested by dissolving and incubating the pellet with 2 ml of TE buffer containing 50 µl of 10 mg/ml RNase A at 37°C for 15 to 30 min. Proteins in the sample were digested by denaturing with 125 µl of 10% SDS followed by incubating with 50 µl of 10 mg/ml proteinase K at 42°C for 1 hour. To extract plasmid DNA, the solution was extracted once with an equal volume of TE-saturated phenol, twice with an equal volume of phenol/chisam (1+1) and once with an equal volume of chisam at room temperature. DNA was precipitated by adding 1/10 volume of 3 M sodium acetate (pH 5.2) and 2.5 volume of ethanol and incubating on ice for at least 20 min or at -20°C overnight. Precipitated DNA was centrifuged at 12,000 rpm and 4°C for 40 minutes, washed twice

with 1 ml of 70% ethanol, dried in a Speed Vac Concentrator (Savant, Farmingdale, NY) and then dissolved in 250  $\mu$ l of TE. 1  $\mu$ l of midi-prep DNA was quantitated by restriction enzyme digestion as described in section 2.6.2 and 2.6.5.

## 2.6.2 DNA Digestion

Plasmid DNA was digested with restriction endonucleases. Usually, 2-5 units of an enzyme was added to per  $\mu$ g of DNA. Digestion reactions were carried out in buffers provided by the manufacturer for each enzyme and under reaction conditions recommended by the manufacturer. Reaction mixtures were run on 0.8-1.2% agarose gels, as described in section 2.6.3, from which purified DNA fragments were extracted, as described in section 2.6.4.

## 2.6.3 DNA Agarose Gel Electrophoresis

DNA fragments were separated on 0.8-1.2% (w/v) agarose gels. 1.12-1.68 g of agarose (weighed in an Analytical Balance, Model XL-400D, Fisher Scientific, Pittsburgh, PA) was dissolved in 140 ml of TAE buffer (1 X TE is 40 mM Tris-HCl, pH 8.0, 20 mM sodium acetate, 2 mM EDTA) by boiling in a microwave. The agarose solution was cooled to approximately 60°C at room temperature before 7  $\mu$ l of ethidium bromide (EtBr) (stock solution is 10 mg/ml) was added to a final concentration of 0.5  $\mu$ g/ml. The mixture was stirred gently before it was poured into a horizontal gel casting tray (15 X 10 cm gel tray, 15 or 20 well comb, 1.5 mm, Bio-RAD, Richmond, CA). The gel was allowed to solidify at room temperature for about 20 min prior to being

transferred to a horizontal electrophoresis chamber (Wide Mini-Sub™ DNA Electrophoresis Cell, Bio-RAD, Richmond, CA) filled with TAE buffer. DNA samples containing tracing dye (0.025% bromophenol blue in 2.5% ficoll and 1X TAE) were loaded into the sample wells of the gel and the electrophoresis was run under constant voltage of 60 V (Power supply: Model FB 135, Fisher Scientific, Pittsburgh, PA) until the dye front migrated to the bottom of the gel. Lambda DNA cleaved with *HindIII* endonuclease and 1 kb DNA ladder (Gibco BRL) were run simultaneously to serve as the molecular weight standards. DNA bands were viewed under an ultra violet light box (312 nm Variable Intensity Transilluminator, FBTIV 614, Fisher Scientific, Pittsburgh, PA) and photographed on a Polaroid 667 film by a Polaroid Camera (Model DS34, Polaroid Corp. Cambridge, MA).

#### 2.6.4 DNA Band Isolation from the Agarose Gel

Digested DNA samples were size fractionated on 0.8-1.2% agarose gels stained with ethidium bromide. DNA fragments were visualized using ultraviolet light as described in section 2.6.3. The appropriate fragments were cut out with a scalpel and extracted from the agarose using the 6 M NaI isolation method described below.

##### 2.6.4.1 6 M NaI Method of DNA Band Isolation

6 M NaI was prepared by dissolving 44.97 g of NaI (FW 149.9 g/mole) in 50 ml deionized water at RT. The DNA-containing agarose was cut into small pieces with a scalpel and transferred into a pre-weighed appropriate tube (either an Eppendorf tube or

a 15 ml-Falcon tube). 2.5 to 3 volumes of 6 M NaI solution per  $\mu\text{g}$  of agarose was added in the tube and incubated at 45-56°C for 10 to 20 minutes until the agarose had melted. The tube was inverted several times during the incubation. 1 ml of Magic Mini Prep Resin (Promega) per 30  $\mu\text{g}$  of DNA was added to the melted agarose, and incubated at room temperature for 5 min. The isolated DNA was eluted from the resin by the procedures as described in Magic Mini prep DNA preparation provided by Promega.

### 2.6.5 Quantitation of DNA

The concentration of the isolated DNA fragment or plasmid was estimated by DNA agarose gel electrophoresis (see section 2.6.3). At least 0.1  $\mu\text{g}$  of DNA was loaded on 0.8-1.0% agarose/TAE gel and the intensity of its EtBr staining was compared to the intensity of a fragment of similar size in  $\lambda$  DNA/*Hind*III standards (Gibco BRL, Gaithersburg, MD) for plasmid and DNA fragments that were larger than 1.6 kb or to Bacteriophage  $\phi$ X174 DNA markers (Gibco BRL, Gaithersburg, MD) for DNA fragments that were smaller than 1.6 kb.

### 2.6.6 Dephosphorylation of DNA Fragment (CIP-treatment)

A kinase reaction is required to prevent the cloning vector from self-ligation.

Dephosphorylation mixture:

DNA digestion mixture: 20-30  $\mu\text{l}$

10x CIP buffer: 5  $\mu\text{l}$

Calf intestinal phosphatase (CIP): 0.01 unit/pmol DNA for 5' overhang)

Deionized H<sub>2</sub>O to 50  $\mu$ l total volume

For 5'-overhangs: the reaction mixture was incubated at 37°C for 30 min, after which another aliquot of CIP was added and the incubation was repeated. For 3'-overhangs or blunt ends: the reaction mixture was incubated at 37°C for 15 min then at 56°C for 15 min, after which another aliquot of CIP was added and the incubation at both temperatures was repeated.

To inactivate the CIP enzyme, 20  $\mu$ l of 500 mM EGTA (pH 8.0) was added to the reaction mixture followed by heat inactivation at 65°C for 45 min or at 68°C for 15 min.

## 2.6.7 DNA Ligation

### 2.6.7.1 Solutions

10 X ligation buffer	250 mM	Tris-HCl, pH 7.6
	100 mM	MgCl <sub>2</sub>
	100 mM	DTT
	100 mM	ATP
10 X Klenow buffer	100 mM	Tris-HCl, pH 7.5
	500 mM	NaCl
	50 mM	DTT (optional)
10 X dNTPs	0.125 mM of each dNTPs	

### 2.6.7.2 Sticky End Ligation of DNA Fragment

A 5-10:1 molar ratio of insert:vector DNA was used to obtain the optimal ligation efficiency. Usually, 0.1  $\mu\text{g}$  of vector DNA was used in the total volume of 15  $\mu\text{l}$  of 1 X ligation buffer. One Weiss unit of T4 DNA ligase (Pharmacia) was added to each ligation mixture. Ligation reactions were allowed to proceed at 15°C overnight (10 to 18 hours). T4 DNA ligase was heat-inactivated at 70°C for 10 minutes before transformation.

### 2.6.7.3 Blunt-End Ligation of DNA Fragment with Phosphorylated Linkers

A 100-200 molar ratio of phosphorylated linker:phosphorylated vector (see section 2.6.6) was usually used for each ligation. Ligation reactions were performed as described in the above section except following the overnight incubation, the ligation reactions were further incubated at room temperature for 4 hours.

### 2.6.7.4 Two-Step Ligation of DNA Fragments

Two-step ligation is a procedure to ligate two fragments that are compatible with only one of their ends.

#### A. First round ligation mixture for enzyme 1 ends:

CIP-treated vector	0.5 $\mu\text{g}$
insert DNA	5-10:1 molar ratio of insert:vector
10 X ligase buffer	1.5-2.0 $\mu\text{l}$
<u>T4 DNA ligase</u>	<u>1 unit</u>
sterile H <sub>2</sub> O	to final volume 15 $\mu\text{l}$ -20 $\mu\text{l}$

Ligation reactions were allowed to proceed at 15°C overnight. T4 DNA ligase was heat inactivated at 70°C for 10 minutes. (The vector self-ligation was stored at -20°C for use as a transformation control.)

B. Klenow enzyme filling in the remaining sticky end:

DNA ligation mixture	15-20 $\mu$ l (from the above)
10 X Klenow buffer	3 $\mu$ l
0.125 mM dNTPs	3 $\mu$ l
100 mM DTT	1.5 $\mu$ l
<u>Klenow</u>	<u>1 unit (diluted in 1 X Klenow buffer)</u>
sterile H <sub>2</sub> O	to final volume 30 $\mu$ l

Incubate at RT (22°C) for 30 min.

C. Second round ligation for the blunt ends:

1) Ligation mixture

10 X ligase buffer	12 $\mu$ l
40% PEG	15 $\mu$ l
100 mM DTT	1.2 $\mu$ l
<u>T4 DNA ligase</u>	<u>1 unit</u>
sterile H <sub>2</sub> O	to final volume 120 $\mu$ l

2) the ligation mixture was added to the 30  $\mu$ l of Klenow reaction mixture;

3) the mixture was incubated at 15°C overnight;

- 4) the following morning, the mixture was incubated at RT for an additional 3 hours;
- 5) the ligase was heat inactivated at 68°C for 10 min.

D. The ligation mixture was transformed into competent HB 101 cells as described in 2.6.8.

- 1) for vector+insert: 50 ng or 100 ng/100  $\mu$ l HB 101;
- 2) for vector control: 100 ng/100  $\mu$ l HB 101.

## 2.6.8 DNA Transformation

For transformation, a 50-100  $\mu$ l aliquot of competent cells (the amount depends on the number of cells) was measured into a cold microcentrifuge tube containing 50-500 ng of plasmid DNA or ligation mixture. The cell/DNA suspension was mixed gently and incubated on ice for 20-30 min, followed by a heat shock in a 42°C water bath for 45 seconds. The tubes were chilled on ice for 2 min and 1 ml of S.O.C. (2% Bacto-trytone, 0.5% yeast extract, 10 mM NaCl, 2.5 mM KCl, 10 mM MgCl<sub>2</sub>, 10 mM MgSO<sub>4</sub>, 20 mM Glucose) was added. The suspension was incubated for 1 hour at 37°C with shaking (225 rpm) to allow expression of the antibiotic-resistant gene before plating onto a LB plate containing ampicillin (100  $\mu$ g/ml) or tetracycline (15  $\mu$ g/ml). Transformants were selected by standard methods described below.



## 2.6.9 Screening for Recombinant DNA

### 2.6.9.1 Blue/white Color Screening

JM109, which contains an F' episome that carries a nutritional requirement for growth (proline biosynthesis), is used for blue/white color screening of the pGEM-Z and pGEM-Zf plasmids (Promega). To prepare plates containing IPTG and X-Gal, 50  $\mu$ l of 2% X-Gal and 100  $\mu$ l of 100 mM IPTG were spread on LB plates and allowed to absorb for 30 min at 37°C prior to plating transformed JM109 cells. The plates were incubated overnight at 37°C. Recombinant colonies were white while nonrecombinant colonies were blue.

### 2.6.9.2 Colony Lift

The following protocol was modified after the procedures described in manufacturer's instruction and Sambrook *et al.* (1989). LB plates with selective agent containing single isolated colonies were cooled at 3°C before use. Nylon membrane (HyBond™-N, Nylon, 0.45  $\mu$ M, X82 mm, Cat# RPN.82N, Amersham, Arlington Heights, IL) was overlaid onto the agar plate to allow uniform wetting. The nylon membrane and agar gel were marked in several places with India ink. The nylon membrane was then placed on a Whatman paper (Whatman 4 filter paper, 9.0 cm, Whatman limited, England) soaked in denaturation solution (2 X SSC and 5% SDS) for 2 minutes (the colony side should be upward). The DNA was fixed to the nylon by microwaving the membrane at high power for 2.5 minutes (650 watts). The bacterial debris was rubbed off with a glove after soaking the membranes in 2 X SSC.

Prehybridization of the membrane was performed in a solution containing 0.5 M sodium pyrophosphate, 1% BSA, 7% SDS, 1 mM EDTA at 65°C for at least 1 hour. Hybridization was performed overnight in the same solution as prehybridization except 2 X 10<sup>6</sup> counts of denatured <sup>32</sup>P-labeled DNA probe was added and incubation temperature was 65°C. The membrane was washed first in 2 X SSC at room temperature for 2-5 minutes and then in 0.1 SSC and 0.1 % SDS at 55°C until the background was low. The holes were labeled with a radioactive pen before autoradiography.

## 2.6.10 Labeling of DNA Probes

### 2.6.10.1 Nick Translation

Radioactive probes were prepared by nick translation using nick translation kit and protocol supplied by BRL. One  $\mu\text{g}$  of probe was added to a mixture containing 100  $\mu\text{Ci}$  [ $\alpha$ -<sup>32</sup>P]-dCTP (Amersham, Arlington Heights, IL), 5  $\mu\text{l}$  of a 0.2 mM solution of three deoxyribonucleoside triphosphates (dNTPs: dATP, dGTP, dCTP), 5  $\mu\text{l}$  of a solution containing 2 units DNA polymerase I and 200 pg DNase I in a total volume of 50  $\mu\text{l}$ . The labeling reaction was incubated at 15°C for 1 h and then stopped by the addition of 5  $\mu\text{l}$  of 300 mM Na<sub>2</sub>EDTA solution on ice. The labeled DNA was immediately separated from unincorporated nucleotides by chromatography on a 0.9 X 1.5 cm G-50 Sephadex™ (Fine) column using the protocol provided by Boehringer Mannheim Corporation (Indianapolis, IN). The specific activity of the labeled probe is 5-10 X 10<sup>7</sup> cpm/ $\mu\text{g}$  DNA.

### 2.6.10.2 Random Priming

25-50 ng template DNA was added with distilled water to bring the total volume to 37  $\mu$ l in a screw-capped microcentrifuge tube. The DNA was denatured by boiling for 5 minutes, immediately placing the tube on ice. The following mixture was added to the DNA solution: 10  $\mu$ l of 5 X C\* buffer (containing 250 mM Tris-HCl, pH=8.0, 25 mM MgCl<sub>2</sub>, 5 mM  $\beta$ -mercaptoethanol, 2 mM each of dATP, dGTP and dTTP, 1 M HEPES (adjusted to pH 6.6 with 4 N NaOH) and 1 mg/ml random primers (mostly hexamers, BRL), 2  $\mu$ l of 10 mg/ml BSA (BRL), 0.5  $\mu$ l of [ $\alpha$ -<sup>32</sup>P]dCTP (Amersham), and 1 unit of the Klenow fragment of *E. coli* DNA polymerase I. The reaction mixture was incubated at room temperature for at least 30 minutes. The specific activity of the labeled probe was determined by counting 1  $\mu$ l of the total reaction mixture in liquid scintillation counter. 10<sup>8</sup>-10<sup>9</sup> cpm/ $\mu$ g is suitable (Sambrook *et al.*, 1989; protocols from GIBCO BRL).

### 2.6.10.3 5' End Labeling

100 pmol (or 50-100 ng) oligonucleotide was phosphorylated by adding 1  $\mu$ l of T4 polynucleotide kinase (8 units/ $\mu$ l in the solution containing 50 mM Tris-HCl, 10 mM MgCl<sub>2</sub>, 10 mM DTT, 1 mM spermidine, and 800  $\mu$ Ci [ $\gamma$ -<sup>32</sup>P] dATP (ICN). The reaction was incubated at 37°C for 30-45 minutes and the kinase was inactivated by heating at 70°C for 10 minutes. The labeled oligonucleotide was immediately separated from unincorporated nucleotides by chromatography on a 0.9 X 1.5 cm of G-25 Sephadex™ (Fine) column using the protocol provided by Boehringer Mannheim Corporation

(Indianapolis, IN). The specific activity of the labeled probe is  $4 \times 10^5$  to  $1.2 \times 10^6$  cpm/ng oligonucleotide.

## 2.7 Site-Directed Mutagenesis

### 2.7.1 Solutions

10 X annealing buffer	200 mM	Tris-HCl, pH 7.5
	100 mM	MgCl <sub>2</sub>
	500 mM	NaCl
10 X M9 solution (per liter)	60 g	Na <sub>2</sub> HPO <sub>4</sub> (MW=131.96)
	30 g	KH <sub>2</sub> PO <sub>4</sub> (MW=136.09)
	5 g	NaCl
	10 g	NH <sub>4</sub> Cl
M9 agar plate (per liter)	100 ml	10 X M9 solution
	875 ml	distilled H <sub>2</sub> O
	15 g	agar
		Autoclave, cool to 55°C and add
	1 ml	MgSO <sub>4</sub>
	100 μl	CaCl <sub>2</sub>
	10 ml	20% (w/v) Glucose
1 ml	10 mg/ml Thiamine	

Pour 20 ml in each plate

Phage precipitation solution	20%	PEG 8000 (Sigma)
	2.5 M	NaCl
10 X synthesis buffer	100 mM	Tris-HCl, pH 7.5
	5 mM	dNTPs
	10 mM	ATP
	20 mM	DTT
TYP broth (per liter)	16 g	Bacto-tryptone
	16 g	Bacto-yeast extract
	5 g	NaCl <sub>2</sub>
	2.5 g	K <sub>2</sub> HPO <sub>4</sub>

### 2.7.2 Preparation of Phagemid Single-Stranded DNA

The following protocol was modified from instructions of Promega Altered Sites kit protocol and an internal protocol. The DNA to be mutated was cloned into the pSelect-1 vector. Recombinant DNA was transformed into competent cells of JM109 or a similar host and selected by plating on the LB-Tet (tetracycline 15  $\mu$ g/ml) and IPTG/X-Gal plate. (The LB-Tet plate was spread with 100  $\mu$ l of 0.1 M IPTG and 50  $\mu$ l of 2% X-Gal, and these components were allowed to absorb for 30 minutes at 37°C prior to

plating cells.) The original pSelect-1 vector was used as a positive control and the pSelect-control phagemid (Promega) was used as a negative control. Several white colonies on the recombinant transformation plate were picked with toothpicks to do mini-preps for confirmation of the correct recombinant clones. The overnight cultures of cells containing pSelect-1, pSelect-control, and correct recombinant DNAs were plated on M9-Tet plate (15  $\mu\text{g/ml}$  tetracycline) to select for the presence of F' which carries a nutritional requirement for growth and decreases the number of false positives. The incubation time was about 40 hrs. An overnight culture was prepared from each M-9 plate by picking individual colonies on M9-Tet plates and inoculating 5 ml of TYP broth containing 15  $\mu\text{g/ml}$  tetracycline and shaking overnight at 37°C. The next morning, 25 ml TYP broth (15  $\mu\text{g/ml}$  tetracycline) was inoculated with 500-1000  $\mu\text{l}$  of overnight cultures. These were shaken vigorously at 37°C for 2-3 hrs until the  $A_{550}=0.5-1.0$ . This was the plating culture and could be stored at 3°C up to 1 week. The culture was infected with helper phage R408 (which obtains high yields when it is used in conjunction with the JM109 strain) at a multiplicity of infection (m.o.i.) of 10. 1 O.D. at  $A_{550}=5 \times 10^8$  cells/ml. The cultures (10-20 ml) were incubated at 37°C for 20 minutes, and then shaken vigorously at 37°C for at least 6 hrs. After shaking, the cultures were transferred to SS34 tubes, and the culture supernatant was harvested by pelleting the cells at 12K rpm/4°C/15 minutes. The supernatant was then transferred to a new SS34 tube, and spun again as described above. 1 ml of each supernatant was saved in 3°C refrigerator. The rest of supernatant was precipitated with 0.25 volume of phage precipitation solution (20% PEG and 2.5 M NaCl) overnight at 3°C. The phage pellet

was then spun down at 12K rpm/3°C/15 min. The tubes were thoroughly drained, spun again for 2 min, and any liquid was removed with a pipeter. The pellet was resuspended in 0.5 ml of TE (pH=7.5-8.0), and transferred to a 1.5-ml microcentrifuge tube. The phagemid DNA was phenol extracted once; phenol:chisam extracted twice; and then chisam extracted once. The phagemid DNA was precipitated with 1/10 volume of 3 M NaAc and 2.5 volume of ethanol at -20°C for 30 minutes or overnight. The pellet was spun down and dried in a Speedvac. The pellet was sometimes difficult to see, and was resuspended in 30  $\mu$ l of TE. 2  $\mu$ l was quantitated on 0.8-1.0% agarose gel. The helper phage band of R408 is 6.4 kb and pSelect-control is 5.6 kb. The single-stranded DNA standard from the sequencing kit (USB) may also be used as the size standard for estimation of single-stranded DNA.

### 2.7.3 5' Phosphorylation of Oligonucleotides

1) The following components were added to a microcentrifuge tube:

oligonucleotide	100 pmol
10 X kinase buffer	2.5 $\mu$ l
10 X ATP (10 mM)	2.5 $\mu$ l
<u>T4 polynucleotide kinase</u>	<u>5 units</u>
sterile H <sub>2</sub> O	to final volume 25 $\mu$ l

2) Incubated the reaction at 37°C for 30 minutes.

3) Incubated the reaction at 70°C for 30 minutes to inactivate the kinase.

4) The reaction products were stored at -20°C or added directly to the annealing

reaction.

#### 2.7.4 Site-Directed Mutagenesis

A phosphorylated mutagenic oligonucleotide (1.25 pmol) and ampicillin repair oligonucleotide (0.25 pmol, Promega) were annealed to the recombinant pSELECT-1 ssDNA (0.05 pmol) in annealing buffer by heating to 70°C for 5 min followed by slowly cooling to room temperature. After extension with T4 DNA polymerase and ligation by T4 DNA ligase in synthesis buffer, DNA strands were used to transform the BMH 71-18 mut S mismatch repair-deficient *E. coli* competent bacteria to select for ampicillin resistant transformants. Total plasmid DNA was prepared and transformed into the JM 109 competent bacteria. Mutant colonies were first screened by the restriction enzyme specific to the site present in the mutagenic oligonucleotide and further confirmed by sequencing as described in section 2.9.

#### 2.8 Reverse Transcription Polymerase Chain Reaction (RT-PCR)

RNA was prepared by using the GIT/CsCl method as described in section 2.12.1.1, and cDNA was synthesized by using the Superscriptase library kit (Gibco BRL).

##### 2.8.1 Synthesis of cDNA Fragment by Reverse Transcriptase (RT)

###### 2.8.1.1 Reagents and Solutions

Amplitaq DNA Polymerase                      200 U/ $\mu$ l



dNTPs	0.1 M	
First strand buffer (5 X)	250 mM	Tris, pH 8.3
	375 mM	KCl
	15 mM	MgCl <sub>2</sub>
Oligo(dT) 15 primer	0.5 $\mu\text{g}/\mu\text{l}$	
PCR buffer (10 X)	100 mM	Tris/HCl (pH 8.0)
	500 mM	KCl
	25 mM	MgCl <sub>2</sub>
	0.1%	gelatin
sense oligonucleotide:	50 pMole/ $\mu\text{l}$	
antisense oligonucleotide:	50 pMole/ $\mu\text{l}$	
rRNasin <sup>®</sup> RNase inhibitor	40 U/ $\mu\text{l}$	

#### 2.8.1.2 Procedure

5  $\mu\text{g}$  of total cellular RNA in TE was precipitated with 1/10 volume of 3 M NaAc (pH 5.2) and 2.5 volumes of EtOH overnight at  $-20^{\circ}\text{C}$ . RNA was pelleted in a

microcentrifuge at 13,000 rpm for 1 hour at 3°C, washed twice in 70% EtOH, air-dried and resuspended in 22.5  $\mu$ l of DEPC-water. The RNA was denatured in the presence of 4  $\mu$ l oligo (dT) primer (0.5  $\mu$ g/ $\mu$ l, Promega) by heating at 65°C for 3 minutes, chilled on ice for 2 minutes, spun briefly, followed by adding 10  $\mu$ l 5 X RT buffer, 5  $\mu$ l 5 mM dNTPs, 5  $\mu$ l 0.1 M DTT, 2  $\mu$ l rRNasin (40 U/ $\mu$ l, Promega, optional), and 1.5  $\mu$ l Superscript Reverse Transcriptase (200 U/ $\mu$ l, GIBCO BRL). Incubated the samples for 10 minutes at room temperature, followed by 1-hour incubation at 42°C. To inactivate reverse transcriptase, the samples were heated for 3 minutes at 95°C in a heat block, chilled on ice and pulse spun. This RNA mixture was usually good for at least 10 PCR reactions. It was either frozen at -20°C, or immediately used for a PCR amplification (see section 2.8.2).

### 2.8.2 PCR Amplification

PCR was performed with 2  $\mu$ l of the cDNA product from *FH* (0.2  $\mu$ g) or 5  $\mu$ l of the cDNA product (0.5  $\mu$ g) from *VXH* or *CH2XH* in a 1.5-ml microcentrifuge tube containing 3.5  $\mu$ l of 10 X PCR buffer, 3.5  $\mu$ l 2 mM dNTPs, 1.0  $\mu$ l forward primer (50  $\mu$ M), 1.0  $\mu$ l reverse primer (50  $\mu$ M), 21  $\mu$ l water, and 0.5 U AmpliTaq polymerase (Taq polymerase, BRL). The mixture was overlaid with 35-50  $\mu$ l of mineral oil and the cDNA was amplified for 30 cycles under the following conditions for each segment in a DNA Thermal Cycler (Perkin Elmer Cetus, Model 480, Emeryville, CA): denaturation, 94°C for 1 minute; annealing, 50°C for 1 minute; extension, 72°C for 2 minutes. After the amplification reaction, 30  $\mu$ l of the PCR products were analyzed on a standard 1%

agarose TAE (or TBE) gel stained with ethidium bromide (Sambrook *et al.*, 1989) to confirm the sizes of synthesized DNA fragments.

PCR amplification of plasmid DNA fragment was performed as described above except that 1 ng of DNA template was used for 25-30 cycles of amplification.

## 2.9 DNA Sequencing

For single-stranded DNA sequencing, the gene segments of interest were subcloned into M13 phage expression vector or pGEM vector (Promega Corp., Madison, WI) and the single-stranded DNA template was prepared as described before (see sections 2.6 and 2.7.2). For double-stranded plasmid sequencing, the single-stranded template DNA was generated by denaturing 5-10  $\mu$ g of plasmid DNA in 2 N NaOH and 2 mM EDTA solution at room temperature for 5 minutes. The mixture was neutralized by adding 0.1 volumes of 3 M  $\text{NH}_4\text{Ac}$  (pH=4.5) and the DNA was precipitated in ethanol at  $-70^\circ\text{C}$  overnight. After washing the pelleted DNA with 70% ethanol, it was dissolved in 7  $\mu$ l of distilled water for the sequencing reaction. Appropriate primer (see section 2.2.1) and the reagents in the Sequenase™ Version 2.0 Kit (United States Biochemical, Cleveland, OH) were used in the sequencing reactions as instructed by the manufacturer. The single-stranded bacteriophage M13mp18 was used as positive control for the sequence reaction.

The samples were denatured at  $80^\circ\text{C}$  for 3-5 minutes prior to loading on 6% urea-polyacrylamide gel. The electrophoresis was performed at 50 watts and  $55^\circ\text{C}$  gel temperature in 1 X TBE buffer. The gel was fixed in 10% methanol and 10% acetic acid

for 15 minutes at room temperature, transferred onto a Whatman filter and dried for 30 minutes at 80°C (Hoefer Scientific, Model SE 1160, San Francisco, CA). The Fluorography was performed by exposing the dried sequencing gel to an X-ray film at room temperature for overnight or 1 day.

## 2.10 Cell Culture Techniques and DNA-Mediated Cell Transfection

### 2.10.1 Cell Maintenance

Mouse plasmacytomas and hybridomas were maintained in RPMI 1640 medium supplemented with 10% (vol/vol) fetal calf serum (FCS, Hyclone Laboratories), 4 mM L-glutamine, 50 units or  $\mu\text{g}$  of a penicillin-streptomycin solution per ml, 0.05 mM  $\beta$ -mercaptoethanol and 1 mM sodium pyruvate at 37°C in a 5% CO<sub>2</sub>-humidified incubator (Heraeus Instrument, S. Plainfield, NJ). This media is referred to as complete RPMI 1640 media. All cell culture reagents were from GIBCO BRL unless specifically indicated.

### 2.10.2 Cell Lines That Were Used in the Dissertation

Mouse pre-B cell line F (Jäck *et al.*, 1989)

Mouse hybridoma FH (LOCB 83.13.13, Jäck *et al.*, 1989)

Mouse hybridoma VXH (GAMO 12.8, Jäck *et al.*, 1989)

Mouse hybridoma CH2XH (GAMO 62.12, Jäck *et al.*, 1989)

Mouse plasmacytoma J558L (Oi *et al.*, 1980)

Mouse plasmacytoma NYCH. $\mu\kappa$  (Bornemann *et al.*, 1995)

Mouse myeloma Ag8.653 (Kearney *et al.*, 1979; Bornemann *et al.*, 1995)

### 2.10.3 Cell Harvesting

Cells were harvested by centrifuging at 1,100 rpm and 4°C for 5 minutes in polypropylene tubes (Silencer® S-103 NA, Rupp & Bowman, Tustin, CA).

### 2.10.4 Freezing and Thawing of Cells

About  $2 \times 10^7$  cell were pelleted, resuspended in 1.5 ml of RPMI freezing media (RPMI 1640 with 30% FCS, 15% dimethyl sulfoxide, and 0.05 mM  $\beta$ -ME), and transferred into an ice-chilled cryogenic tube (Vangard CRYOS™, Sumitomo Bakelite Co., Ltd., Japan). The tubes were kept in a styrofoam box overnight at -70°C to allow for slow freezing and stored in liquid nitrogen (Nitrogen tank type 5k, Taylor-Wharton, Theodore, AL).

To thaw cells, the frozen tubes were warmed up in a 37°C water bath until most of the cells were thawed, then completely thawed on ice. Then the cells were transferred into a 50-ml Falcon tube, washed once with 25 ml of complete RPMI 1640 media, and cultured in 10 ml of the complete media.

### 2.10.5 Cell Counting

Cells were diluted in an equal volume of trypan blue solution and counted in a Neubauer hemacytometer chamber (Bright-Line®, 0.1 mm, American Optical Co., Buffalo, NY). The cell number was determined by the following equation:

$$\text{Cells/ml} = \text{cells per large square} \times 2 \times 10^4$$

### 2.10.6 Subcloning

Hybridoma cell lines were subcloned by limiting dilution in 96-well plates (0.15 cells/100  $\mu$ l/well, Costar, Cambridge, MA). 100  $\mu$ l of the complete RPMI 1640 media was added to each well after 7-10 days. The wells were screened for colony growth under the light microscope (400 X, Labovert Inverted Microscope FS, Leitz Wetzlar, Germany) after 12 to 15 days. Subclones were analyzed for Ig expression by cytoplasmic immunofluorescence analysis as described in section 2.13.1, or the presence of  $\mu$  gene by PCR as described in section 2.8.2.

### 2.10.7 Transfection

For electroporation,  $5 \times 10^6$  cells were removed and washed twice in ice-cold protein-free RPMI 1640 medium (the complete RPMI 1640 media without FCS), and resuspended in 500  $\mu$ l of the same medium. After addition of 5-20  $\mu$ g DNA (in 1 X TE, total volume <20  $\mu$ l), the cells were incubated on ice for 10 minutes and subjected to 1 pulse of 330  $\mu$ F, 285 volts at low conductivity with a Cell Porator (BRL, Gaithersburg, MD). The transfected cells were immediately transferred into 50 ml-flasks and grown in 10 ml of 20% FCS-RPMI 1640 media for 48 hours. To isolate stable transfectants, we grew the transfected cells that were plated in 96-well plates (Costar, Cambridge, MA) at the density of  $5 \times 10^4$  cells per ml media, 100  $\mu$ l media per well in growth media containing 2.5  $\mu$ g of mycophenolic acid (MPA) and 250  $\mu$ g of xanthine per ml for 7-10

days (Jäck *et al.*, 1989). The MPA positive stable transfectants were screened by cytoplasmic immunofluorescence for  $\mu$  protein expression (see section 2.13.1).

## 2.11 DNA Isolation from Mammalian Cells and Analysis

### 2.11.1 DNA Isolation by Guanidinium Isothiocyanate (GIT)/Cesium Chloride (CsCl) Method

High molecular weight DNA was isolated as described in Sambrook *et al.*, 1989. Briefly, DNA bands in cesium chloride phase (see section 2.12.1.1 below) were aspirated into a pasteur pipette and washed twice with 10 ml of 70% ethanol in 50 ml-Falcon tube. After air-drying briefly, the DNA was digested with 200  $\mu$ g/ml proteinase K (PK) in 10 ml of PK buffer at 42°C overnight (about 16 hours). To remove the proteins, the DNA solution was extracted once with equal volume of TE-saturated phenol, twice with phenol/chisam (1+1) and once with chisam. The extracted DNA was then precipitated with 2 volumes of 100% ethanol, spooled onto a pasteur pipette, washed once in 80% ethanol, briefly dried, resuspended in TE (pH 8.0), and incubated overnight at 37°C to facilitate the dissolving process. The concentration of DNA was determined by photometric measurement at 260 nm as described in 2.11.2. DNA preparations were stored at 4°C.

### 2.11.2 Quantitation of DNA

The concentration of DNA was quantitated by measuring the absorption or optical density (OD) at 260 nm (Spectrophotometer, Spectronic 20, Bausch & Lomb, Rochester, NY).

**1 OD at 260 nm = 50  $\mu$ g/ml DNA.**

The purity of DNA was determined by the ratio of the absorbance of DNA at 260 nm to its absorbance at 280 nm. Our samples were in the range of 1.8 to 2.2.

### 2.11.3 Southern Blot Analysis

#### 2.11.3.1 Solutions

Alkali solution	0.5 N	NaOH
	1.5 M	NaCl
Neutralization solution	0.5 M	Tris-HCl, pH 7.4
	3 M	NaCl
Washing solutions	1) 0.4 N	NaOH
	2) 0.2 M	Tris-HCl, pH 7.5
	2 X	SSC
10 X SSC (pH 7.0)	0.15 M	Citric Acid
	1.5 M	NaCl

#### 2.11.3.2 Procedure

High molecular weight DNA that was prepared as described in section 2.11.1 was digested to completion (overnight) with the appropriate restriction enzymes, and electrophoresed on a 0.8% agarose gel. The gel was then denatured in 250 ml of alkali



solution under shaking at room temperature for 30 minutes and neutralized with 250 ml of neutralization solution for 30 minutes. The DNA was capillarilly transferred onto the concave side of genescreen plus® (DuPont Biotechnology System NEN® Research Product, Boston, MA) in 10 X SSC at room temperature overnight. The genescreen filter was washed first with 0.4 N NaOH for 30 seconds, and then washed with 0.2 M Tris-HCl (pH 7.5) and 2 X SSC for 2 minutes. The filter was dried under an infrared lamp or between 2 Whatman papers (3MM). The filters were prehybridized in 10% Dextran sulfate, 1% SDS and 1 M NaCl at 65°C for about 2 hours and hybridized with 100  $\mu$ Ci of <sup>32</sup>P-nick-translation labeled DNA probes and 200  $\mu$ g/ml of salmon sperm DNA in 10% Dextran sulfate, 1% SDS and 1 M NaCl at 65°C overnight. The filter was washed as described in section 2.12.5 except at 65°C.

## 2.12 RNA Isolation from Mammalian Cells and Analysis

### 2.12.1 Total RNA Isolation

#### 2.12.1.1 GIT/CsCl Method

Total RNA was prepared from cells with guanidinium thiocyanate followed by centrifugation in cesium chloride solutions (Sambrook *et al.*, 1989). Briefly, 1-2 X 10<sup>7</sup> cells were removed and washed twice with ice-cold phosphate-buffered saline (PBS, GIBCO BRL) without calcium and magnesium. Then the cells were transferred in 1 ml of PBS into a 15 ml-Falcon tube and lysed in 2 ml of GIT homogenization buffer (4 M GIT, 0.12 M  $\beta$ -Mercaptoethanol, and 25 mM Sodium acetate, pH 5.6-6.0). The resulting homogenate was then layered on a 2 ml cushion of cesium chloride (CsCl) solution (5.7

M CsCl, 25 mM NaAc, pH 5.2) in a clear ultracentrifuge tube (Nalgene™ UltraTubes, thin wall/polyallomer, open-top, size 13 X 51 mm, Nalge Company, Rochester, NY). The tubes were balanced with GIT homogenation buffer. The gradient was centrifuged at 35 K rpm for at least 20 hours at 20°C in a Beckman SW50.1 rotor (Preparative Ultracentrifuge, Model L8-70, Beckman, Palo Alto, CA). After centrifugation, the DNA band was collected (if preparation of DNA was desired, see section 2.11.1), the remaining supernatant was aspirated until the CsCl layer. The rest of CsCl layer was poured off and briefly air-dried. The bottom of the tube was cut off with a razor blade, the RNA pellet (may be not visible) was resuspended in 270  $\mu$ l (3 x 90  $\mu$ l) of TE, and transferred to an Eppendorf tube. 30  $\mu$ l of 3 M sodium acetate (pH 5.2) and 750  $\mu$ l of absolute ethanol were added to precipitate the RNA at -20°C overnight. The precipitate was dissolved in TE buffer (10 mM Tris-HCl, 1 mM EDTA, pH 8.0).

#### 2.12.1.2 Trizol or RNazol™ B Method

Total RNA was rapidly isolated for the screening of hybridoma subclones by a single-step method (Chomczynski and Sacchi, 1987; Kedzierski and Porter, 1991) using TRIzol Reagent (GIBCO BRL Cat No. 15596-026) and protocol supplied by BRL. Briefly, 5 X 10<sup>6</sup> plasmacytoma cells were pelleted by centrifugation as described in section 2.10.3. The cells were lysed in 1 ml of the TRIzol Reagent by repetitive pipetting, and the samples were transferred to microcentrifuge tubes. The homogenized samples were then incubated for 5 minutes at room temperature to permit the complete dissociation of nucleoprotein complexes. 200  $\mu$ l of chloroform was added to the samples,

shaken vigorously by hand for 15 seconds and incubated at room temperature for 2 to 3 minutes. The samples were centrifuged at 12,000 X g for 15 minutes at 4°C, and 500  $\mu$ l of the upper aqueous phase was transferred to a fresh tube. The RNA was precipitated by incubating samples with an equal volume of isopropanol at room temperature for 10 minutes and centrifuging at 12,000 X g for 10 minutes at 4°C. The RNA pellet was washed once with 1 ml 70% ethanol by centrifugation, briefly air-dried, and dissolved in 25  $\mu$ l of RNase-free water or TE by passing the solution a few times through a pipette tip. If the RNA pellet was not completely dissolved, the tubes were incubated for 10 minutes at 55°C-60°C. The isolated RNA had an  $A_{260/280}$  ratio of 1.6-1.8.

The isolation of RNA using RNAzol™ B solution (Tel-Test, INC., Friendswood, TX) is based on the same principle and similar procedures as suggested by the manufacturer.

### 2.12.2 Cytoplasmic RNA Isolation

Cytoplasmic RNA was isolated by the Nonidet P-40/Phenol method (modified from Favaloro *et al.*, 1980). Briefly,  $5 \times 10^6$  cells were removed, centrifuged, washed with PBS once in an Eppendorf tube. Cells were lysed in 200  $\mu$ l of ice-cold lysis buffer (5 Prime to 3 Prime, Inc.®, 0.14 M NaCl, 1.5 mM MgCl<sub>2</sub>, 0.5 % Nonidet-P40, 10 mM Tris, pH 8.6, and 0.05 unit/ml rRNasin from Promega) for 10 minutes on ice. The nuclei and unlysed cells were removed by centrifugation at 13 K rpm (12,000 X g) and 4°C for 5 minutes. 175  $\mu$ l of the supernatant was transferred to a new Eppendorf tube and digested with 0.2 mg Proteinase K (Boehringer Mannheim) in 175  $\mu$ l of preheated

2 X proteinase K buffer (0.3 M NaCl, 2 mM EDTA, 2% SDS, 0.2 M Tris, pH 7.6) at 42°C for 1-2 hours. The RNA solution was then extracted three times with 300  $\mu$ l of phenol/chloroform (1+1) and once with 300  $\mu$ l of chisam at room temperature, and precipitated with sodium acetate and absolute ethanol as described above. The precipitate was dissolved in 25  $\mu$ l of TE buffer. The concentration of RNA was determined by measuring the absorbance at 260 nm as described in section 2.12.4. The RNA yield was 60  $\mu$ g per 5 X 10<sup>6</sup> hybridoma cells and 35-40  $\mu$ g per 5 X 10<sup>6</sup> plasmacytoma cells.

### 2.12.3 Nuclear RNA Isolation

#### 2.12.3.1 RNA Isolation for Crude Nuclei Fractions

To prepare nuclear RNA, the nuclear pellet from NP-40 lysis method was washed twice with 1 ml of ice-cold PBS, then 1 ml of GIT homogenization buffer (described previously) was added followed by vortexing for 15 sec to completely lyse the nuclei. The nuclear lysate was diluted with GIT homogenation buffer and layered over a 2 ml cushion of 5.7 M cesium chloride (CsCl) solution as described above. The gradient was centrifuged in a SW50.1 rotor at 45 K rpm for at least 20 hr at 20-24°C (Wilkinson *et al.*, 1988). The rest of the procedures were as the same as those for total RNA isolation.

#### 2.12.3.2 RNA Isolation for Purified Nuclei

##### 2.12.3.2.1 Solutions and Reagents

PBS (GIBCO)

Dulbecco's Phosphate-Buffered Saline,  
without CaCl<sub>2</sub> and MgCl<sub>2</sub> (GIBCO)

2 X Isotonic high salt lysis buffer	0.02 M	Tris-HCl, pH 8.4
	0.28 M	NaCl
	0.003 M	MgCl <sub>2</sub>
	1% (v/v)	Nonidet-P 40
	0.1%	DEPC water
2 X 0.88 M Sucrose	Dissolve 120.49 g Sucrose (MW 342.3 g/molar) in 200 ml 0.1% DEPC water at 65°C. Vigorously shake until dissolving.	
0.88 M Sucrose-Lysis buffer	Mix equal volume of 2 X lysis buffer with 2 X 0.88 M Sucrose	
2 M Sucrose	Dissolve 136.92 g Sucrose in 200 ml 0.1% DEPC water at 65°C.	
2 M Sucrose cushion	2M	sucrose
	5 mM	magnesium acetate
	0.1 mM	EDTA
	10 mM	Tris, pH 8.0
	1 mM	DTT

10% Tween 20	10 % (w/w) in 0.1% DEPC water	
10 X Tween-Doc	3.3% (v/v) of 10% sodium deoxycholate 6.6% (v/v) of 10% Tween 20	
DNase I buffer	0.5 M	NaCl
	0.05 M	MgCl <sub>2</sub>
	0.01 M	Tris-HCl, pH 7.4
	(Holtzman <i>et al.</i> , 1966)	

#### 2.12.3.2.2 Procedure

The following protocol was generated by modifying several protocols (Nevins, 1980; Birnie, 1978; and Penman, 1966).  $2.5 \times 10^7$  hybridoma cells were collected by centrifugation at 1,100 rpm and 4°C for 5 minutes. The pelleted cells were resuspended with 10 ml of ice-cold PBS (GIBCO BRL), transferred into a 15-ml polypropylene tube (17 X 100 mm culture tube, Gemini, Chicago, IL), and centrifuged again. The pellet of washed cells was suspended in 5 ml of ice-cold isotonic-high salt lysis buffer by pipetting the solution 10 times. The samples were incubated for 10 minutes on ice and vortexed gently for 5 seconds. One drop of the lysis solution was placed on a glass slide (25 X 75 mm, 1 mm, VWR Scientific, Media, PA) overlaid with a cover slide (18 mm square, VWR Scientific, Media, PA), and the nuclei were examined under the phase-contrast microscope (1,000 X, Biological Microscope, OPTIPHOT, Nikon Corporation, Tokyo,

Japan) to determine whether the cells were completely lysed and whether the cytoplasmic components are removed from the nuclei. If the majority of cells (95%) were lysed and there was no obvious cytoplasmic contamination to the nuclei, the homogenized nuclei solution was layered over 5 ml of 0.88 M sucrose-lysis buffer solution in a new 15-ml polypropylene tube, and the nuclei were purified by centrifugation at 800 X g (2750 rpm) (Silencer® S-103 NA) and 4°C for 10 min. Cell debris was found at the interface between the lysis buffer and 0.88 M sucrose solutions. The nuclei were found at the bottom of the tube after centrifugation. The lysis and sucrose solutions were removed phase by phase by aspiration without disturbing the nuclei. The nuclei pellet was resuspended very well by tapping vigorously with the hand and repetitive pipetting. In most cases, the pellet could not be dispersed very well. Thus it was digested with 50  $\mu$ l of RNase-free DNase I (40 units/ $\mu$ l, Promega) in 500  $\mu$ l DNase I buffer for 20 to 40 minutes at room temperature. 5 ml of lysis buffer and 500  $\mu$ l of Tween-Doc solution were then added, vortexed for 5 seconds and incubated on ice for 5 minutes. This mixture was overlaid with either 5 ml of 0.88 M sucrose-lysis buffer and centrifuged as described above, or 5 ml of 2 M sucrose cushion in a SW41 polyallomer tube (Nalgene™ UltraTubes, thin wall/polyallomer, open-top, size 14 X 98 mm, Nalge Company, Rochester, NY) and centrifuged at 25 K for 1 hour at 4°C (Preparative Ultracentrifuge, Model L8-70, Beckman, Palo Alto, CA). After purification of nuclei by centrifugation, a drop of the lysis solution was checked under the phase-contrast microscope to determine whether the nuclei were still intact and free of visible cytoplasmic contamination. The 0.88 M sucrose cushion centrifugation was repeated until no visible

cytoplasmic tab was attached to the pure nuclei. To remove the sucrose from nuclei preparation, the nuclei were washed twice with 1 ml of lysis buffer and the RNA isolated from nuclei by the GIT/CsCl method as described in section 2.12.3.2.

#### 2.12.4 Quantitation of RNA

The concentration of RNA was quantitated by measuring the absorption or optical density (OD) at 260 nm.

$$1 \text{ OD at } 260 \text{ nm} = 40 \mu\text{g/ml RNA}$$

The purity of RNA was determined by the ratio of the absorbance of RNA at 260 nm to its absorbance at 280 nm. My samples were in the range of 1.8 to 2.2. The typical yields of different cell lines are summarized in Table 1.



**Table 1. Average Yield of RNA Isolation**

Cell lines	RNA ( $\mu\text{g}/10^7$ )		
	Total	Cytoplasmic	Nuclear
<b>Ag8.653</b>	90 to 100	ND	ND
<b>J558L</b>	90 to 120	80 to 220	ND
<b>FH</b>	180 to 220	80 to 180	12 to 15
<b>VXH</b>	100 to 160	100 to 150	12 to 15
<b>CH2XH</b>	100 to 120	50 to 90	12 to 15

Values are determined from the results of several experiments  
 ND, not determined.

## 2.12.5 Northern Blot Analysis

### 2.12.5.1 Solutions

10 X MOPS	0.2 M	MOPS (sodium base)
	10 mM	sodium EDTA
	50 mM	sodium acetate
	0.1%	DEPC water
	Adjust pH to 7.0 with glacial acid	

5 X RNA loading buffer	1 X	MOPS
	2.5%	Ficoll
	0.025%	bromophenol blue
	0.1%	DEPC water

RNA sampling buffer	1 X	MOPS
	2.2 M	formaldehyde
	50%	deionized formamide (dFA)
	0.1%	DEPC water

Gel overlay buffer	1 X	MOPS
	2.2 M	formaldehyde
	0.1%	DEPC water

deionized formamide (dFA) formamide (Ultrapure, Boehringer Mannheim) was deionized with 5 g per 100 ml AG 501-X8(0) and Bio-Rex MSZ 501 mixed bed resins (Bio-Rad) by stirring very slowly at room temperature for about 1 hour, filtered through 0.45- $\mu$ m filter (Schleicher & Schuell) and stored at -20°C in aliquot.

50 X Denhardt's reagent	1%	bovine serum albumin
	1%	polyvinylpyrrolidone
	1%	Ficoll (DL-400)
	0.1%	DEPC water

1 M sodium phosphate buffer (NaP, pH 7.0, per liter)

200 ml of 1 M  $\text{NaH}_2\text{PO}_4$

600-700 ml of 1 M  $\text{Na}_2\text{HPO}_4$

fill to 1 L with deionized water

Prehybridization solution	0.1%	SDS
	50%	dFA
	5 X	SSC

	5 X	Denhardt's reagent
	50 mM	sodium phosphate buffer
	0.25 mg/ml	denatured sheared salmon sperm DNA (from 10 mg/ml stock solution)
Hybridization solution	0.1%	SDS
	50%	dFA
	5 X	SSC
	1 X	Denhardt's reagent
	20 mM	sodium phosphate buffer
	10%	Dextran sulfate
	0.3 mg/ml	denatured sheared salmon sperm DNA

#### 2.12.5.2 Procedure

5-10  $\mu\text{g}$  RNA (with 3  $\mu\text{g}$  of ethidium bromide per lane) was loaded in the sample wells of a formaldehyde agarose electrophoresis gel (1.2% agarose, 2.2 M formaldehyde, 1 X MOPS in 0.1% DEPC water) submerged in overlay buffer. RNA size markers (RNA ladder, GIBCO-BRL) were usually also run on the gels. The electrophoresis was performed in 1 X MOPS buffer in a horizontal gel electrophoresis chamber (Model H3, BRL) under a constant current of 10-15 mA (about 35-40 volts) for 15-20 hours until the

bromophenol blue migrated to the bottom of the gel. After capillary transfer of RNA onto a nitrocellulose filter (0.45  $\mu\text{m}$ , Schleicher & Schuell, Inc., Keene, NH) in 20 X SSC for overnight at room temperature, the blot was baked for 2 hours in 80°C vacuum oven (VWR 1410, VWR Scientific, San Francisco, CA). Hybridization was performed with an Omniblot system (ABN) according to the manufacturer's instructions. The prehybridization was performed in a 11 cm X 15 cm milliblot plastic bag (Millipore Corporation, Bedford, MA) at 42°C for at least 1 hour in a 21 ml mixture of 0.1% SDS, 50% deionized formamide, 5 X SSC, 5 X Denhardt's reagent, 50 mM sodium phosphate buffer (NaP, pH 7.0), and 5 mg of denatured sheared salmon sperm DNA (from 10 mg/ml stock solution). The radioactive DNA probe was denatured by boiling for 5 min and put immediately on ice. Once chilled, the probe was added to 15 ml hybridization solution containing 0.1% SDS, 50% dFA, 5 X SSC, 1 X Denhardt's reagent, 20 mM NaP, 10% dextran sulfate, and 1.5 mg denatured sheared salmon sperm DNA. Then the blot was hybridized with 1-2 X 10<sup>6</sup> cpm per ml of a denatured <sup>32</sup>P nick-translated  $\mu$  cDNA probe (covering the region between C $\mu$ 1 and part of C $\mu$ 4) for 12-18 hours at 42°C. The filter was washed consecutively with 2 X SSC and 0.1% SDS for 10 minutes once and with 0.1 X SSC and 0.1% SDS for 20-30 minutes at 55-60°C several times until the background detected by Geiger counter (Mini-Instrument, LTD., Model 900, Essex, England, through Research Products International Corp., Mount Prospect, IL) on the filter was low. After washing, the blot was dried briefly, and the position of RNA standards and ribosomal RNAs was labeled with radioactive ink. The blot was then wrapped with Saran wrap and exposed to X-ray film (Kodak X-OMAT™ AR or X-ONAR

LS, Eastman Kodak Company, Rochester, NY) between intensifying screens (Fisher Biotech, Pittsburgh, PA) for appropriate time at  $-70^{\circ}\text{C}$  before processed by Developer X-Ray Film Processor (Model QX-60A, Konica, Tokyo, Japan).

The amount of RNA on the blot was quantitated with a Betagen Radioanalytic imaging system (Betascope 603 Blot Analyzer, Betagen Corp., Mountain View, CA). The sizes of specific RNA bands were determined by measuring the distance from the loading well to each of the bands of RNA on the autoradiograph. The  $\log_{10}$  of the size of the fragments of standard RNA was plotted against the distance migrated. The resulting curve was used to calculate the sizes of the RNA species detected by hybridization. RNA size standard used was RNA Ladder (GIBCO-BRL) and ribosomal rRNAs (Rogers *et al.*, 1981).

To control for the copy number of active transcripts of plasmids in stable transfectants, Northern blots from stable transfection with  $\mu^{\text{gpt}}\Delta\text{M}$  plasmids, blots were stripped of hybridized DNA probe by washing them twice with boiled 0.1% SDS-0.1 X SSC, and subsequently rehybridized to a 1.055 kb of *HindIII-ApaI* fragment or a 1.335 kb of *PvuII-BamHI* fragment of *gpt* gene from pSV2 $\mu^{\text{gpt}}$ .2*XhoI* (SF#189). The relative amount of  $\mu$  mRNA per sample was calculated by dividing the amount of  $\mu$  mRNA by the amount of *gpt* mRNA from the same blot.

To control for RNA loading on each lane, Northern blots from hybridoma cell lines, the blots were rehybridized with a 1.3 kb *BamHI-EcoRI* fragment of rabbit GAPDH or a 1.918kb *HindIII-EcoRI* fragment of mouse  $\beta$ -actin probe.

### 2.12.6 mRNA Decay Rates Measured by Actinomycin C1 or DRB Treatment

Decay rates of individual mRNAs in different hybridoma cell lines were measured by two transcriptional inhibitors, Actinomycin C1 and DRB as described before (Jäck *et al.*, 1988). Briefly, cells were seeded in complete RPMI medium to a density of  $5 \times 10^5$  cells/ml, and preincubated for 1 hr at 37°C before addition of Actinomycin C1 (Boehringer Mannheim, Mannheim, Germany) or DRB (Calbiochem, San Diego, CA). The final concentration of Actinomycin C1 was 5  $\mu$ g/ml from a stock solution of 10 mg/ml in dimethyl sulfoxide (DMSO). The final concentration of DRB was 1.2 mM from a stock solution of 120 mM in DMSO. At 0, 4, and 8 hr, 20 ml (about  $10^7$ ) or 10 ml (about  $5 \times 10^6$ ) of cells were removed, centrifuged, and subjected to total RNA isolation by the GIT method and cytoplasmic RNA isolation by the NP-40/phenol method, respectively. Total viable cell counts at each time point were determined using 5  $\mu$ g/ml fluorescein diacetate (FDA) stain and a hemocytometer under a fluorescence microscope (630 X, Leica Photofluorescence Microscope, Leitz Wetzlar, Germany). This method is based on the principle that only living cells cleave diacetate from FDA, which releases the fluorescein molecule that can be visualized under the fluorescence microscope. The amount of mRNA left at each time point after the addition of the transcriptional inhibitor was determined by Northern blot analysis as described before. The absolute amount of radiolabeled probe hybridized to specific bands was quantitated on a Betascope Blot Analyzer (Betagen, Mountain View, CA) and normalized to the amount of  $\beta$ -actin mRNA. The efficiency of transcriptional inhibition was determined by rehybridizing the blot with H2b or c-myc probe, whose mRNA has a short half-life of 15 to 120-min (Old

and Woodlane, 1984; Dani *et al.*, 1984a; Herrick and Ross, 1994). Thus, I should not detect H2b or c-myc mRNA at 2 hr after the addition of the drug.

#### 2.12.7 DRB Titration Experiment

The DRB titration experiment was performed as following: *FH* cells were maintained in complete RPMI 1640 media. After counting, 2 ml of *FH* cells (at a density of  $5 \times 10^5$  cells/ml) were distributed into wells of 24-well Costar plate and kept for 1 hr at 37°C before addition of DRB (Calbiochem, San Diego, CA). The final concentration of DRB is 0, 0.12 mM, 0.24 mM, 0.48 mM and 0.96 mM, respectively, from a stock solution of 120 mM in dimethyl sulfoxide (DMSO, Sigma). At 0 and 4 hr, 2 ml (about  $10^6$ ) of cells were removed, centrifuged, and subjected to cytoplasmic RNA isolation by the NP-40/phenol method. Total viable cell counts at each time point and after overnight incubation were determined using 5  $\mu$ g/ml fluorescein diacetate (FDA) stain and a hemocytometer under a fluorescence microscope (630 X, Leica Photofluorescence Microscope, Model LABOVERT FS, Leitz Wetzlar, Germany). The amount of H2b mRNAs left at each time points after the addition of the transcriptional inhibitor were determined by Northern blot analysis. The absolute amount of radiolabeled probes hybridized to specific bands was quantitated on a Betascope Blot Analyzer (Betagen, Mountain View, CA) and normalized to the amount of GAPDH mRNA. The inhibitory effect of DRB on transcription was also determined by rehybridizing the blot with a  $^{32}$ P nick-translated 1 kb *Cla*I-*Sma*I human *c-myc* cDNA probe (Dr. Jeff Ross), whose mRNA is transcribed from a single copy gene and has a short half-life.



## 2.13 Analysis of Proteins

### 2.13.1 Immunofluorescence Analysis

To detect cytoplasmic proteins,  $1-5 \times 10^4$  cells in 200-300  $\mu\text{l}$  of RPMI 1640 media were centrifuged onto a glass slide at 1200 rpm for 3 minutes (Shandon centrifuge, London, England). After air-drying the pellets, cells were fixed in ethanol for 5 minutes, and rehydrated in PBSF solution (PBS - 0.1% bovine serum albumin - 0.1%  $\text{NaN}_3$ ) for at least 1 hr. The expression of transfected mouse heavy chain genes was detected by incubating the cells with 10  $\mu\text{l}$  of 1:20 diluted FITC-conjugated goat antibodies (50  $\mu\text{g}/\text{ml}$ ) specific for mouse heavy chain isotypes in a wet chamber for 10 minutes at room temperature (Burrows *et al.*, 1981). After mounting with Cytoseal (VWR Scientific, Media, PA), the fluorescence-labeled cells were examined under a fluorescence microscope (Leica Photofluorescence Microscope, Model LABOVERT FS, Leitz Wetzlar, Germany).

To detect membrane proteins,  $2 \times 10^6$  cells in suspension were incubated with fluorescein (FITC)-labeled goat anti-mouse IgM antibody for 20 minutes on ice. The cells were centrifuged and fixed onto a glass slide in absolute ethanol and overlaid with Cytoseal (VWR Scientific, Media, PA) as described above.

### 2.13.2 Metabolic Labeling and Immunoprecipitation

#### 2.13.2.1 Solutions and Reagents

RPMI labeling medium	500 ml	Methionine-free RPMI 1640
		(GIBCO)

50 ml Fetal calf serum (Hyclone)

10 ml 200 mM L-Glutamine(GIBCO)

0.5 ml 1 M Sodium pyruvate

5 ml 500 units/ml Penicillin-Streptomycin  
(GIBCO)

2.5 ml 10 mM  $\beta$ -mercaptoethanol

10 X NET

500 mM Tris base, pH 7.4

1.5 M NaCl

50 mM NaEDTA

1%  $\text{NaN}_3$

Store at  $-20^\circ\text{C}$

1 X NET/Triton (100 ml)

10 ml 10 X NET

2.5 ml 20% Triton X-100 in water

Store at  $-20^\circ\text{C}$

0.1 M PMSF

0.1 M in ethanol, store at  $-20^\circ\text{C}$

10 X NET lysis buffer

500 mM Tris base, pH 7.4

1.5 M NaCl

50 mM NaEDTA

	1%	NaN <sub>3</sub>
	0.5%	Triton X-100
	0.1 M	PMSF
10% <i>Staphylococcus aureus</i>		<i>S. aureus</i> in PBS and Azide
<i>S. aureus</i> wash buffer	50 mM	Tris, pH 8.2-8.5
	5 mM	EDTA
	0.5 mM	NaCl
	0.02%	NaN <sub>3</sub>
	0.1%	SDS
	0.5%	Triton X-100
	0.5%	NaDOC
	1 mM	methionine
		supplemented with 1 mg/ml ovalbumin (albumin chicken egg, Sigma)
SDS sampling buffer	0.0625 M	Tris-HCl, pH 6.8
	5%	β-mercaptoethanol
	2.5%	SDS
	0.002%	bromophenol blue
	10%	glycerol

### 2.13.2.2 Procedure

For continuous labeling,  $1-3 \times 10^6$  cells were starved for 1 hr in 1 ml methionine-free RPMI 1640 medium with 10% dialyzed FCS and then metabolically radiolabeled with 75  $\mu\text{Ci/ml}$  Trans- $^{35}\text{S}$  label (1076 Ci/mmol, ICN) for 30-180 min in 5%  $\text{CO}_2$  at 37°C. After washing, cells were lysed with NET lysis buffer supplemented with the protease inhibitor phenylmethylsulfonyl fluoride (PMSF, 1 mM) by incubating on ice for 20 minutes. Ig proteins were precipitated from cell culture supernatants and cell lysates with goat anti-mouse IgM ( $\mu$  heavy chain specific) (Southern Biotechnology Associates, Inc., Birmingham, AL). The incubation was carried out at 4°C shaker for 2-3 hours (sometimes overnight), followed by with formalin-fixed and heated-denatured 10% *S. aureus* that was prepared as described by Kessler (Kessler, 1975). The *S. aureus* pellets were washed in *S. aureus* wash buffer for 2 to 3 times and low salt washing buffer (50 mM Tris, pH=8.0) once (Burrow *et al.*, 1981). The washed precipitates were resuspended in equal volumes of SDS sample buffer, boiled for 3 minutes, cooled in a water bath to room temperature, and analyzed by 10% SDS-PAGE under reducing or nonreducing conditions as described below.

### 2.13.3 Protein SDS Polyacrylamide Gel Electrophoresis

#### 2.13.3.1 Solutions

40% Acrylamide/1.07% BIS	Solve 40 g acrylamide and 1.07 g bisacrylamide in about 90 ml water, heat slightly up to solve and make the volume to
--------------------------	---

100 ml. Filter sterilizes and store at 4°C in an aluminium foil-wrapped bottle.

3 M Tris, pH 8.8

Solve 72.7 g Tris in 170 ml water, pH to 8.8 with 5 N HCl and make the volume to 200 ml. Filter sterilizes and store at 4°C.

0.5 M Tris, pH 6.8

Solve 6.05 g Tris in 80 ml water, pH to 6.8 with 5 N HCl and make the volume to 100 ml. Filter sterilizes and store at 4°C.

10% APS

100 mg APS in an Eppendorf tube, add 1 ml water. Prepare fresh.

10 X Laemmli electrode buffer

0.25 M Tris

1.92 M Glycine

1% SDS

### 2.13.3.2 Procedure

The SDS polyacrylamide gel electrophoresis was carried out according to the method of Laemmli with modifications (Laemmli, 1970). Immunoprecipitated proteins from about  $10^6$  cells in sample buffer was loaded in each well. The separating gel was

made of 7.5-12.5% (w/v) acrylamide, 0.20-0.33% (w/v) N,N'-methylene bisacrylamide, 0.375 M Tris-HCl (pH 8.8), 0.1% (w/v) SDS, 0.1% (w/v) ammonium persulfate, 0.05% (v/v) TEMED. The stacking gel was made of 3.8% (w/v) acrylamide, 0.09% (w/v) bisacrylamide, 125 mM Tris-HCl (pH 6.8), 0.1% (w/v) SDS, 0.1% (w/v) ammonium persulfate, 0.05% (v/v) TEMED. The electrophoresis was run in a vertical slab gel electrophoresis unit (Hoefer Scientific, Model SE 600, San Francisco, CA) under a constant current of 10 mA/1.5 mm gel overnight, or 40 mA/ 1.5 mm gel for approximately 4-5 hours. The gels were fixed by shaking in 5% glacial acetic acid and 5% methanol for 30 min to 1 hour. The gel was incubated with Intensify solutions (EN<sup>3</sup>HANCE™ Autoradiography Enhancer, E.I. DuPont de Nemours & Co., Boston, MA): A for 40 minutes and solution B for 40 minutes with shaking at room temperature. The gel was then dried at 80 °C for 2 hours under vacuum in a slab gel dryer (Hoefer Scientific, Model SE 1160, San Francisco, CA). The dried gel was exposed to X-ray films (Kodak X-Omat OR) between 2 intensifier screens at -70 °C for appropriate time. Selected bands were quantitated by counting the radioactivity in dried gels with a Betascope blot analyzer.

## CHAPTER III

### IMMUNOGLOBULIN $\mu$ mRNA WITH A NONSENSE CODON IS DECREASED IN BOTH THE NUCLEUS AND THE CYTOPLASM OF PLASMA CELLS

#### 3.1 Characterization of the Cell Lines That Are Used in This Chapter

The 18-81 cell line is the Abelson-virus-transformed mouse pre-B cell line that synthesizes only H chain (as well as some that synthesize no Ig chain) (Alt *et al.*, 1982; Burrow *et al.*, 1981). The majority of cells synthesize  $\mu$  chain, while some cells can switch from  $\mu$  to  $\gamma 2b$  chain synthesis *in vitro* (Burrow *et al.*, 1983). The 18-81 cell line is diploid for the H chain loci (Burrows *et al.*, 1981) on chromosome 12 (Meo *et al.*, 1980). Both alleles have correctly joined VDJ segments, containing either a  $J_2$  or a  $J_3$  gene segment (Alt *et al.*, 1982; Burrow *et al.*, 1983). Thus the variable region alleles are named V2 and V3, respectively. Cells of the 18-81 line usually express only the V3 allele, because the V2 allele contains an amber nonsense codon in the  $C\mu 2$  exon (Alt *et al.*, 1982). However, a few cells continuously produce H Chain from both alleles by reversion of the amber nonsense codon (Wabl *et al.*, 1984; Jäck and Wabl, 1987).

In order to study the expression of  $\mu$  mRNA from a single allele, variants of the 18-81 cell line that have switched from  $\mu$  to  $\gamma 2b$  chain synthesis were fused with the myeloma P3X63-Ag8.653 (called Ag8.653 here after, which has lost its functional Ig genes) to generate hybridomas (Wabl and Burrows, 1984). This switch of heavy chain

from  $\mu$  to  $\gamma 2b$  is accompanied by a loss of DNA sequences between the joining region and  $\gamma 2b$  constant region gene segments, including the  $C\mu$  gene segments, on the V3 allele (Burrow *et al.*, 1983). However, all these cells retain the  $\mu$  gene without (*FH*) or with (*VXH* or *CH2XH*) a nonsense codon on the V2 allele (Jäck *et al.*, 1989). Thus, these hybridomas contain two alleles of Ig genes: the V2 allele expresses  $\mu$  transcript and the V3 expresses  $\gamma 2b$  transcript. The genomic configuration of endogenous  $\mu$  gene on the V2 allele in hybridomas used in this chapter is diagrammed in Figure 1. Hybridoma *FH* has a functional  $\mu$  gene that directs the synthesis of full-length  $\mu$  chain. Hybridoma *VXH* has an amber nonsense codon (TAG) in its diversity (D) segment of  $\mu$  gene, and *CH2XH* has an opal nonsense codon (TGA) in the  $C\mu 2$  exon of  $\mu$  gene. The gene dosage is approximately the same in the three hybridomas as determined by Southern blot analysis (Jäck *et al.*, 1989). One characteristic of the 18-81 cell line is that it has spontaneous deletions at the H chain locus at high rate (Jäck and Wabl, 1987). The spontaneous deletions in the largest  $J_H$ - $C\mu$  intron accumulate during growth in vitro (Alt *et al.*, 1982; Burrow *et al.*, 1983), and contribute to the different lengths of precursor  $\mu$  transcript in hybridomas *FH*, *VXH* and *CH2XH*. The sizes of these deletions were determined by Southern blot analysis (Figure 2B), and are depicted in Figure 1a.

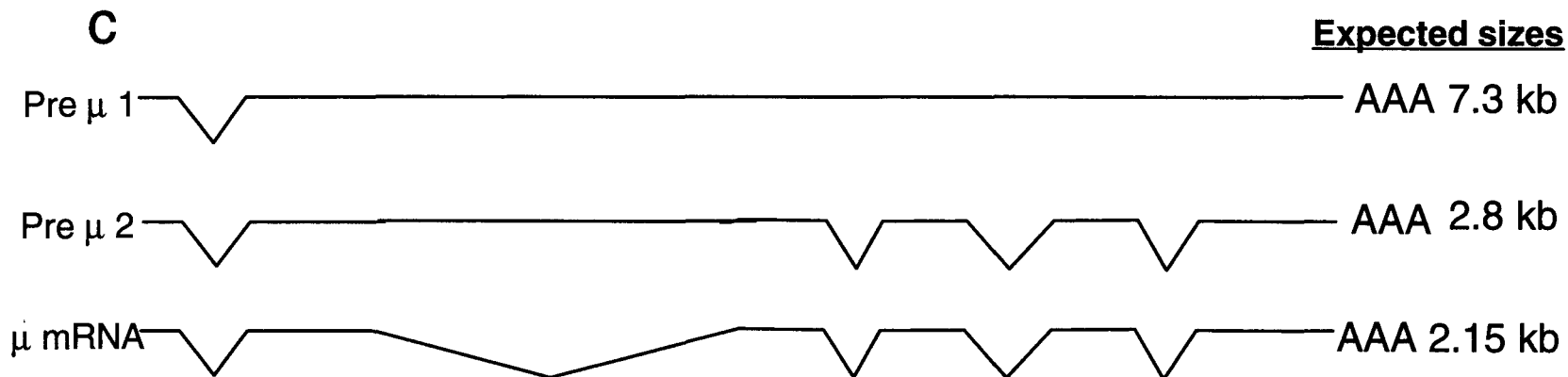
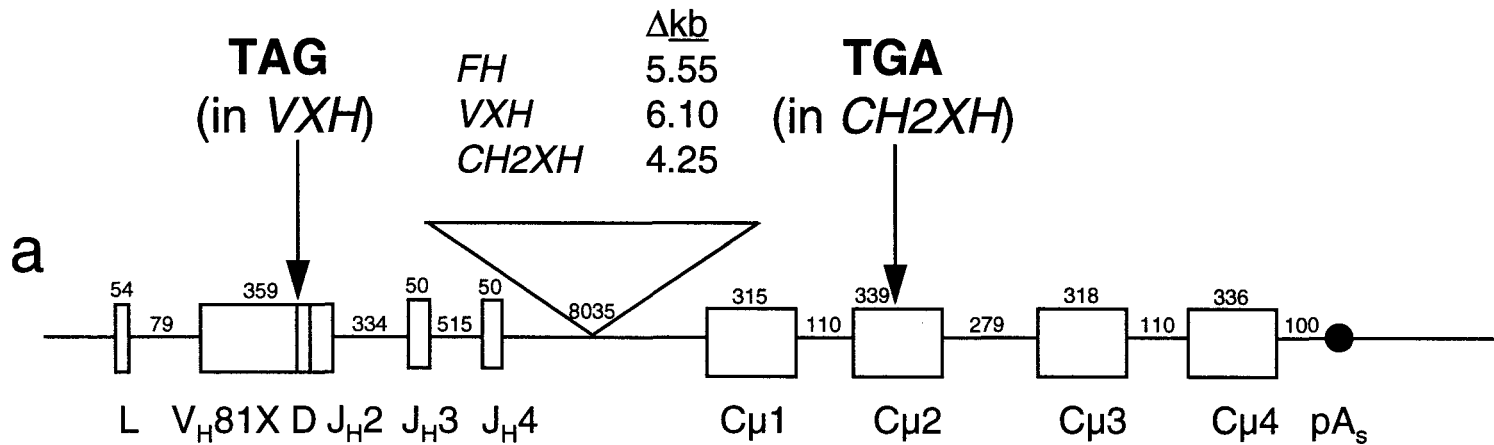
Since hybridomas are polyploid cells that often lose chromosomes and spontaneous deletions at Ig H chain locus occur at high rate, we subcloned all three hybridomas by limiting dilution just before using them in the experiments described below. The subclones were screened for the presence of the  $\gamma 2b$  (that is expressed from the V3 allele) by cytoplasmic immunofluorescence (CIF) using Texas Red-labeled goat



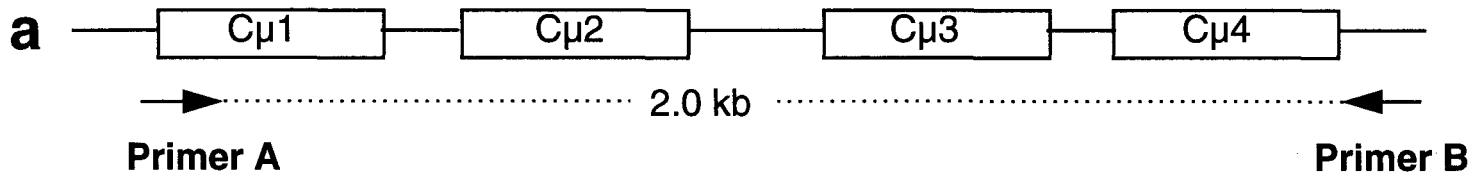
anti-mouse  $\gamma 2b$ . In the case of *FH* subclones, the expression of  $\mu$  chain was determined by CIF using FITC-labeled goat anti-mouse IgM antibodies. Since the  $\mu$  chain is not expressed in hybridomas *VXH* and *CH2XH* that contain nonsense codons in their  $\mu$  genes on the V2 allele (Figure 1a), the presence of the  $\mu$  gene in these hybridomas was determined by PCR using two sets of primers. Primer A and B amplified the genomic  $C\mu$  gene segments in the  $\mu$  gene, and the resulting products are revealed in Figure 2A. One subclone from the  $\mu$ -producing hybridoma *FH*, *FH.8*, was used as a positive control. As shown in panel b of Figure 2A, we identified seven subclones of *CH2XH* and five subclones of *VXH*, all of which contain the complete  $C\mu$  region of 2.0 kb (only visible on the original gel). The presence of variable region in all subclones was also confirmed by PCR using primers that are specific for the  $V_H$  exon (Beck-Engeser, unpublished result). These data suggest that  $V_H$  exon and the constant region of  $\mu$  genes are present in all subclones.

To determine the size of the large  $J_H-C\mu$  intron in the  $\mu$  gene, we isolated cellular DNAs from various subclones, digested them with different restriction enzymes, and analyzed the DNA fragments containing Ig gene segments using Southern blotting (Figure 2B). We found that  $\mu$  gene in *FH* had a deletion of 1.3 kb and  $\mu$  gene in *VXH* had a deletion of 1.85 kb when compared to the  $\mu$  gene in *CH2XH*. All these deletions are in the region of a 4.8 kb *HindIII* fragment in the large  $J_H-C\mu$  intron. However, the *CH2XH* itself was shown to have a deletion of 4.25 kb in this region (Wabl and Burrows, 1984). The sizes of these deletions were determined by Southern blot analysis (Figure 2B), and are depicted in Figure 1a.

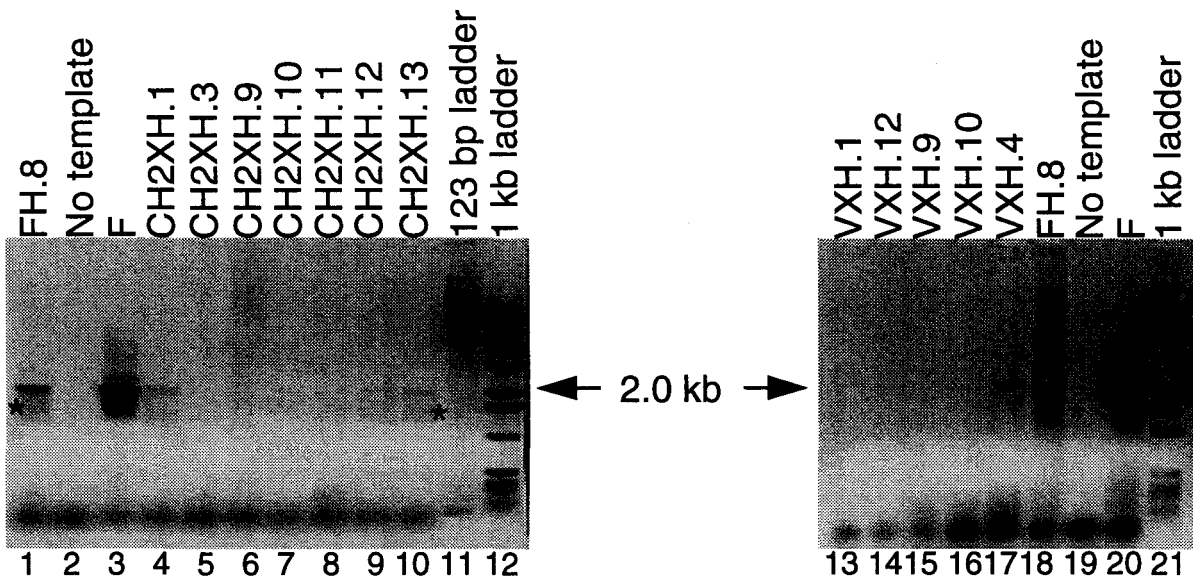
**Figure 1 Schematic Representations of DNA Structures, Hybridization Probes and  $\mu$  Transcripts.** (a) DNA structures of endogenous  $\mu$  genes in hybridomas that are used in this Chapter. For the V2 allele that has a completely assembled  $\mu$  gene, open boxed and interspersed lines designate, respectively, exons and introns of the mouse  $\mu$  gene in hybridoma *FH*. The numbers above indicate the size of respective exons and introns in base pairs (not drawn to scale). Arrows above the structure specify the sites at which spontaneous point mutations have generated nonsense codons in the  $\mu$  gene of hybridomas *VXH* and *CH2XH*. The variations of spontaneous deletions in the large  $J_H-C\mu$  intron as determined by Southern blot analysis (Figure 2B) have also been shown with an inverted triangle above the structure. (b) Bold lines represent the DNA probes used in the hybridizations. (c) Expected sizes of precursor and mature  $\mu$  transcripts. Pre, precursor transcript. TAG, an amber nonsense codon; TGA, an opal nonsense codon.



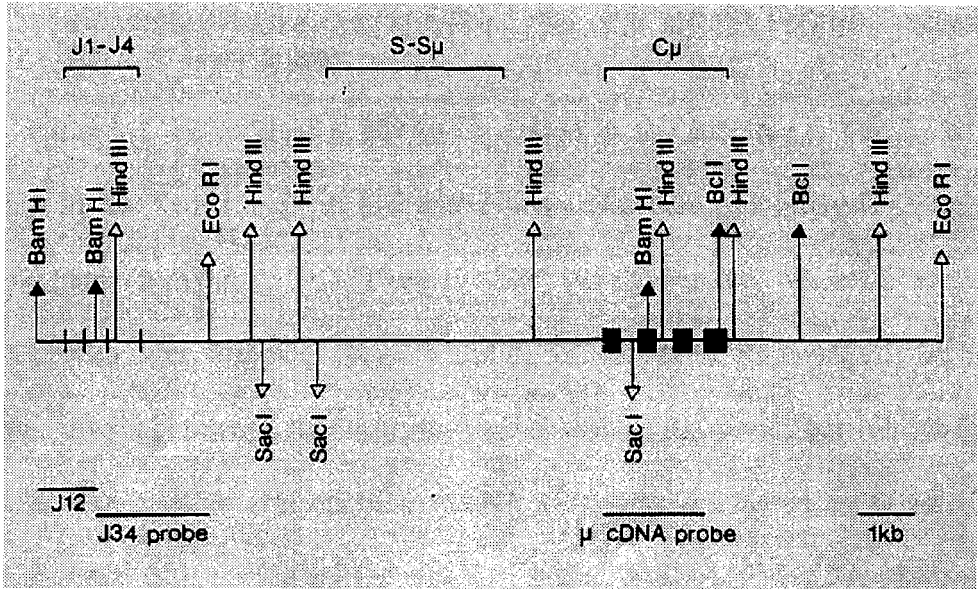
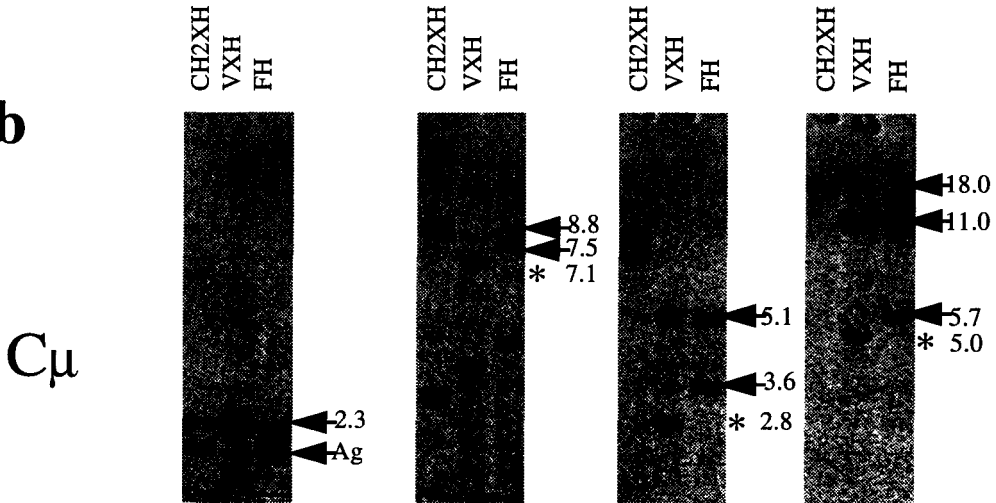
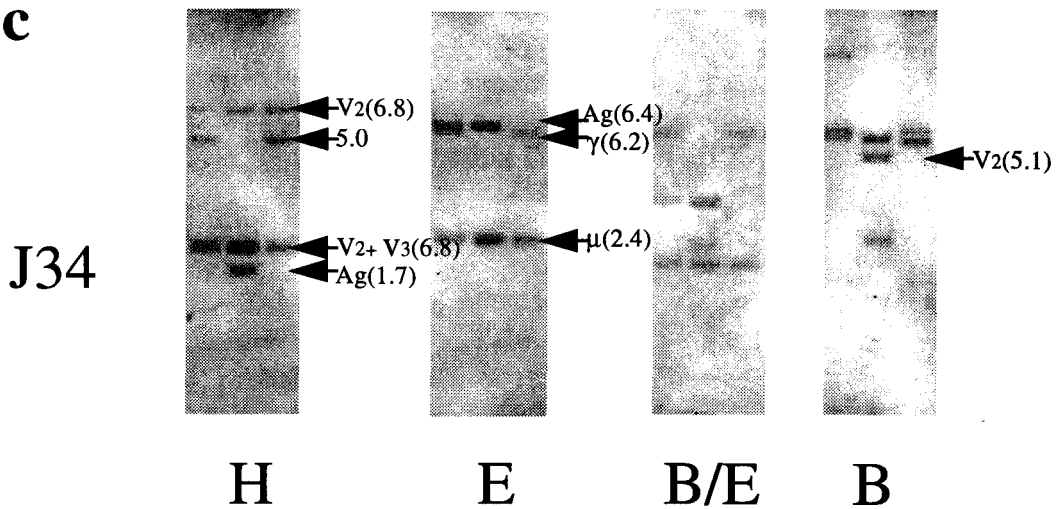
**Figure 2A PCR Analysis to Screen for the Presence of  $C\mu$  Gene Segments in Hybridoma Subclones.** (a) Schematic representation of the positions of primers A and B used in the PCR and the expected size of PCR product. (b) DNA isolated from  $2.5 \times 10^4$  cells of each subclone was amplified by PCR using 5' $C\mu$ 1. Forward (Primer A) and 3' $C\mu$ 4. Backward (Primer B) primers (For primer sequences, see section 2.2.1.2.1) for 35 cycles under the following conditions for each cycle: denaturation at 94°C for 20 seconds; annealing at 65°C for 1 minute; extension at 72°C for 1 minute. The resulting products were resolved by electrophoresis in a 1% TBE agarose gel and visualized by ethidium bromide staining. The  $C\mu$  gene segments (2.0 kb) were present in all sample lanes on the original gel, including lanes 5 to 8 and lanes 13 to 16 even though the bands are not visible in this figure. DNA isolated from *F* (the progenitor cell line) and *FH* (a hybridoma that contains a functional  $\mu$  gene) were used as positive controls. Asterisk (\*) indicates nonspecific priming products of PCR.



**b**



**Figure 2B Southern Blot Analysis to Identify the Deletion in the  $J_H$ - $C\mu$  Intron of  $\mu$  Gene on the V2 Allele.** (a) Restriction enzyme cleavage map of the embryonic DNA that contains the  $J_H$  and  $C\mu$  gene segments. The DNA probes used in the hybridizations are diagrammed below. (b and c) Southern Blot Analysis of the hybridomas. High molecular weight DNA was isolated from the various hybridomas, digested to completion with different restriction enzymes, electrophoresed in a 0.8% agarose gel and transferred to nitrocellulose filters. The filters were hybridized with a  $\mu$  cDNA probe (b), stripped and rehybridized with the J34 probe (c). The size of respective bands (in kb) was determined on a semi-logarithmic plot of the apparent size of standard DNA fragments versus their migration distance (indicated in kb). A copy of the autoradiogram (exposed for 2 weeks at  $-70^\circ\text{C}$ ) for  $C\mu$  hybridization was used in panel b because the original film is lost (as suggested by Dr. H.M. Jäck). The autoradiogram for J34 hybridization was exposed for 1 week at  $-70^\circ\text{C}$ . Ba, *Bam*HI; H, *Hind*III; E, *Eco*RI; Ag, Ag8.653 (the fusion partner).

**a****b****c**

### 3.2 Nonsense Codons Decrease the Level of $\mu$ mRNA but not Precursor $\mu$ RNA in Hybridomas

To determine the level of  $\mu$  RNAs expressed in the subclones, I isolated total cellular RNA by the Trizol method, and performed a Northern blot analysis using a  $C\mu$  cDNA probe (panel a in Figure 3A). The same blot was sequentially rehybridized to  $\gamma 2b$  and  $\beta$ -actin probes after stripping (panel b and c, respectively). Radioactivity of bands was determined by a betascope blot analyzer, which detects the counts per minute (cpm) of the bands. The relative amount of  $\mu$  mRNA ( $[\mu]$ ) was calculated by dividing the hybridization signal of  $\mu$  mRNA by the signal of  $\beta$ -actin mRNA. Table 2A summarizes the results of Figure 3A. I found that all subclones that contain  $\mu$  gene with nonsense codons produced less  $\mu$  mRNA than the subclone that expresses productive  $\mu$  gene (in hybridoma *FH.8*): subclones of hybridoma *VXH* produce about 30 fold less  $\mu$  mRNA, while subclones of hybridoma *CH2XH* produce about 125 fold less  $\mu$  mRNA. These values are the averages calculated from four different subclones in Figure 3A. The expression of  $\mu$  mRNA also varied within subclones of the same hybridomas (e.g. lane 7 to lane 10 in Figure 3A). The progenitor cell line 18-81 of the hybridomas acquires spontaneous deletions within the  $J_H$ - $C\mu$  intron during growth *in vitro* (Alt *et al.*, 1982b; Burrow *et al.*, 1983). Although the enhancer element in the  $J_H$ - $C\mu$  intron is not required for the a high level of H chain production (Wabl *et al.*, 1984), the deletion around this region (Figure 2B) still might be responsible for the variation of  $\mu$  mRNA expression in subclones in Figure 3A. The levels of  $\gamma 2b$  mRNA ( $[\gamma 2b]$  in Table 2A) also varied between subclones, probably for the same reason. From these data, I confirmed that the presence of a nonsense codon in the  $\mu$  gene decreases the steady-state level of  $\mu$  mRNA



in plasma cells.

In contrast to the decrease in the level of  $\mu$  mRNA with a nonsense codon, I found that the presence of a nonsense codon did not decrease the level of precursor  $\mu$  RNA ([pre  $\mu$ ] in Table 2A). Since the transcriptional rates for  $\mu$  gene with or without a nonsense codon are the same in hybridomas (Jäck *et al.*, 1989), this finding may result from the  $\mu$  mRNA with a nonsense codon in the plasma cell being degraded faster than  $\mu$  mRNA without a nonsense codon. Alternatively, the higher relative (rel) [pre  $\mu$ ] level may result from a nonsense codon preventing the splicing of precursor  $\mu$  RNA.

I also found that  $\mu$  RNAs (including precursor  $\mu$  RNA and  $\mu$  mRNA) in hybridomas *VXH* and *CH2XH* (lane 5' and 7', respectively in Figure 3A) had different gel mobility than  $\mu$  RNAs in hybridoma *FH* (lane 6' in Figure 3A). Possible mechanisms that account for the differences in gel mobility of  $\mu$  RNAs between hybridomas will be discussed and studied in detail in section 3.4.

Since the results of Northern blot analysis using total cellular RNA isolated by the Trizol method are sometimes not reproducible, I also isolated total cellular RNA by the conventional GIT/CsCl method, and quantified the levels of  $\mu$  RNAs by Northern blot analysis (Figure 3B). The results summarized in Table 2B are similar to those obtained by the Trizol method (Table 2A). The slower gel mobility of the precursor  $\mu$  RNA and  $\mu$  mRNA in hybridomas *VXH* and *CH2XH* than those in hybridoma *FH* is more obvious in Figure 3B than Figure 3A.

In summary, the presence of nonsense codons decreases the level of  $\mu$  mRNA of the total cellular fraction in hybridomas by about 30 fold in *VXH* and about 100 fold in

*CH2XH*, when compared to the wild-type  $\mu$  mRNA in hybridoma *FH*. Subclones *FH.8*, *VXH.10* (34 fold lower than *FH.8*, calculated from the average of two experiments from Table 3A and 3B) and *CH2XH.1* (76 fold lower than *FH.8*, calculated from the average of two experiments from Table 3A and 3B) were selected for further studies. Total cellular RNA will be only isolated by the GIT/CsCl method.

**Figure 3A Northern Blot Analysis of Total Cellular RNA Isolated from Various Subclones.** Total RNA from various subclones was isolated by the Trizol method. 5  $\mu$ g of RNA was loaded onto each lane, electrophoresed on a gel (1.2% agarose; 1 X MOPS; 2.2 M formaldehyde), and transferred onto a nitrocellulose filter. The filter was hybridized, stripped, and rehybridized sequentially with  $^{32}$ P-labeled DNA probes. The filter was then washed, dried and exposed at  $-70^{\circ}\text{C}$  to X-ray film between two intensifier screens. (a) Autoradiogram of the nitrocellulose blot that was hybridized with a  $C\mu$  cDNA probe, as indicated in Figure 1. Film was exposed for 18 hr at  $-70^{\circ}\text{C}$ . The diminished exposure (film exposure was for 18 hr at room temperature) of lanes 5, 6 and 7 is shown on the right in Figure 3.1 as lanes 5', 6', and 7'. (b) The same blot was stripped, and rehybridized with a  $\beta$ -actin probe to control for the amount of RNA loaded onto each lane. Film was exposed for 18 hr at room temperature. (c) The same blot was rehybridized with a  $\gamma 2b$  probe. Film was exposed for 24 hr at  $-70^{\circ}\text{C}$ . (d) Ethidium bromide staining of the same gel revealed the integrity and the positions of pre-rRNA and rRNA markers. RNA standards used to determine the sizes of RNAs: 28S rRNA, 5.0 kb; 18S rRNA, 1.84 kb (Rogers *et al.*, 1981). The 4.4 kb in lane 6' (panel a) is present in several Northern blot analyses, although its identity is unknown. The results of this figure are summarized in Table 3A.

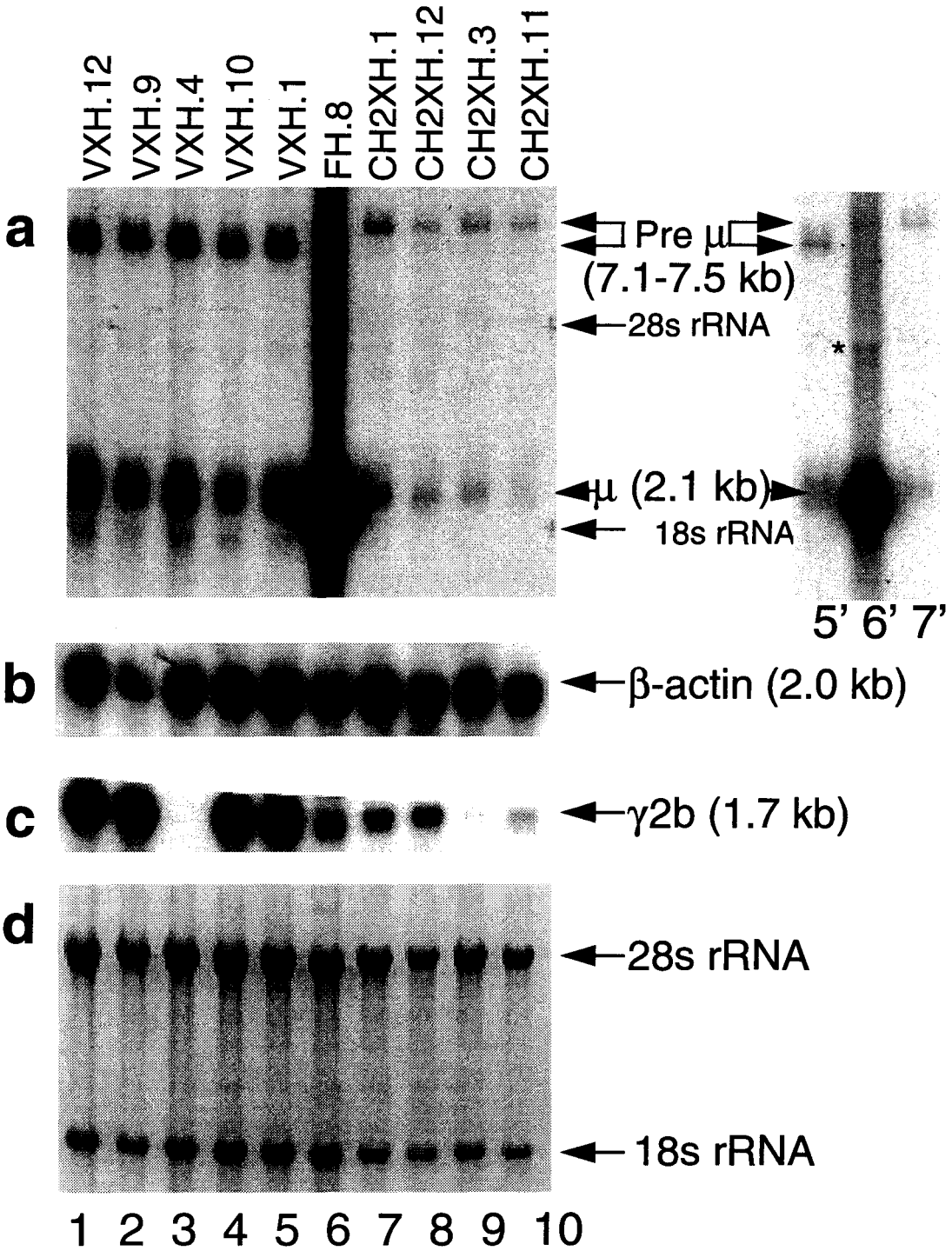


**Table 2A Quantitation of Northern Blot Analysis in Figure 3A**

Hybridomas	Method	RNA loaded	Pre $\mu$	$\mu$	$\gamma$ 2b	$\beta$ -actin	rel [pre- $\mu$ ] (pre- $\mu$ /actin)	rel [ $\mu$ ] ( $\mu$ /actin)	% [ $\mu$ ] %FH.8	[ $\gamma$ 2b] ( $\gamma$ 2b/actin)
			[cpm]							
FH.8	Trizol	5 $\mu$ g	4	1398.2	23.6	106.2	<0.1	13.2	<b>100%</b>	0.2
VXH.12	Trizol	5 $\mu$ g	22.5	63.5	124.9	110.2	0.2	0.6	4.4%	1.1
VXH.9	Trizol	5 $\mu$ g	19.2	32.6	108.7	34.8*				
VXH.10	Trizol	5 $\mu$ g	26.3	48.2	< 0.1	108.4	0.2	0.4	3.4%	<0.1
VXH.4	Trizol	5 $\mu$ g	19.5	22.7	125.8	124.8	0.2	0.2	1.4%	1.0
VXH.1	Trizol	5 $\mu$ g	24.5	65.7	135.6	149.6	0.2	0.4	3.3%	0.9
average								0.4	<b>3.1%</b>	
CH2XH.1	Trizol	5 $\mu$ g	8.2	30	16.8	132.9	0.1	0.2	1.7%	0.1
CH2XH.12	Trizol	5 $\mu$ g	3.7	6.8	15.3	74.1	<0.1	0.1	0.7%	0.2
CH2XH.13	Trizol	5 $\mu$ g	4.1	5.3	2.0	89.3	<0.1	0.1	0.5%	<0.1
CH2XH.11	Trizol	5 $\mu$ g	3.1	2.2	4.9	63.9	<0.1	0.0	0.3%	0.1
average								0.1	<b>0.8%</b>	

Radioactivity of respective bands (cpm) was determined by betascope scanning of Northern blot analysis. Relative steady-state level ([x]) of respective RNA was calculated by dividing cpm of band x by cpm of  $\beta$ -actin in the same lane. Background of respective bands have been subtracted.

%[ $\mu$ ] is the percent of [ $\mu$ ] relative to that of FH.8 by setting FH.8 value equal to 100%.

\* Value is not included in the calculation for average because  $\beta$ -actin hybridization is visibly not accurate.

**Figure 3B Northern Blot Analysis of Total Cellular RNA Isolated from Various Subclones.** Total RNA from various subclones was isolated by the GIT/CsCl method. 0.4  $\mu$ g of RNA from *FH* and 8  $\mu$ g of RNA from *VXH* and *CH2XH* were loaded onto each lane and Northern blot analysis was performed as described in Figure 3A using a  $C\mu$  probe (panel a, film was exposed for 4 days at  $-70^{\circ}\text{C}$ ), or a  $\beta$ -actin probe after stripping to control for the amount of RNA loaded onto each lane (panel b, film was exposed for 4.5 hr at  $-70^{\circ}\text{C}$ ), or a  $\gamma 2b$  probe to detect the expression of  $\gamma 2b$  mRNA (panel c, film was exposed for 18 hr at  $-70^{\circ}\text{C}$ ). In panel d, ethidium bromide staining of the agarose gel revealed the integrity and the positions of pre-rRNA and rRNA markers. Lane 7: Ag8.653 that does not express  $\mu$  mRNA was used as a negative control for  $\mu$  specific hybridization. The results of this figure are summarized in Table 3B. Asterisk (\*) indicates an unidentified band that is hybridized to the  $C\mu$  cDNA probe.

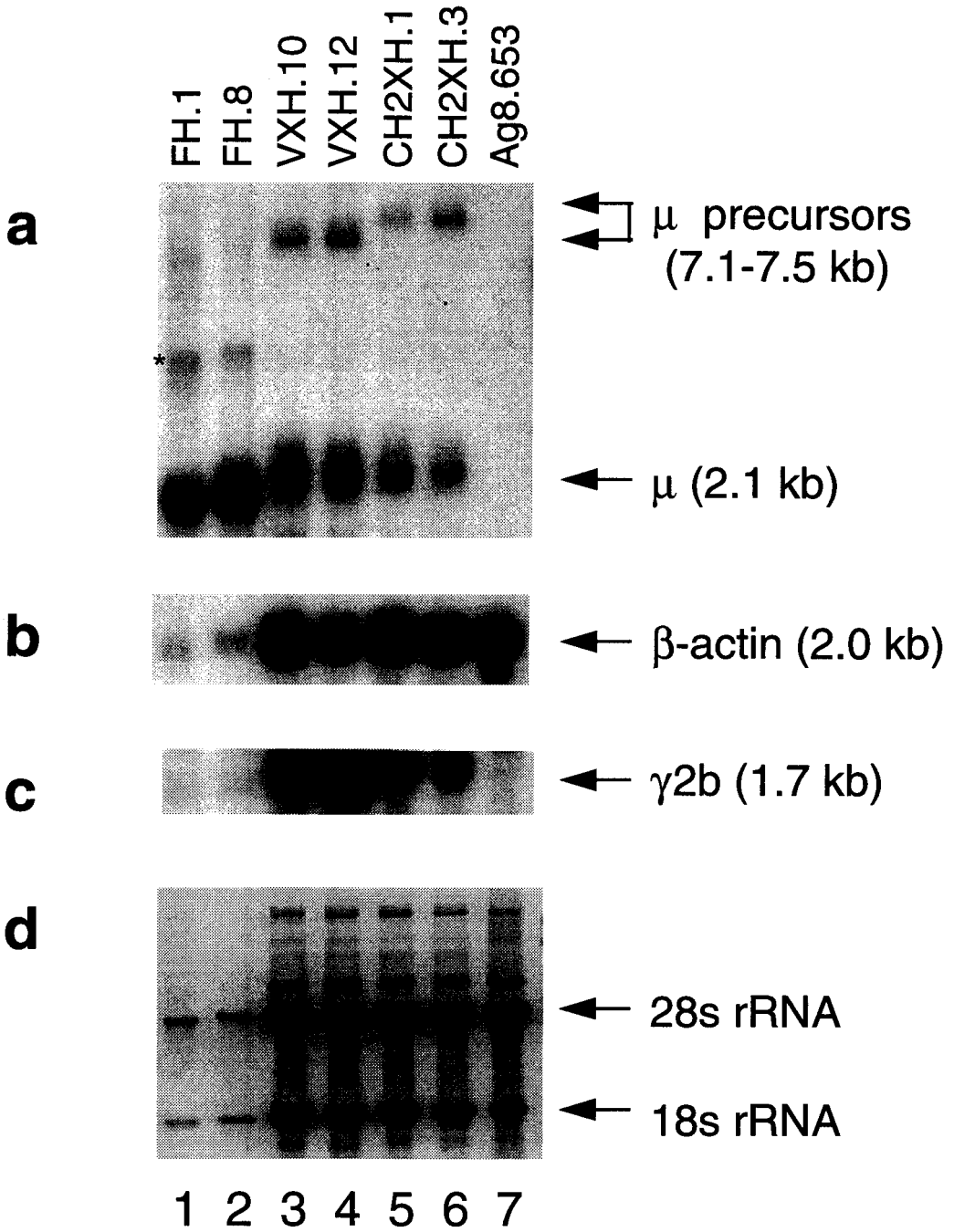


**Table 2B Quantitation of Northern Blot Analysis in Figure 3B**

Hybridomas	Method	RNA loaded	Pre $\mu$ RNA $\mu$ mRNA $\beta$ -actin mRNA			relative pre- $\mu$ (pre- $\mu$ /actin)	relative $\mu$ ( $\mu$ /actin)	relative $\mu$ (%)
			Pre $\mu$ RNA	$\mu$ mRNA	$\beta$ -actin mRNA			
FH.8	GIT	0.4 $\mu$ g	0.2	77.8	48.3	<0.1	1.6	<b>100.0%</b>
FH.1	GIT	0.4 $\mu$ g	1.1	40.6	29.0	<0.1	1.4	87.0%
VXH.12	GIT	8 $\mu$ g	4.6	25.5	425.3	<0.1	0.1	3.7%
VXH.10	GIT	8 $\mu$ g	3.8	27.4	717.2	<0.1	<0.1	2.5%
average						<0.1	<0.1	<b>3.1%</b>
CH2XH.1	GIT	8 $\mu$ g	2.7	8.0	536.3	<0.1	<0.1	0.9%
CH2XH.13	GIT	8 $\mu$ g	1.5	13.6	711.0	<0.1	<0.1	1.2%
average						<0.1	<0.1	<b>1.1%</b>



### 3.3 Nonsense Codons Reduce the Steady-state Level of $\mu$ RNA in the Nucleus

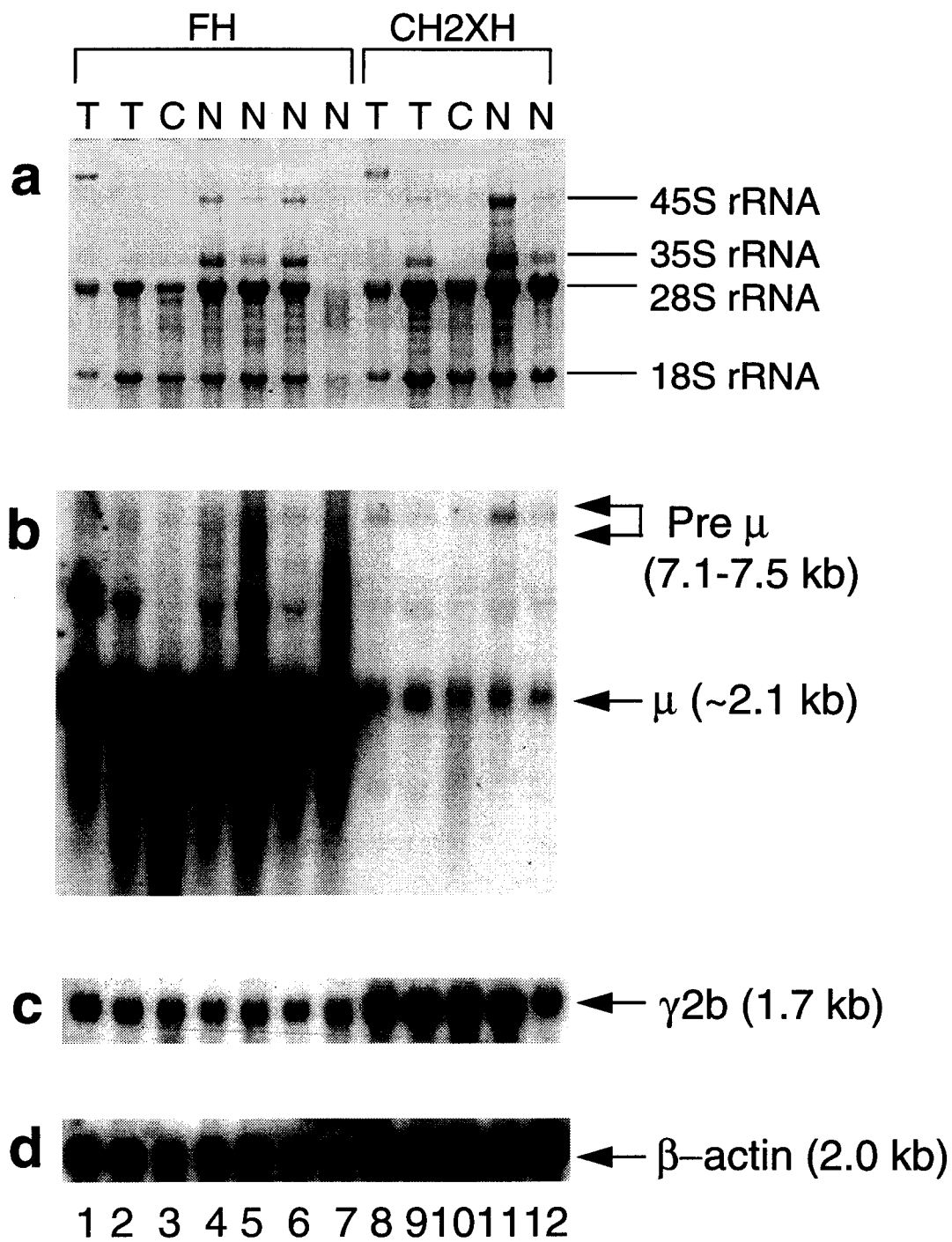
To determine whether the lower total steady-state level of  $\mu$  mRNA with a nonsense codon results from either cytoplasmic or nuclear RNA reduction, I isolated RNA from the nuclear and cytoplasmic fractions, and quantified the levels of  $\mu$  RNA in the two subcellular compartments by Northern blot analysis.

The isolation of nuclear RNA is a very difficult task, mainly because of its low abundance when compared with cytoplasmic RNA (Schibler *et al.*, 1978) and the technical difficulty in separating the nuclei from the endoplasmic reticulum in the cytoplasm. Endoplasmic reticulum binds the majority of cytoplasmic mRNA. Thus, I first compared several published methods to isolate nuclear RNA from hybridomas *FH* and *CH2XH*. Briefly, cell pellets from the lysate of NP-40-containing lysis buffer (the lysis buffer for cytoplasmic RNA isolation) were purified through 2 M sucrose cushion by either microcentrifugation or centrifugation, washed twice with PBS and taken as the crude nuclei. The nuclear RNA was isolated by either the GIT/CsCl or Trizol method, and quantified by Northern blot analysis (Figure 4). I found that the level of nuclear  $\mu$  mRNA was visibly lower in *CH2XH* (lane 11 and 12 in panel b) when compared to that of *FH* (lane 4 to 7 in panel b). Since cytoplasmic RNA is about nine fold more abundant than nuclear RNA (Schibler *et al.*, 1978), this lower steady-state level of nuclear  $\mu$  mRNA in *CH2XH* might result from either the nuclear  $\mu$  mRNA level being lower, or the nuclear RNA measured in Figure 4 reflects the steady-state level of cytoplasmic RNA that was contaminated with nuclei during nuclear RNA isolation. Thus, I needed to establish a reliable protocol to exclude cytoplasmic RNA contamination in the procedure

Figure 4

**Comparison of Methods to Isolate Nuclear RNA from Hybridomas *FH* and *CH2XH*.** Nuclei from *FH* and *CH2XH* were purified by either washing the pellets of NP-40 lysed homogenate twice with PBS (lane 5, 6, 7, and 12) or centrifugation through a 2 M sucrose cushion in a microcentrifuge tube (lane 4 and 11). Nuclear RNA was either isolated by the GIT/CsCl method (lane 5, 6, and 12) or the Trizol method (lane 4, 7, and 11). Total RNA was isolated by either the Trizol method (lane 1 and 8) or the GIT/CsCl method (lane 2 and 9). Cytoplasmic RNA was isolated by the NP-40/phenol method (lane 3 and 10). 5  $\mu$ g of RNA from *FH* or 10  $\mu$ g RNA from *CH2XH* was loaded onto each lane and Northern blot analysis was performed as described in the legend to Figure 3A. (a) Ethidium bromide staining of a representative gel shows the integrity and the positions of pre-rRNA and rRNA markers. The identity of rRNA precursors (45S and 35S) is suggested by the sizes of RNAs measured on the autoradiogram correlate with the published sizes of precursor rRNAs (Penman, 1966). (b) Autoradiogram (65 hr exposure) of the nitrocellulose blot that was hybridized with a  $C\mu$  cDNA probe. (c) The same blot was rehybridized with a  $\gamma 2b$  probe. Film was exposed for 24 hr at  $-70^{\circ}\text{C}$ . (d) After stripping, the same blot was rehybridized with a  $\beta$ -actin probe to control for the amount of RNA loading onto each lane. Film was exposed for 45 hr at  $-70^{\circ}\text{C}$ . T, total cellular RNA; C, cytoplasmic RNA; and N, nuclear RNA. Since the hybridomas *FH* and *CH2XH* used in this

experiment were not subcloned after a long time in culture, the amounts of  $\gamma 2b$  expression are different from those shown in Figure 3A.



of nuclear RNA isolation in order to evaluate the level of nuclear RNA. Since the use of microcentrifugation and the Trizol method did not generate reproducible results (Li and Jäck, unpublished results), I chose a 2 M sucrose cushion centrifugation method to purify the nuclei and the GIT/CsCl method to isolate nuclear RNA in future experiments.

Since the outer membrane of nuclei is continuous with the membrane of the endoplasmic reticulum in the cytoplasm (Arnstein and Cox, 1992), an efficient way to eliminate the cytoplasmic RNA contamination is to remove the outer nuclear membrane in the nuclear RNA isolation procedure. Thus I used ionic and nonionic detergents to remove the outer membrane of the nuclei (Nevins, 1980) and subsequently used 0.88 M (Birnie, 1978) or 2 M (Nevins, 1980) sucrose cushion centrifugation to remove the cytoplasmic RNA, polyribosomes, the outer membranes of nuclei and endoplasmic reticulum from the nuclei. As shown in Figure 5c by ethidium bromide staining of the agarose gel, I found that the rRNA precursors (45S and 35S) were enriched and the ratios of 28S rRNA to 18S rRNA were visibly increased in the nuclear RNA preparation of *FH* (lane 4 and 5). This suggested that the preparation was enriched in the nuclear fraction (Penman, 1966). The removal of cytoplasmic components was determined by phase-contrast microscopy after each step of nuclear RNA isolation. Representative photographs are shown in Figure 6. I found that there were no obvious cytoplasmic tabs in the examined fields after I purified the nuclei. I also attempted to examine the removal of outer nuclear membrane by electron microscopy (Holtzman, 1966) with the help of Dr. McNulty's laboratory. Due to the difficulty in counting enough nuclei to ensure their purity and DNase I-mediated disruption of the chromosome structure inside the nuclei,

I decided to use a novel approach to determine the removal of cytoplasmic components in nuclear RNA isolation.

As discussed above, one efficient way to ensure the purity of nuclear RNA is to eliminate all cytoplasmic components in the procedure of nuclear RNA isolation. Since the nuclear and cytoplasmic fractions of the same cell type contain the same type of RNAs, it is hard to distinguish the nuclear RNA from the cytoplasmic RNA. However, hybridoma *FH* expresses only the heavy chain but no light chain of Ig. Thus by mixing cytoplasmic RNA isolated from plasmacytoma *J558L* (that expresses only a lambda ( $\lambda$ ) light chain but no heavy chain) with the cell homogenate of hybridoma *FH*, I was able to determine whether my modified nuclear RNA isolation protocol can efficiently remove the exogenous cytoplasmic RNA. The main steps are illustrated in Figure 5A. Briefly, I mixed the cell homogenate from  $2.5 \times 10^7$  hybridoma *FH* (that expresses only  $\mu$  but no  $\lambda$  mRNA) with post-nuclear supernatant containing cytoplasmic RNA either in polyribosome-bound form or free mRNA form isolated from same number of cells of plasmacytoma *J558L* (that expresses only  $\lambda$  but no  $\mu$  mRNA). The mixture was then subjected to the nuclear RNA isolation procedure, and the amount of  $\lambda$  mRNA by Northern blot analysis was quantified by Northern blot analysis and betascope scanning. The extent of cytoplasmic RNA contamination was determined by comparing the signal of  $\lambda$  mRNA in nuclear RNA isolated from *FH* (lane 5 in Figure 5B, panel a) to the signal of  $\lambda$  mRNA in cytoplasmic RNA isolated from the same number of *J558L* cells (lane 6 in panel a of Figure 5B and Table 3A). The amount of nuclear  $\mu$  mRNA isolated from the mixture (lane 5 in panel b) was comparable to that of *FH* (lane 4 in panel b),

suggesting equal amounts of RNA were loaded in lane 4 and 5. These results are summarized in Table 3A. I found that the amount of cytoplasmic  $\lambda$  RNA contamination in nuclear RNA isolated from *FH* was 0.001% in the polyribosome-bound form of cytoplasmic RNA (experiment 2) and 0.009% in the free cytoplasmic mRNA form (experiment 1). Thus I concluded that the extent of cytoplasmic RNA contamination to the nuclear RNA isolation can be ignored in my modified protocol.

# Nuclear RNA Isolation Procedure

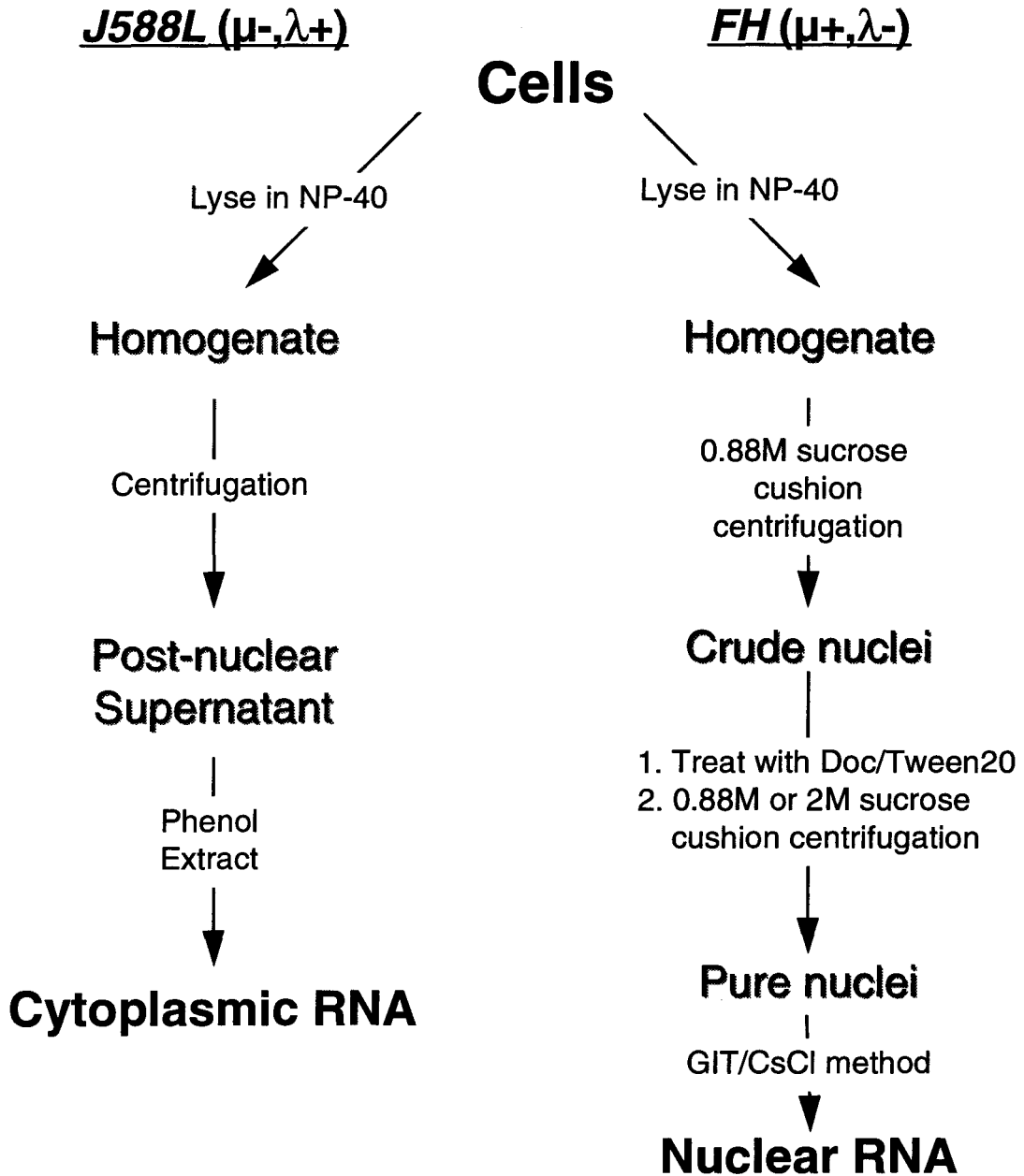




**Figure 5B      Quantitation of the Extent of Cytoplasmic mRNA Contamination in Purified Nuclei by Northern Blot Analysis.** Cell homogenate from  $2.5 \times 10^7$  hybridoma *FH* in 5 ml lysis buffer was mixed with either 5 ml post-nuclear supernatant (for the polyribosome-bound cytoplasmic RNA) or cytoplasmic RNA extract (for the free cytoplasmic RNA) isolated from the same number of cells of plasmacytoma *J558L*, and the mixture was subjected to the subsequent established nuclear RNA isolation procedure as described in section 2.12.3.2. 8  $\mu\text{g}$  of RNA was loaded onto each lane and Northern blot analysis was performed as described in the legend to Figure 3A. Table 3 summarizes the results of two independent experiments. (a) Autoradiogram of a representative nitrocellulose blot that was hybridized with a  $V\lambda 1$  probe. (b) The same blot was rehybridized with a  $C\mu$  cDNA probe to control for the amount of nuclear RNA (lane 4 and 5) loaded onto each lane of the blot. (c) Ethidium bromide staining of the gel revealed the amount of RNA loaded on the gel, and the integrity and positions of pre-rRNA and rRNA markers.

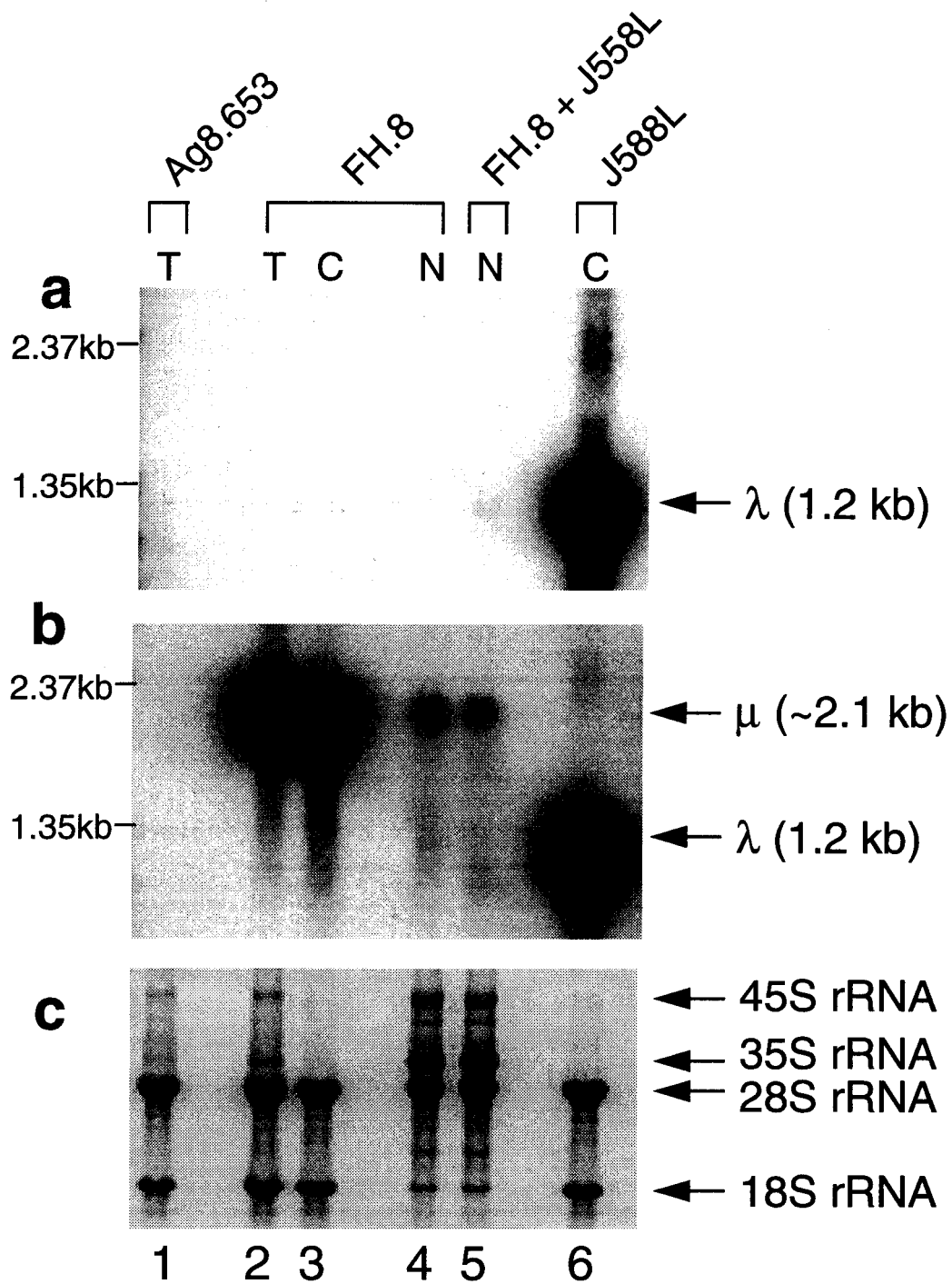


**Table 3 Quantitation of the Amount of Cytoplasmic RNA Contamination in the Purified Nuclei (Fig 5B)**

**Experiment 1**

Cell line RNA Isolation	FH			FH.Nuc+	J558L
	Total	Cytoplasmic	Nuclear	J558L.Cyto	Cyto
RNA loaded ( $\mu\text{g}$ )	8	8	8	8	8
Cell # ( $\times 10^5$ ) loaded	3.6	6.6	55.5	84.4	11.85
$\lambda_1$ mRNA (cpm)	<0.1	<0.1	0.2	2.5	1368.3
$\mu$ mRNA (cpm)	388.3	319.6	30.4	21.7	7.8
$[\lambda]$ ( $\lambda/\mu$ )			<0.1	0.1	175.4
$[\lambda]/10^5$ Cells			<0.1	<0.1	14.8
% $[\lambda]$ left			<0.1	<0.1	100.0

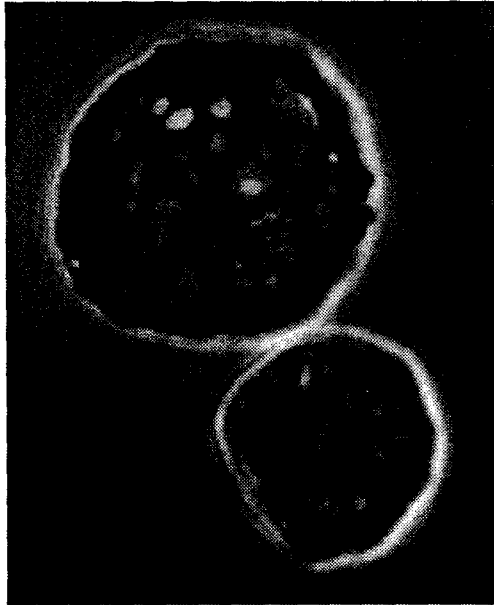
**Experiment 2**

Cell line RNA Isolation	FH			FH.Nuc +	J558L
	Total	Cytoplasmic	Nuclear	J558L.Cyto	C
RNA loaded ( $\mu\text{g}$ )	8	8	8	8	8
Cell # ( $\times 10^5$ )	3.6	10.2	57.0	67.0	10.0
$\lambda_1$ mRNA (cpm)	<0.1	<0.1	<0.1	3.7	1014.3
$\mu$ mRNA (cpm)	1681.7	1264.6	180.7	107.9	2.7
$[\lambda]$ ( $\lambda/\mu$ )			<0.1	<0.1	375.7
$[\lambda]/10^5$ Cells			<0.1	<0.1	37.6
% $[\lambda]$ left			<0.1	<0.1	100.0

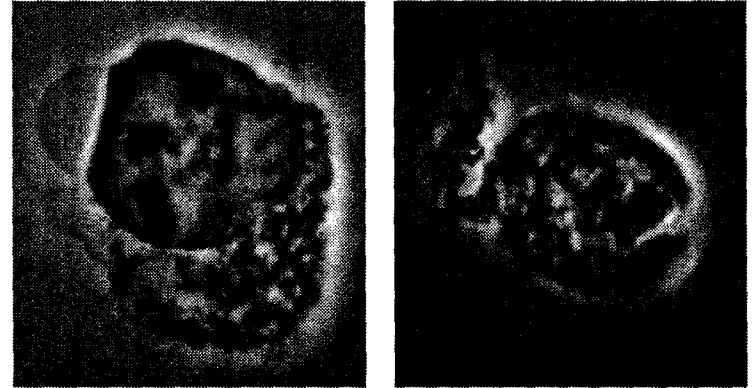
**Figure 6**      **Representative Photographs of Nuclei in the Nuclei Isolation Procedure.** Intact cells of hybridoma *FH* (in panel a) were lysed in 5 ml NP-40 lysis buffer, and the resulting cell homogenate was centrifuged through a 0.88 M sucrose cushion to isolate nuclei (termed "crude nuclei"). Only about 5% of the crude nuclei had visible cytoplasmic tabs (in panel b). The outer membrane of crude nuclei was removed by ionic and nonionic detergents and pure nuclei were purified by centrifugation through either a 0.88 M or a 2 M sucrose cushion as illustrated Figure 5A. None of the nuclei examined had visible cytoplasmic tabs. A representative picture is showed in panel c. All of the photographs were viewed at the same magnification (more than 100X).

# Representative Photographs of Nuclei in the Procedure of Nuclear RNA Isolation

**a**



**b**



**c**



By the established methods diagrammed in Figure 7, I isolated RNA from different compartments of hybridomas and analyzed the RNA by Northern blot analysis as revealed in Figure 8. The Northern blot was first hybridized to a  $C\mu$  cDNA probe (Figure 8b). The relative amounts of  $\mu$  mRNA in each lane (Figure 8b) were normalized to the levels of  $\beta$ -actin hybridization signal (Figure 8d). The steady-state levels of  $\mu$  RNA in each subcellular compartment (obtained from three Northern blot analyses of two independent RNA isolations) are summarized in Table 4 and illustrated in a bar graph (Figure 8f). I found that in both mutant hybridomas (*VXH* and *CH2XH*), the nuclear levels of nonsense codon-containing  $\mu$  mRNA (lane 7 and lane 10 in Figure 8, respectively; nuclear [ $\mu$ ] in Table 4) were decreased by about 7 fold as compared to the functional  $\mu$  mRNA in hybridoma *FH* (lane 4,  $p < 0.01$ ). This suggests that Ig mRNA with a nonsense codon starts to decrease in the nucleus. The same parameters as discussed before, such as the presence of enriched rRNA precursors and the increased ratio of 28S to 18S rRNA (Figure 8a) and the lack of visible cytoplasmic tabs to the purified nuclei as determined by phase-contrast microscopy (data not shown), were used to determine the removal of cytoplasmic components in the nuclear RNA isolation procedure. In addition, since mature histone mRNA is exported rapidly to the cytoplasm (Sun *et al.*, 1992), I should find the amount of H2b is lower in the nuclear fraction than in the cytoplasmic fraction of RNA isolations. Thus I rehybridized the Northern blot with a H2b probe and found the levels of H2b mRNA in nuclear fractions were low as predicted (lane 4, 7, and 10 in Figure 8e; H2b in experiment 2 of Table 4).

The presence of precursor  $\mu$  RNA in all fractions of hybridomas in Figure 8b was

verified by rehybridizing the blot with an intron probe (1.0 kb *Xba*I fragment of the IgH enhancer in the large J<sub>H</sub>-C $\mu$  intron) as shown in Figure 8c. The presence of precursor  $\mu$  RNA in the cytoplasmic fraction may result from the cytoplasmic RNA being contaminated with nuclear RNA during the isolation procedure. This possibility could not be ruled out by the lack of precursor 45S and 35S rRNAs in the RNAs isolated from the cytoplasmic fraction (lane 4, 7 and 10 in panel a of Figure 8), since the precursor rRNAs are processed in the nucleolus which is unlikely affected by the removal of nuclear membrane (Sommerville, 1986). However, the amount of nuclear Ig RNA is only about one ninth that of the cytoplasmic Ig RNA (Schibler *et al.*, 1978). Thus the cells loaded in lanes of cytoplasmic RNA were far less than those of the nuclear RNA. Therefore, the majority of precursor  $\mu$  RNA in Figure 8b and 8c should not have resulted from nuclear RNA contamination. Alternatively, the presence of precursor  $\mu$  RNA is a unique phenomenon in hybridoma cells used in this study. Usually unspliced precursor RNAs are not exported from the nucleus, presumably by the effect of spliceosome-retention (Legrain and Rosbash, 1989; Green, 1991). However, the transport of precursor RNA can be facilitated by some RNA-binding proteins. The best example is the Rev protein, which binds to a specific sequence in the precursor RNA of human immunodeficiency virus-1 and facilitates viral precursor RNA nuclear export (Malim *et al.*, 1989). The mechanism for the presence of precursor  $\mu$  RNA might also be mediated by a Rev like protein.

## A Flow Chart of RNA Isolation Procedures

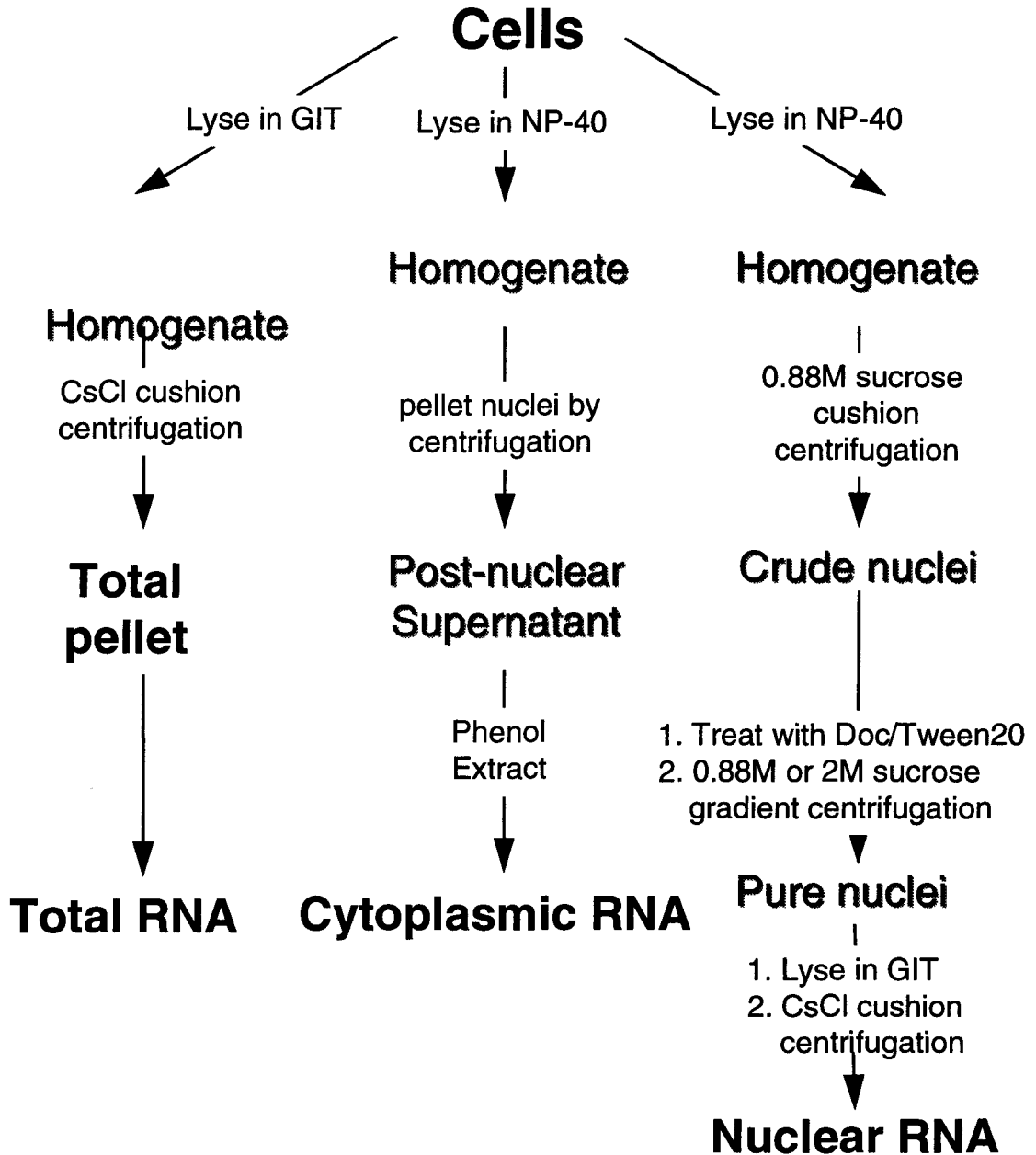




**Figure 8 Northern Blot Analysis to Quantify the Steady-state Levels of RNAs in Subcellular Compartments of Hybridomas.** Total RNA was isolated by the GIT/CsCl method (lane 1, 2, 5, and 8). Cytoplasmic RNA was isolated by the NP-40/phenol method (lane 3, 6, and 9). Nuclear RNA was isolated by established protocol as described in section 3.3.3.2 (lane 4, 7, and 10). 8  $\mu$ g of RNA was loaded on each lane and Northern blot analysis was performed as described in the legend to Figure 3A. Table 4 summarizes the results from three Northern blot analyses of two independent RNA isolations. (a) Ethidium bromide staining of a representative gel shows the amount of RNA loaded, and the integrity and positions of pre-rRNA and rRNA markers. (b) Autoradiogram (exposure time was 7 days at  $-70^{\circ}\text{C}$ ) of the nitrocellulose blot that was hybridized with a  $C\mu$  cDNA probe (as shown in Figure 1). The diminished exposure (16 hr) of *FH* RNA (lanes 2, 3, and 4) was shown on the right as lanes 2', 3', and 4'. (c) The identity of precursor  $\mu$  transcripts was verified by rehybridizing the blot with an intron probe in the large  $J_H$ - $C\mu$  intron (as illustrated in Figure 1b) after stripping. Film was exposed for 8 days. (d) The same blot was rehybridized with a  $\beta$ -actin probe after stripping to control for the loading of RNA. Film was exposed for 6 hr. (e) The same blot was rehybridized with a H2b probe to determine the level of H2b mRNA in different fractions of RNA isolation. Film was exposed for 3 days. Lane 1: Ag8.653 that expresses no  $\mu$  RNA was used as a negative

control for  $\mu$  specific hybridizations. By comparing RNA to RNA size markers (as indicated at left), I estimated the size of each RNA (as indicated at right). The mechanism for precursor  $\mu$  RNA present in the cytoplasmic fractions of hybridomas (lane 3, 6, and 9) is unknown. (f) A bar chart indicates the levels of  $\mu$  transcripts in subcellular compartments relative to the wild-type  $\mu$  RNAs in *FH*. The means and standard errors were calculated from the results of three Northern blot analyses of two independent RNA isolations and are listed in the summary tables in Table 4 (the levels of  $\mu$  RNAs for each experiment in *FH* is defined as 100%, see [ $\mu$ ] and [pre  $\mu$ ] in Table 4). \*:  $p < 0.01$  when compared to the control in *FH* (Newman-Keuls' multiple range test).

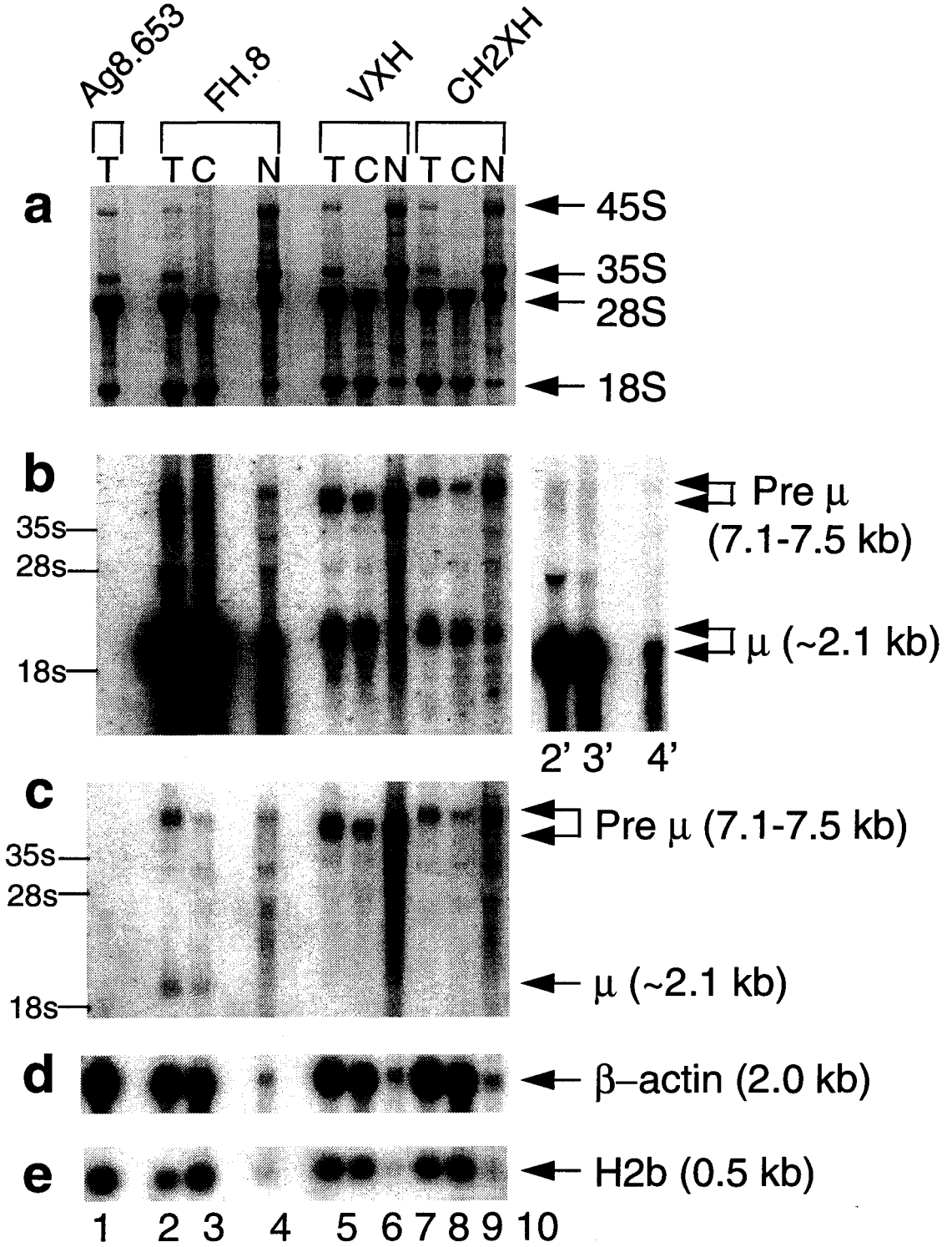


**Table 4. Steady-State Levels of RNA Transcripts**

**Experiment 1**

Hybridoma	RNA Loaded	$\mu$	$\text{pre } \mu^4$	$\text{enh}^4$	H2b	$\beta\text{-actin}$	$[\mu]^2$	$\%[\mu]^3$	$[\text{pre } \mu]^2$	$\%[\text{pre } \mu]^3$	[enh]	[H2b]
		[cpm] <sup>1</sup>					( $\mu/\text{actin}$ )	% FH.8	( $\mu/\text{actin}$ )	% FH.8		
<b>a. Total Cellular RNAs</b>												
<b>FH.8</b>	0.4 $\mu\text{g}$	70.6	N.D.	N.D.	N.D.	19.4	3.6	100.0		100.0		
<b>VXH.10</b>	8 $\mu\text{g}$	27.0	13.3	1.8	N.D.	403.2	0.1	1.8	<0.1		<0.1	
<b>CH2XH.1</b>	8 $\mu\text{g}$	10.4	5.9	0.9	N.D.	571.0	<0.1	0.5	<0.1		<0.1	
<b>b. Cytoplasmic RNAs</b>												
<b>FH.8</b>	0.4 $\mu\text{g}$	33.6	N.D.	N.D.	N.D.	15.0	2.2	100.0		100.0		
<b>VXH.10</b>	8 $\mu\text{g}$	21.4	8.4	1.1	N.D.	292.6	0.1	3.3	<0.1		<0.1	
<b>CH2XH.1</b>	8 $\mu\text{g}$	10.3	4.4	0.6	N.D.	470.0	0.0	1.0	<0.1		<0.1	
<b>c. Nuclear RNAs</b>												
<b>FH.8</b>	8 $\mu\text{g}$	54.0	4.8	N.D.	N.D.	23.7	2.3	100.0	0.2	100.0		
<b>VXH.10</b>	8 $\mu\text{g}$	9.7	17.7	2.2	N.D.	34.0	0.3	12.5	0.5	257.0	0.1	
<b>CH2XH.1</b>	8 $\mu\text{g}$	4.6	7.8	1.4	N.D.	30.5	0.2	6.6	0.3	126.3	<0.1	

1. Radioactivity of respective bands ([cpm]) was determined by a betascope blot analyzer.
2.  $[\mu]$  and  $[\text{pre } \mu]$  were calculated by dividing cpm of band  $\mu$  or  $\text{pre } \mu$  by cpm of  $\beta\text{-actin}$  in the same lane.
3.  $\%[\mu]$  and  $\%[\text{pre } \mu]$  are the percent of  $[\mu]$  and  $[\text{pre } \mu]$  of respective cell line related to those of FH.8
4.  $\text{pre } \mu$ , precursor  $\mu$ ;  $\text{enh}$ , enhancer.

**Table 4. Steady-State Levels of RNA Transcripts (Continued)**

**A. Experiment 2 (Figure 8)**

Hybridoma	RNA	$\mu$	pre $\mu^4$	enh <sup>4</sup>	H2b	$\beta$ -actin	$[\mu]^2$	% $[\mu]^3$	[pre $\mu]^2$	%[pre $\mu]^3$	[enh]	[H2b]
	Loaded	[cpm] <sup>1</sup>					( $\mu$ /actin)	% FH.8	( $\mu$ /actin)	% FH.8		
<b>a. Total Cellular RNAs</b>												
<b>FH.8</b>	8 $\mu$ g	174	2.6	1.9	5.0	497.9	0.3	100.0	<0.1	100.0	<0.1	<0.1
<b>VXH.10</b>	8 $\mu$ g	4.9	2.4	5.1	7.4	553.2	<0.1	2.5	<0.1	83.1	<0.1	<0.1
<b>CH2XH.1</b>	8 $\mu$ g	2.5	1.6	2.4	6.0	661.6	<0.1	1.1	<0.1	46.3	<0.1	<0.1
<b>b. Cytoplasmic RNAs</b>												
<b>FH.8</b>	8 $\mu$ g	58.9	1.4	0.6	9.5	414.1	0.1	100.0	<0.1	100.0	<0.1	<0.1
<b>VXH.10</b>	8 $\mu$ g	3.6	1.5	2.8	5.3	335.4	<0.1	7.5	<0.1	132.3	<0.1	<0.1
<b>CH2XH.1</b>	8 $\mu$ g	2.4	1.4	1.8	7.0	440.5	<0.1	3.8	<0.1	94.0	<0.1	<0.1
<b>c. Nuclear RNAs</b>												
<b>FH.8</b>	8 $\mu$ g	5.9	0.5	1.3	1.3	34.4	0.2	100.0	<0.1	100.0	<0.1	<0.1
<b>VXH.10</b>	8 $\mu$ g	2.2	3.5	7.7	1.1	64.8	<0.1	19.8	0.1	371.6	0.1	<0.1
<b>CH2XH.1</b>	8 $\mu$ g	1.5	2.4	3.6	1	44.3	<0.1	19.7	0.1	372.7	0.1	<0.1

1. Radioactivity of respective bands ([cpm]) was determined by a betascope blot analyzer.
2.  $[\mu]$  and [pre  $\mu$ ] were calculated by dividing cpm of band  $\mu$  or pre  $\mu$  by cpm of  $\beta$ -actin in the same lane.
3. % $[\mu]$  and %[pre  $\mu$ ] are the percent of  $[\mu]$  and [pre  $\mu$ ] of respective cell line related to those of FH.8
4. pre  $\mu$ , precursor  $\mu$ ; enh, enhancer.

**Table 4. Steady-State Levels of RNA Transcripts (Continued)**

**A. Experiment 3**

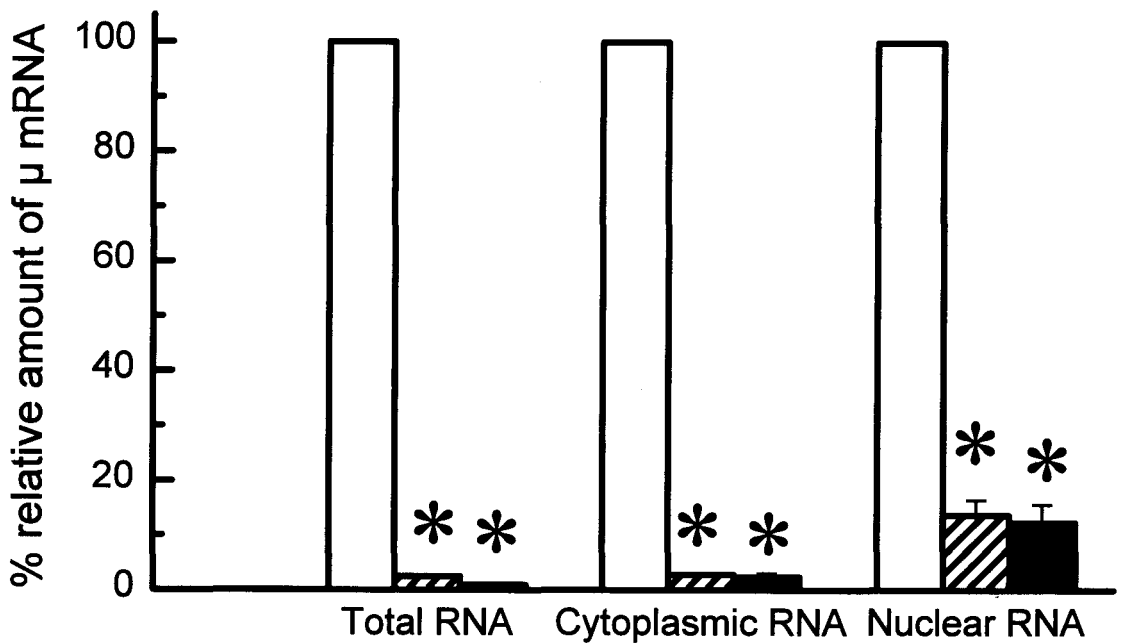
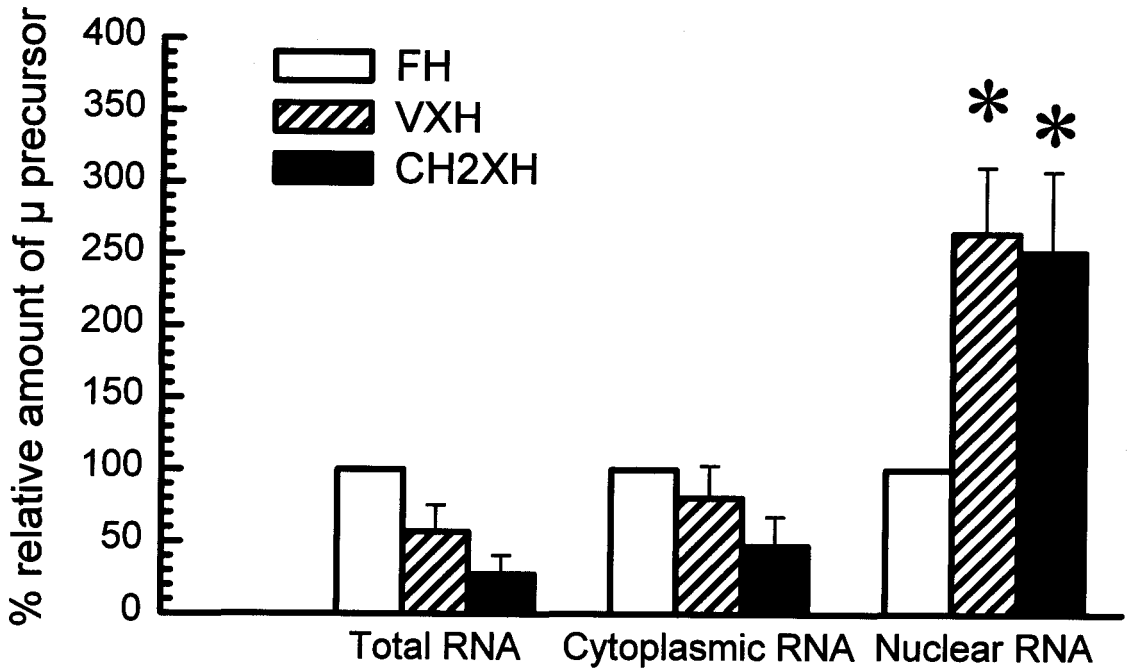
Hybridoma	RNA Loaded	$\mu$	pre $\mu^4$	enh <sup>4</sup>	H2b	$\beta$ -actin	$[\mu]^2$	% $[\mu]^3$	$[\text{pre } \mu]^2$	% $[\text{pre } \mu]^3$	[enh]	[H2b]
		[cpm] <sup>1</sup>					( $\mu$ /actin)	% FH.8	( $\mu$ /actin)	% FH.8		
<b>a. Total Cellular RNAs</b>												
<b>FH.8</b>	8 $\mu$ g	2186	84.1	N.D.	N.D.	656.5	3.3	100.0	0.1	100.0		
<b>VXH.10</b>	8 $\mu$ g	60.0	23.9	N.D.	N.D.	617.2	0.1	2.9	<0.1	30.2		
<b>CH2XH.1</b>	8 $\mu$ g	30.3	8.1	N.D.	N.D.	753.5	<0.1	1.2	<0.1	8.4		
<b>b. Cytoplasmic RNAs</b>												
<b>FH.8</b>	8 $\mu$ g	1696	27.4	N.D.	N.D.	461.5	3.7	100.0	0.1	100.0		
<b>VXH.10</b>	8 $\mu$ g	42.7	15.4	N.D.	N.D.	499.5	0.1	2.3	<0.1	51.9		
<b>CH2XH.1</b>	8 $\mu$ g	14.6	2.5	N.D.	N.D.	185.1	0.1	2.1	<0.1	22.7		
<b>c. Nuclear RNAs</b>												
<b>FH.8</b>	8 $\mu$ g	230.7	13.4	N.D.	N.D.	58.1	4.0	100.0	0.2	100.0		
<b>VXH.10</b>	8 mg	12.6	18.5	N.D.	N.D.	38.1	0.3	8.3	0.5	210.5		
<b>CH2XH.1</b>	8 mg	10.1	13.4	N.D.	N.D.	24.8	0.4	10.3	0.5	234.3		

1. Radioactivity of respective bands ([cpm]) was determined by a betascope blot analyzer.
2.  $[\mu]$  and  $[\text{pre } \mu]$  were calculated by dividing cpm of band  $\mu$  or  $\text{pre } \mu$  by cpm of  $\beta$ -actin in the same lane.
3. % $[\mu]$  and % $[\text{pre } \mu]$  are the percent of  $[\mu]$  and  $[\text{pre } \mu]$  of respective cell line related to those of FH.8
4.  $\text{pre } \mu$ , precursor  $\mu$ ;  $\text{enh}$ , enhancer.

### Summary of The Relative Steady-State Levels of $\mu$ RNA

	Total Cellular $\mu$			Cytoplasmic $\mu$			Nuclear $\mu$		
	FH.8	VXH.10	CH2XH.1	FH.8	VXH.10	CH2XH.1	FH.8	VXH.10	CH2XH.1
<b>Exp 1</b>	100.0	1.8	0.5	100.0	3.3	1.0	100.0	12.5	6.6
<b>Exp 2</b>	100.0	2.5	1.1	100.0	7.5	3.8	100.0	19.8	19.7
<b>Exp 3</b>	100.0	2.9	1.2	100.0	2.3	2.1	100.0	8.3	10.3
<b>Mean</b>	<b>100.0</b>	<b>2.4</b>	<b>0.9</b>	<b>100.0</b>	<b>4.4</b>	<b>2.3</b>	<b>100.0</b>	<b>13.5</b>	<b>12.2</b>
<b>SE</b>		0.3	0.2		2.8	1.4		5.8	6.8

# Quantitation of $\mu$ Transcripts in Subcellular Compartments





### 3.4 Cytoplasmic Decay Rates of $\mu$ mRNA With or Without a Nonsense Codon

Since cytoplasmic degradation could be an independent event from nuclear degradation, I further determined whether  $\mu$  mRNA with a nonsense codon is degraded in the cytoplasm of plasma cells in addition to the reduction observed in the nucleus. The cytoplasmic decay rates of  $\mu$  mRNA were measured using two transcriptional inhibitors (Actinomycin C1, Figure 9A and DRB, Figure 9B).

Actinomycin C1 is a transcriptional inhibitor that blocks all DNA-dependent RNA polymerases by binding to guanine-rich region of duplex DNA (Perry and Kelly, 1970). Although various effects of Actinomycin C1 on mRNA stability have been reported in the literature (Belasco and Brawerman, 1993), 5  $\mu$ g/ml of Actinomycin C1 was shown to almost completely inhibit the transcription in *FH* cell lines within an hour as measured by the [ $^3$ H] uridine incorporation into RNA (Jäck, 1988). Cytoplasmic RNA was isolated from the cells at 0, 4, and 8 hrs after addition of Actinomycin C1 to the culture. The levels of  $\mu$  mRNA left in the cells were determined by Northern blot analysis using a  $C\mu$  cDNA probe (Figure 9Aa). The amount of  $\mu$  mRNA was quantitated by a betascope blot analyzer. The size of GAPDH mRNA is smaller than  $\mu$  mRNA. Although the amount of GAPDH expressed in three different hybridomas is different, it remains the same within the same hybridomas. Thus GAPDH was used instead of  $\beta$ -actin as the control for RNA loading at different time points of the same hybridoma (panel b in Figure 9A). The results from three independent experiments are summarized in Table 5A. I found that the relative level of  $\mu$  mRNA ( $[\mu]$ ) with a nonsense codon decreased by about 1.5 fold in both *VXH* and *CH2XH* during the 8-hour drug treatment. In contrast, the relative level

of  $\mu$  mRNA without a nonsense codon was increased in the *FH* cell line during the 8-hour drug treatment. This increase probably occurs because GAPDH mRNA, which has a half-life of 8 hr (Dani *et al.*, 1984b), is less stable than functional  $\mu$  mRNA (that has a half-life of 13-34 hr) (Mason *et al.*, 1988; Cox and Emtage, 1989; Genovese and Milcarek, 1990). The almost undetectable amount of GAPDH at 8 hr after addition of Actinomycin C1 probably accounts for the two-phase decay rate of  $\mu$  mRNA in hybridoma *VXH*. Alternatively, *VXH* might be more sensitive to Actinomycin C1 treatment. At 4 hr and 8 hr after addition of the drug, rRNAs were degraded in hybridoma *VXH* as evidenced in lane 6 and 7 of panel e in Figure 9A. Thus it would be wise to isolate cytoplasmic RNA between time points 0 to 4 hr while the RNA in hybridoma *VXH* are not degraded.

DRB, an adenosine analogue, is a protein kinase inhibitor, which only blocks the initiation of RNA polymerase II-mediated transcription (Zandomeni *et al.*, 1983; Chodosh *et al.*, 1989; Dubois *et al.*, 1994). It does not influence the transcription of tRNA and rRNA (Zandomeni *et al.*, 1983). I used this drug as an alternative to measure the decay rate of  $\mu$  mRNA without or with a nonsense codon. Unlike Actinomycin C1, 0.12 mM of DRB was shown to inhibit only the transcription of mRNA but not rRNA in the *FH* cell line within an hour as measured by the [<sup>3</sup>H] uridine incorporation (Jäck, 1988). As shown in Figure 9B and summarized in Table 5B, the half-life of  $\mu$  mRNA with a nonsense codon was decreased from being relatively stable in *FH* to 3-4 hours in hybridomas *VXH* and *CH2XH* during 8 hour-treatment.

As time went by,  $\mu$  mRNA in hybridomas *VXH* and *CH2XH* migrated faster

through the gel (panel a in Figure 9A and 9B). The degradation of mRNA in eukaryotic cells is initiated by endonucleolytic cleavage, by shortening of the poly A tail, or by decapping. Among them, control of poly A tail length has an important effect on RNA degradation. For some mRNAs, decapping requires prior deadenylation (Jackson, 1993). Thus the progressive shortening of  $\mu$  mRNA as a result of ribonuclease digestion most likely results from  $\mu$  mRNA deadenylation. However, premature translational termination in yeast can trigger deadenylation-independent mRNA decapping (Muhlrad and Parker, 1994). Thus it is also possible that  $\mu$  mRNA with a nonsense codon is degraded by deadenylation-independent decapping mechanism.

The inhibitory effect of Actinomycin C1 or DRB on transcription in each experiment was evaluated by rehybridizing the same blot with probes that detected the mRNAs with short half-lives of 15 to 30 minutes, including Histone 2b (Old and Woodland, 1984) or c-myc (Dani *et al.*, 1984a; Herrick and Ross, 1994) (panel c and d, respectively, in Figure 9A and Figure 9B). I found that the levels of c-myc mRNA were visibly decreased with time in panel d of both Figure 9A and 9B, suggesting that the transcriptional inhibitors (Actinomycin C1 and DRB) efficiently blocked the transcription of mRNAs in each experiment. The differences in the size of c-myc mRNA in different cell lines are probably attributable to differential DNA rearrangements at the myc oncogene locus (Shen-Ong *et al.*, 1982). The amount of H2b mRNA decreased significantly after 4 hours of treatment with Actinomycin C1, which is consistent with the reported half-life of H2b mRNA as discussed above. Surprisingly, the amount of H2b mRNA was exceptionally stable after 8 hours of treatment with DRB.

**Figure 9A Northern Blot Analysis of Cytoplasmic Decay Rates of  $\mu$  RNA in Hybridomas by Using the Actinomycin C1 Method.** Cytoplasmic RNA was isolated from  $5 \times 10^6$  cells at 0, 4, and 8 hours after the addition of Actinomycin C1 ( $5 \mu\text{g/ml}$ ) to the culture, and analyzed by Northern blot analysis as described in the legend to Figure 3A. Table 5A summarizes the results from three independent RNA isolations. As time went by, the mRNAs migrated faster through the gel because they became progressively shorter as a result of ribonuclease digestion. Only the darkest band of  $\mu$  mRNA in each lane was quantified. (a) Autoradiogram (exposure time was 7 days at  $-70^\circ\text{C}$ ) of a representative nitrocellulose blot that was hybridized with a  $C\mu$  cDNA probe. (b) The same blot was rehybridized with a GAPDH probe to control for RNA loading onto each lane of the blot. Film was exposed for 10 days. The inhibitory effect of Act C1 on transcription in each experiment was determined by sequentially rehybridizing the blot with a H2b probe (panel c, exposure time was 15 hr) or a 1 kb *ClaI-SmaI* human c-myc cDNA probe (panel d, exposure time was 7 days). The virtual disappearance of H2b, c-myc mRNAs at 4 hr in lanes 2, 6 and 9 shows that they were degraded faster than  $\mu$  mRNA in *FH*. (e) Ethidium bromide staining of the gel revealed the integrity and positions of pre-rRNA and rRNA markers. Lane 4: Ag8.653 was used as a negative control for  $\mu$  specific hybridization.

# Cytoplasmic Decay Rates of RNAs (the Act C1 Method)

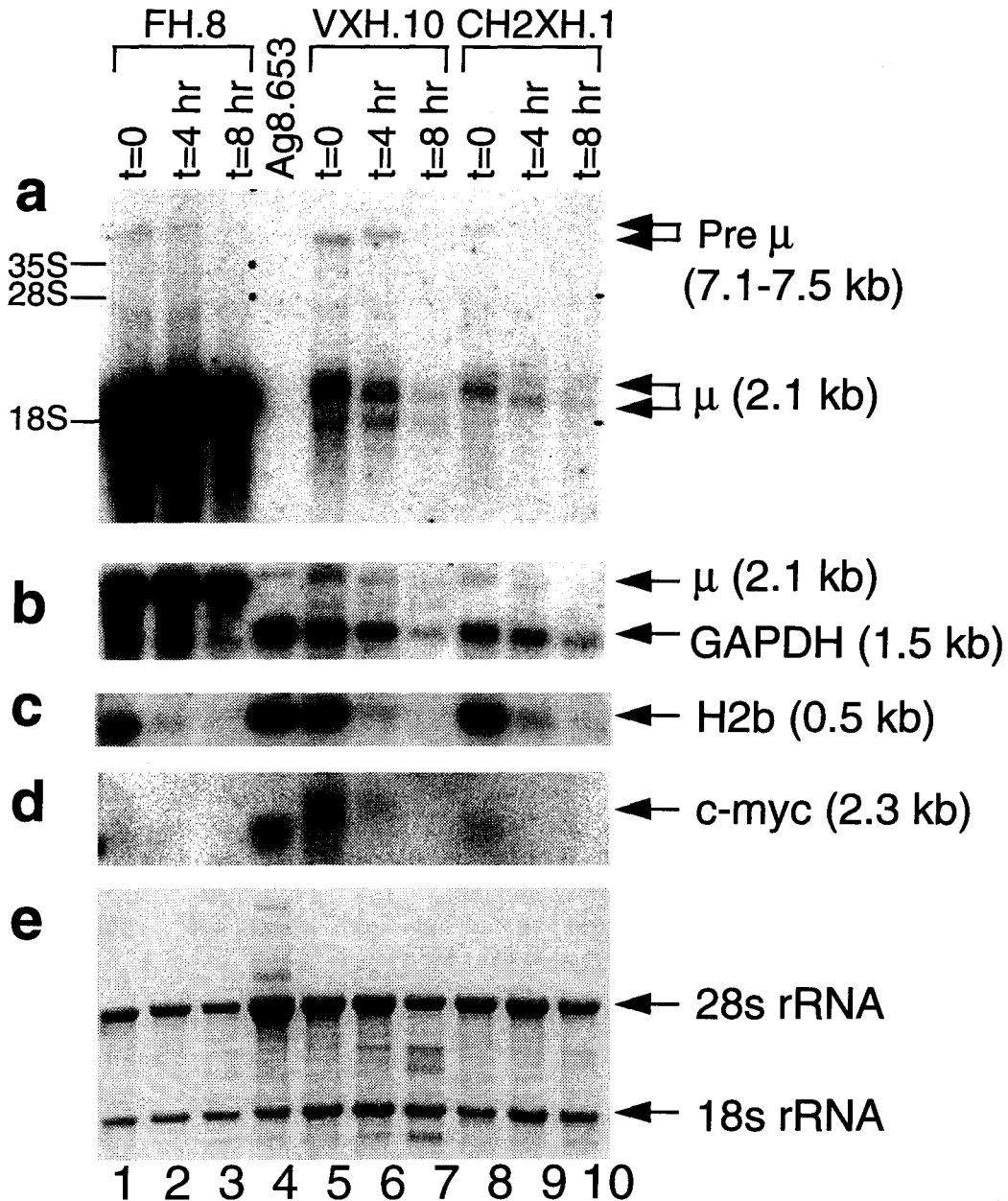


Table 5A. Cytoplasmic Decay Rates of RNAs (the Actinomycin C1 Method)

Hybridoma	Time (hr)	RNA Loaded	$\mu$	H2b c-myc GAPDH			[ $\mu$ ]	%[ $\mu$ ] %t=0	[H2b]	%[H2b] %t=0	
				$\mu$	[cpm]	[cpm]					
FH.8	t=0	Exp 1	4 $\mu$ g	262.4	12.1	0.9	5.0	52.5	100.0	2.4	100.0
		Exp 2	8 $\mu$ g	297.6	83.4	N.D.	31.2	9.5	100.0	2.7	100.0
		Exp 3	8 $\mu$ g	1041	161	N.D.	59.5	17.5	100.0	2.7	100.0
FH.8	t=4	Exp 1	4 $\mu$ g	289.1	1.2	0.2	4.5	64.2	122.4	0.3	11.0
		Exp 2	8 $\mu$ g	239.6	0.4	N.D.	20.8	11.5	120.8	<0.1	0.7
		Exp 3	8 $\mu$ g	924.2	35.2	N.D.	60.1	15.4	87.9	0.6	21.7
		mean							110.3		11.1
		SE						8.7		4.1	
FH.8	t=8	Exp 1	4 $\mu$ g	158.6	<0.1	0.1	1.7	93.3	177.8	<0.1	<0.1
		Exp 2	8 $\mu$ g	131.1	<0.1	N.D.	12.2	10.7	112.7	<0.1	<0.1
		Exp 3	8 $\mu$ g	443.5	17.6	N.D.	27.5	16.1	92.1	0.6	23.7
		mean							127.5		7.9
		SE						19.3		6.1	
VXH.10	t=0	Exp 1	8 $\mu$ g	14.5	26.8	3.0	7.1	2.0	100.0	3.8	100.0
		Exp 2	8 $\mu$ g	9.7	168	N.D.	39.9	0.2	100.0	4.2	100.0
		Exp 3	8 $\mu$ g	6.4	155	N.D.	15.2	0.4	100.0	10.2	100.0
VXH.10	t=4	Exp 1	8 $\mu$ g	7.0	2.2	1.4	4.7	1.5	72.9	0.5	12.4
		Exp 2	8 $\mu$ g	2.9	21.8	N.D.	19.6	0.1	60.9	1.1	26.4
		Exp 3	8 $\mu$ g	3.7	39.3	N.D.	18.8	0.2	46.7	2.1	20.6
		mean							60.2		19.8
		SE						5.2		2.8	
VXH.10	t=8	Exp 1	8 $\mu$ g	1.7	<0.1	0.7	0.6	2.8	138.7	<0.1	<0.1
		Exp 2	8 $\mu$ g	1.5	13.8	N.D.	7.6	0.2	81.2	1.8	43.1
		Exp 3	8 $\mu$ g	2.3	24.0	N.D.	9.3	0.2	58.7	2.6	25.4
		mean							92.9		22.8
		SE						17.6		8.8	
CH2XH.1	t=0	Exp 1	8 $\mu$ g	4.9	23.3	2.3	3.3	1.5	100.0	7.1	100.0
		Exp 2	8 $\mu$ g	7.7	149	N.D.	22.6	0.3	100.0	6.6	100.0
		Exp 3	8 $\mu$ g	6.8	95.1	N.D.	17.2	0.4	100.0	5.5	100.0
CH2XH.1	t=4	Exp 1	8 $\mu$ g	2.7	3.0	0.6	2.6	1.0	69.9	1.2	16.3
		Exp 2	8 $\mu$ g	2.4	14.7	N.D.	7.9	0.3	89.2	1.9	28.1
		Exp 3	8 $\mu$ g	2.7	47.7	N.D.	15.7	0.2	43.5	3.0	54.9
		mean							67.5		33.1
		SE						9.3		8.4	
CH2XH.1	t=8	Exp 1	8 $\mu$ g	1.4	<0.1	0.3	1.2	1.2	78.6	<0.1	<0.1
		Exp 2	8 $\mu$ g	0.8	13.6	N.D.	4.2	0.2	55.9	3.2	49.0
		Exp 3	8 $\mu$ g	1.5	45.2	N.D.	8.0	0.2	47.4	5.7	102.2
		mean							60.6		50.4
		SE						6.9		19.9	

**Figure 9B Northern Blot Analysis of Cytoplasmic Decay Rates of  $\mu$  RNA in Hybridomas Using the DRB Method.** Cytoplasmic RNA was isolated from  $5 \times 10^6$  cells at 0, 4, and 8 hours after the addition of DRB (0.12 mM) to the culture. 4  $\mu$ g of RNA from *FH* and 8  $\mu$ g of RNA from *VXH* and *CH2XH* were loaded onto each lane and Northern blot analysis was performed as described in the legend to Figure 9A. Table 5B summarizes the results from three independent RNA isolations. As time went by, the mRNAs migrated faster through the gel because they became progressively shorter as a result of ribonuclease digestion. Only the darkest band of  $\mu$  mRNA in each lane was quantified. (a) Autoradiogram (exposure time was 7 days) of a representative nitrocellulose blot that was hybridized with a  $C\mu$  cDNA probe. (b) The same blot was rehybridized with a GAPDH probe to control for the amount of RNA loaded onto each lane of the blot. Film was exposed for 8 days. The inhibitory effect of DRB on transcription in each experiment was determined by sequentially rehybridizing the blot with an H2b probe (panel c, exposure time was 15 hr) or a c-myc probe (panel d, exposure time was 8 days). The virtual disappearance of H2b, c-myc mRNAs at 4 hr in lane 2 shows that they were degraded faster than  $\mu$  mRNA in *FH*. (e) Ethidium bromide staining of the gel revealed the integrity and positions of pre-rRNA and rRNA markers. Lane 4: Ag8.653 was used as a negative control for  $\mu$  specific hybridization.

# Cytoplasmic Decay Rates of RNAs (the DRB Method)

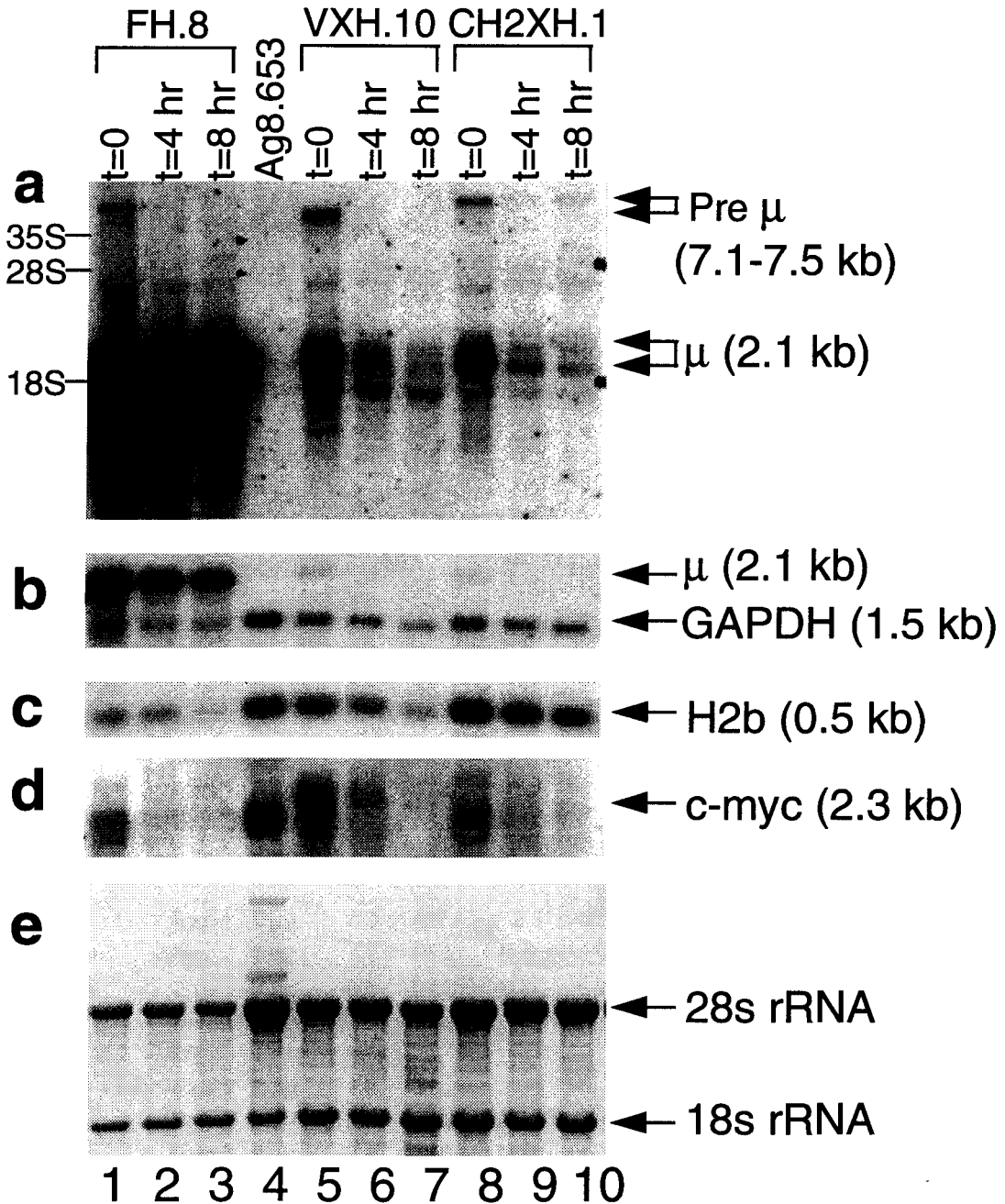




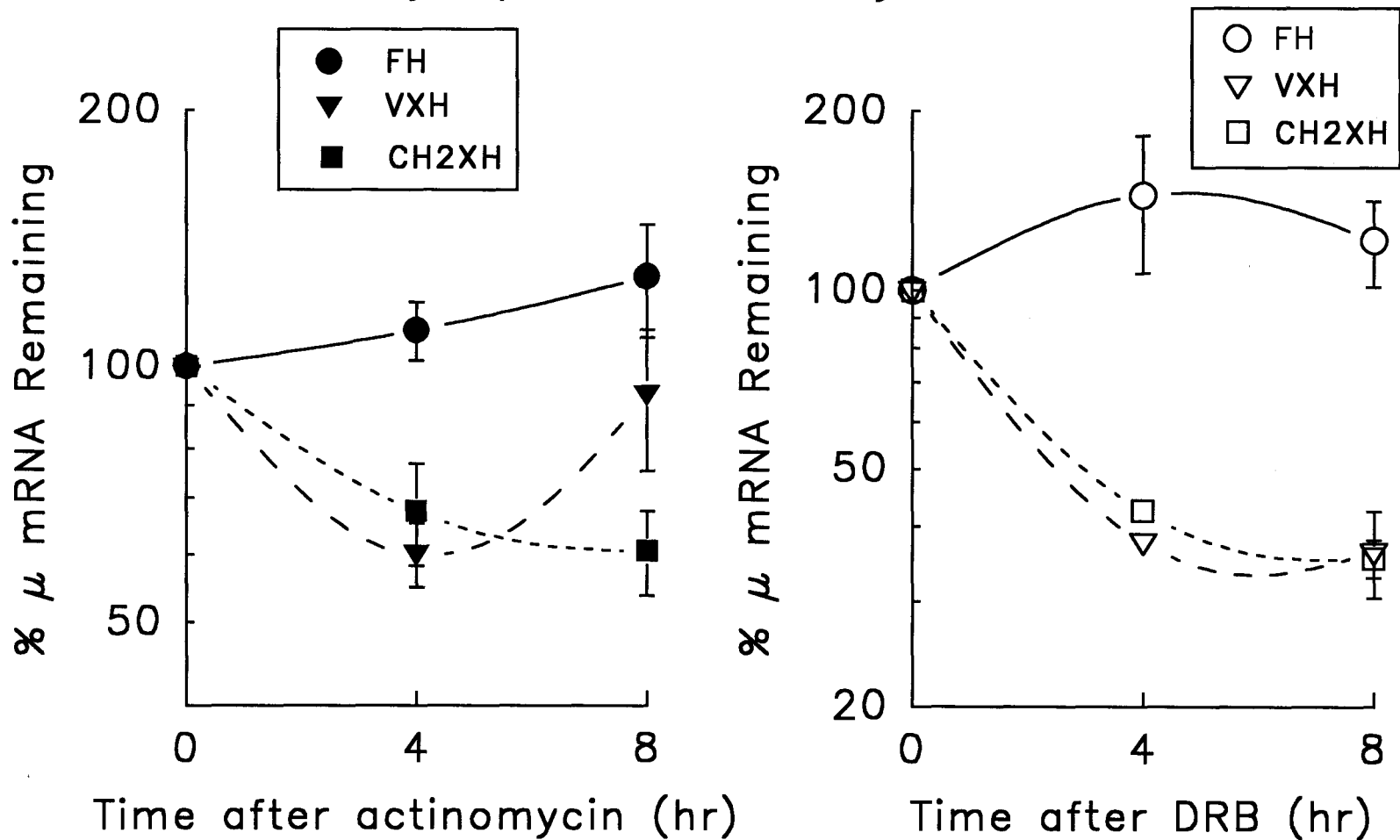
Table 5B. Cytoplasmic Decay Rates of RNAs (the DRB Method, Figure 9B)

Hybridoma	Time (hr)	RNA Loaded	RNA $\mu$	H2b c-myc GAPDH			[ $\mu$ ]	% [ $\mu$ ] %t=0	[H2b] % [H2b]		
				[cpm]					%t=0		
FH.8	t=0	Exp 1	4 $\mu$ g	304.2	17.9	3.6	9.6	31.7	100.0	1.9	100.0
		Exp 2	8 $\mu$ g	977.6	30.8	N.D.	18.0	54.3	100.0	1.7	100.0
		Exp 3	8 $\mu$ g	541.4	31.1	N.D.	16.2	33.4	100.0	1.9	100.0
FH.8	t=4	Exp 1	4 $\mu$ g	316.8	15.0	1.0	5.5	57.6	181.8	2.7	146.3
		Exp 2	8 $\mu$ g	921.9	23.8	N.D.	11.8	78.1	143.9	2.0	117.9
		Exp 3	8 $\mu$ g	2260	70.5	N.D.	62.9	35.9	107.5	1.1	58.4
		mean							<b>144.4</b>		<b>107.5</b>
		SE						<b>14.4</b>		<b>18.9</b>	
FH.8	t=8	Exp 1	4 $\mu$ g	182.1	7.8	0.9	4.7	38.7	122.3	1.7	89.0
		Exp 2	8 $\mu$ g	942.3	28.7	N.D.	12.3	76.6	141.1	2.3	136.4
		Exp 3	8 $\mu$ g	1926	59.1	N.D.	57.3	33.6	100.6	1.0	53.7
		mean							<b>121.3</b>		<b>93.0</b>
		SE						<b>8.0</b>		<b>16.7</b>	
VXH.10	t=0	Exp 1	8 $\mu$ g	14.1	35.6	7.4	7.2	2.0	100.0	4.9	100.0
		Exp 2	8 $\mu$ g	26.8	76.7	N.D.	29.8	0.9	100.0	2.6	100.0
		Exp 3	8 $\mu$ g	16.0	62.5	N.D.	38.7	0.4	100.0	1.6	100.0
VXH.10	t=4	Exp 1	8 $\mu$ g	3.7	23.1	3.9	5	0.7	37.8	4.6	93.4
		Exp 2	8 $\mu$ g	3.4	25.0	N.D.	9.2	0.4	41.1	2.7	105.6
		Exp 3	8 $\mu$ g	12.5	124	N.D.	87.4	0.1	34.6	1.4	87.9
		mean							<b>37.8</b>		<b>95.6</b>
		SE						<b>1.3</b>		<b>3.8</b>	
VXH.10	t=8	Exp 1	8 $\mu$ g	1.8	13.3	2.1	3.7	0.5	24.8	3.6	72.7
		Exp 2	8 $\mu$ g	5.9	30.7	N.D.	14.5	0.4	45.2	2.1	82.3
		Exp 3	8 $\mu$ g	3.1	30.4	N.D.	19.2	0.2	39.1	1.6	98.0
		mean							<b>36.4</b>		<b>84.3</b>
		SE						<b>4.4</b>		<b>5.3</b>	
CH2XH.1	t=0	Exp 1	8 $\mu$ g	8.5	57.6	5.2	8.1	1.0	100.0	7.1	100.0
		Exp 2	8 $\mu$ g	22.9	86.9	N.D.	27.2	0.8	100.0	3.2	100.0
		Exp 3	8 $\mu$ g	11.7	74.6	N.D.	42.2	0.3	100.0	1.8	100.0
CH2XH.1	t=4	Exp 1	8 $\mu$ g	2.3	42.5	2.1	5.1	0.5	43.0	8.3	117.2
		Exp 2	8 $\mu$ g	7.1	55.2	N.D.	20.0	0.4	42.2	2.8	86.4
		Exp 3	8 $\mu$ g	6.3	64.3	N.D.	53.2	0.1	42.7	1.2	68.4
		mean							<b>42.6</b>		<b>90.6</b>
		SE						<b>0.2</b>		<b>10.2</b>	
CH2XH.1	t=8	Exp 1	8 $\mu$ g	1.8	31.2	1	4.7	0.4	36.5	6.6	93.4
		Exp 2	8 $\mu$ g	5.2	57.2	N.D.	15.8	0.3	39.1	3.6	113.3
		Exp 3	8 $\mu$ g	2.4	33.5	N.D.	28.4	0.1	30.5	1.2	66.7
		mean							<b>35.4</b>		<b>91.1</b>
		SE						<b>1.9</b>		<b>9.4</b>	

**Figure 9C      Cytoplasmic Decay Rates of  $\mu$  mRNA in Hybridomas by the Use of Actinomycin C1 or DRB Method (Continued).**

The amount of  $\mu$  mRNA remaining in the cells after the addition of the drug at each time point was determined by a betascope blot analyzer, and normalized to the amount of GAPDH mRNA. Only the darkest band of  $\mu$  mRNA in each lane was quantified. The relative amount of  $\mu$  mRNA ( $[\mu]$ ) at 0 hr was defined as 100% and later time points were calculated as a percentage thereof. The log of these relative  $\mu$  mRNA levels after addition of the drug was plotted as a function of time by SigmaPlot 5.0. The values represent the means of three independent RNA isolations and the error bars represent the standard errors of the mean. Solid circles, triangles and squares denote the curves obtained from the experiments depicted in Figure 9A and Table 5A; open circles, triangles and squares denote the curves obtained from the experiments depicted in Figure 9B and Table 5B.

# Influence of Nonsense Codons on $\mu$ mRNA Cytoplasmic Decay Rates

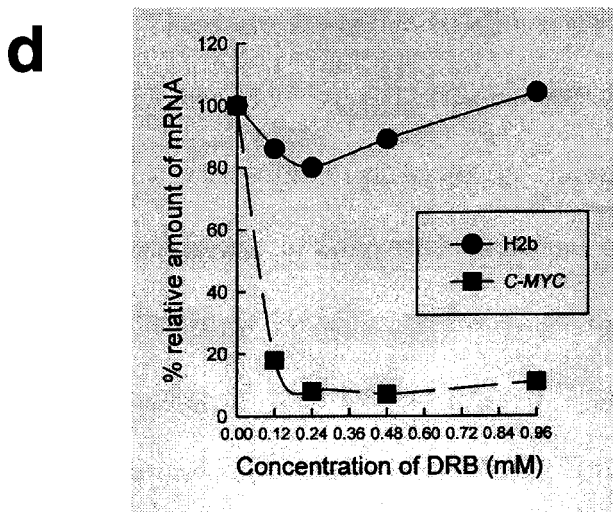
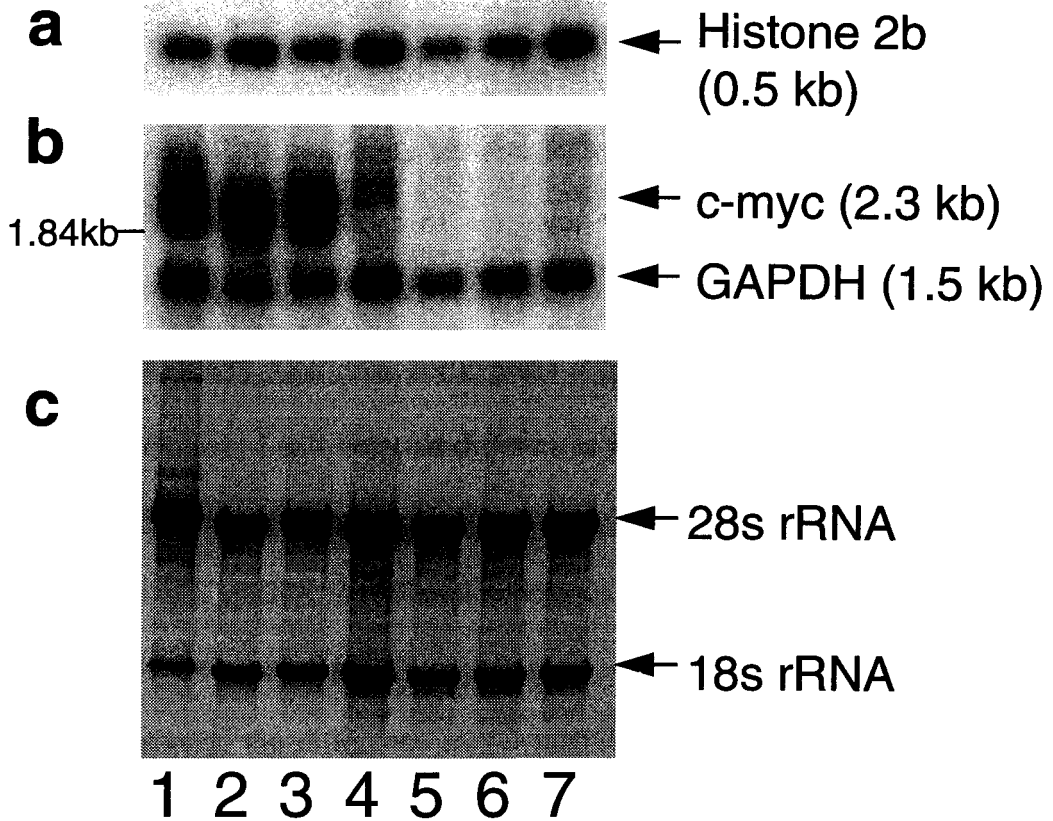


Histone genes are intronless multicopy genes which encode small basic polypeptides that are essential elements of the eukaryotic nucleosome (Marzluff and Hanson, 1993). Unlike other eukaryotic mRNAs, histone RNAs in most organisms do not have poly A tails but instead contain a conserved stem-loop sequence at their 3' end (Marzluff and Pandey, 1988). All histone mRNAs with this 3' end stem-loop structure are regulated coordinately with DNA synthesis, mainly by changing the stability of histone mRNA (Gallwitz, 1975). Histone mRNA levels increase rapidly at the onset of DNA synthesis, and decline equally rapidly at the end of DNA synthesis. The levels varies 30- to 50-fold during the cell cycle (Marzluff and Pandey, 1988). Thus, the finding that the amount of H2b mRNA remained relatively stable during the 8 hour-treatment with DRB might result if: 1) the concentration of DRB used in the experiment was not enough to block the transcription of abundant H2b mRNA or, 2) the regulation of H2b mRNA decay is different from those of  $\mu$  and c-myc mRNAs in the case of DRB treatment. To distinguish between these possibilities, I treated hybridoma *FH* with increasing concentrations of DRB (0, 0.12 mM, 0.24 mM, 0.48 mM and 0.96 mM, respectively), and quantified by Northern blot analysis the amount of H2B mRNA left at 0 and 4 hr after addition of DRB (Figure 10). If the concentration of DRB I used before (0.12 mM) was not enough to block all H2B mRNA transcription in *FH*, I would expect to find the amount of H2B mRNA left in the cells would decrease as the concentration of DRB increased. If the H2B mRNA is subjected to different regulation pathway, I would expect to find that the increased concentration of DRB has no significant effect on H2B mRNA level. As shown in panel a and summarized in panel

d of Figure 10, the increased concentration of DRB did not alter the amount of H2b mRNA (panel a in Figure 10). In contrast, the same amount of DRB reduced the amount of c-myc mRNA. From these data, I conclude that the exceptionally stable amount of H2b mRNA during the 8 hour-treatment with DRB is not due to DRB concentration too low to block the transcription of abundant H2b mRNA. Instead it might result from the metabolism of H2b mRNA being subjected to a different regulation pathway from that of  $\mu$  or c-myc mRNA.

**Figure 10 Northern Blot Analysis to Determine the Effect of DRB Concentration on the Level of H2b mRNA.** After counting, 2 ml of *FH* cells (at a density of  $5 \times 10^5$  cells/ml) were distributed into wells of 24-well Costar plate and kept for 1 hr at  $37^\circ\text{C}$  before addition of DRB. The final concentration of DRB is 0, 0.12 mM, 0.24 mM, 0.48 mM and 0.96 mM, respectively. At 0 and 4 hr, 2 ml (about  $10^6$ ) of cells were removed, centrifuged, and subjected to cytoplasmic RNA isolation by the NP-40/phenol method. 8  $\mu\text{g}$  of RNA was loaded onto each lane and Northern blot analysis was performed as described in the legend to Figure 9A. (a) Autoradiogram of the nitrocellulose blot that was hybridized with an H2b probe. (b) The same blot was rehybridized with a GAPDH probe to control for the amount of RNA loaded onto each lane of the blot. To quantify the effect of DRB on transcription, the blot was rehybridized with a c-myc probe. Lane 4: Ag, Ag8.653, total RNA isolated from Ag8.653 (that expressed no  $\mu$  mRNA). (c) The amount of RNA loaded in each lane, and the integrity and positions of pre-rRNA and rRNA markers were visualized by staining with ethidium bromide. (d) A graph. The relative amount of H2b or c-myc mRNA without DRB treatment at 0 hr was defined as 100% and later H2b or c-myc mRNA amounts were calculated as a percentage thereof. The relative H2b or c-myc mRNA levels after addition of DRB was plotted as a function of concentration by SigmaPlot 5.0.

Cell Line	Ag	FH.8						
DRB	0	0	0	.12	.24	.48	.96	[ $\mu$ M]
Time	0	0	4	4	4	4	4	[hrs]



### 3.5 Nonsense Codons Affect the Size of $\mu$ mRNA

I showed previously that  $\mu$  mRNA in hybridomas *VXH* and *CH2XH* (lane 5' and 7', respectively in Figure 3A) had slower gel mobility than  $\mu$  mRNA in hybridoma *FH* (lane 6' in Figure 3A). The differences in gel mobility of  $\mu$  mRNA may be attributed to the different amounts of RNA loaded on the agarose gel (0.4  $\mu$ g for *FH* and 8  $\mu$ g for *VXH* and *CH2XH*). This possibility was further studied by a mixing experiment (Figure 11). I made five serial dilutions of 1:5 each of 5  $\mu$ g RNA isolated from *FH* and compensated for the amount of RNA in each lane to 5  $\mu$ g by the addition of RNA isolated from Ag8.653 (that does not express  $\mu$  mRNA). With equal amounts of RNA loaded onto each lane, I still detected differences in the size of  $\mu$  mRNA in hybridomas *VXH* and *CH2XH* from *FH* (panel a in Figure 11). Thus, I concluded that the differences in gel mobility of  $\mu$  mRNA in different subclones were not due to different amounts of RNA loaded on the agarose gel.

Alternatively, the difference in gel mobility of  $\mu$  mRNA may result from the observation that  $\mu$  mRNA in hybridomas *VXH* and *CH2XH* is larger in size than  $\mu$  mRNA in *FH*. There are several possibilities which may explain the larger size of  $\mu$  mRNA in hybridomas *VXH* and *CH2XH* (that contain nonsense codons in their  $\mu$  genes), such as: 1) the  $\mu$  transcripts in different hybridomas use different transcriptional start sites, 2) the  $\mu$  transcripts in different hybridomas use different polyadenylation sites or the length of their poly A tail is different, or 3) the presence of a nonsense codon prevents the splicing of small introns that are in the constant region of  $\mu$  RNA, which results in the increase in the size of  $\mu$  mRNA by 300 to 500 bp. The last possibility was



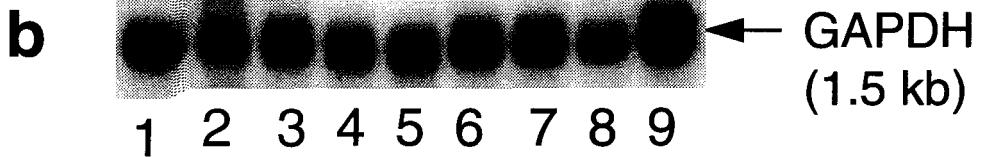
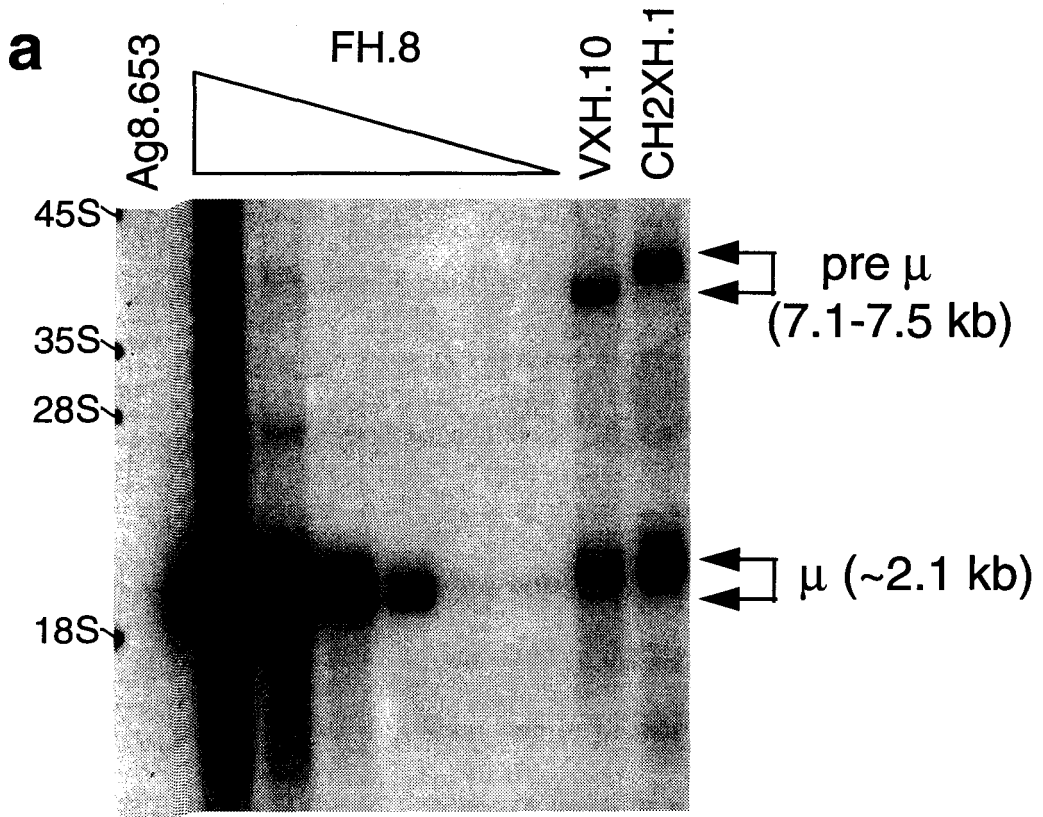
studied here by using 3 sets of primers that are specific for the coding region of  $\mu$  mRNA. If the presence of a nonsense codon prevents the splicing of small introns in the constant region of  $\mu$  RNA, I should be able to detect the RT-PCR products from hybridomas *VXH* and *CH2XH* as being bigger than that from hybridoma *FH*. As shown in Figure 12, all RT-PCR products detected by 3 sets of primers were the same in all hybridomas. Thus, I suggest that the presence of a nonsense codon does not prevent the splicing of small introns in the constant region of  $\mu$  mRNA, which may contribute to the size increase in  $\mu$  mRNA with a nonsense codon in hybridomas *VXH* and *CH2XH*.

The possibility that the presence of a nonsense codon affects the use of different polyadenylation sites in  $\mu$  gene or the length of the poly A tail in  $\mu$  mRNA was studied by ribonuclease H digestion. Ribonuclease H is an enzyme that digests duplex RNAs. Total cellular RNA isolated from different hybridomas was incubated with oligo d(T), which hybridizes to the poly A tail. By treating the mixture with ribonuclease H, the RNA-DNA duplex of poly A tail and oligo d(T) was digested away. If the larger size of  $\mu$  mRNA in hybridomas *VXH* and *CH2XH* (that contain nonsense codons in their  $\mu$  genes) results from it having a longer poly A tail than that of  $\mu$  mRNA in hybridomas *FH*, they should have the same gel mobility after the ribonuclease H treatment. This was exactly what we found (data not shown). Thus, I conclude that the presence of a nonsense codon can influence the length of poly A tail in  $\mu$  mRNA, which contributes, at least in part, to the slower gel mobility of  $\mu$  mRNA in hybridomas *VXH* and *CH2XH*. The remaining possibility is that the length of the 5'-untranslated regions may be influenced by a nonsense codon. This hypothesis can be studied by RNase protection

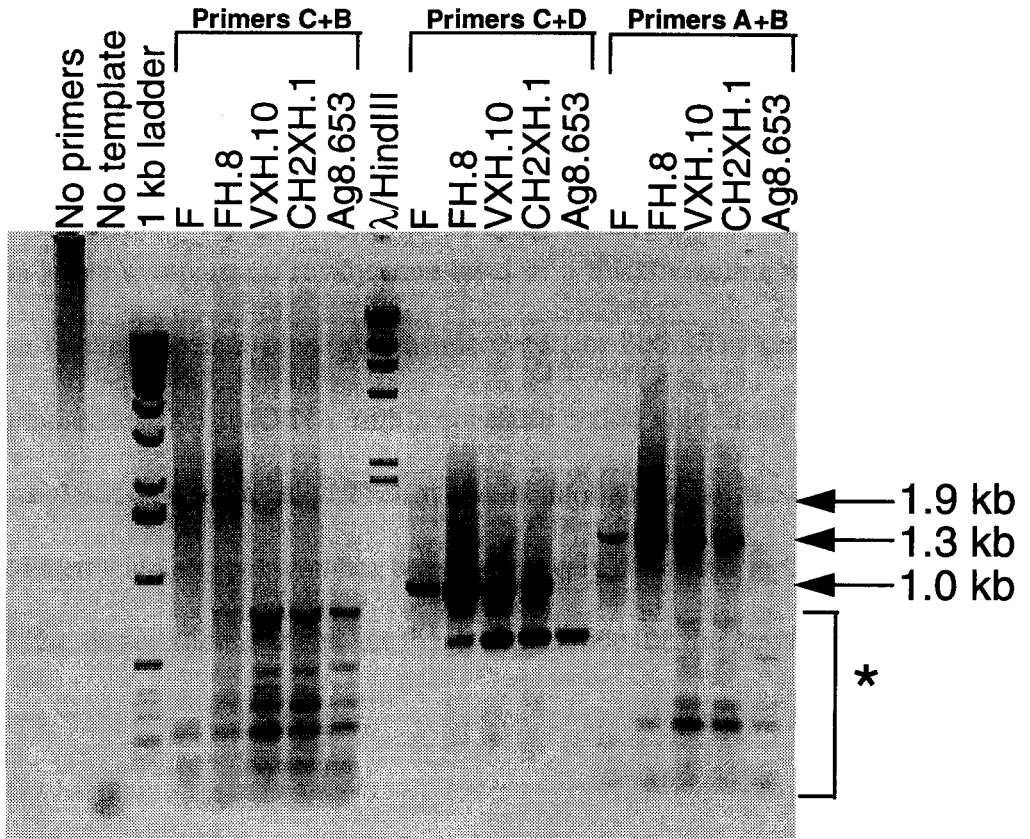
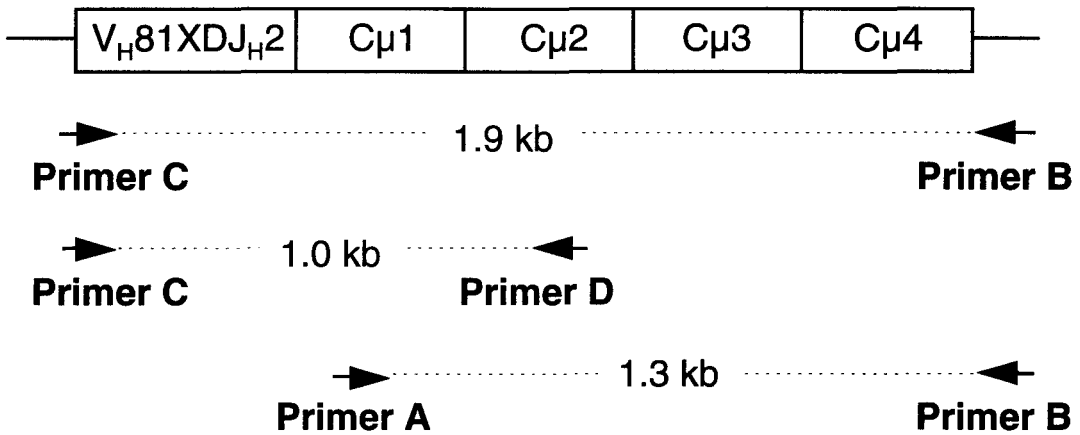
analysis using a probe that is specific for the 5'-untranslated region of  $\mu$  RNA.

All these mechanisms that account for the size differences in  $\mu$  mRNA can also apply to the size differences in precursor  $\mu$  RNA. Since the precursor  $\mu$  RNA contains introns, the variations in the size of introns, such as different deletions in the large  $J_H$ - $C\mu$  intron on the V2 allele as discussed before, may be attributed to the size differences in precursor  $\mu$  RNA with or without a nonsense codon. As revealed by Southern blot analysis, the  $\mu$  gene in  $FH$  has a deletion of about 1.3 kb and  $VXH$  has a deletion of about 1.85 kb when compared to that of  $CH2XH$  (Figure 2B). Based on these results, I suggest that the various deletions in the large  $J_H$ - $C\mu$  intron on the V2 allele attribute, at least partially, to the size differences between precursor  $\mu$  RNAs with (in hybridomas  $VXH$  and  $CH2XH$ ) or without a nonsense codon ( $FH$ ). However, the relationship between the presence of a nonsense codon and deletion in the large  $J_H$ - $C\mu$  intron of  $\mu$  gene is unknown.

**Figure 11 Northern Blot Analysis to Test the Effect of RNA Loading on Mobility.** Total RNA isolated from hybridoma *FH.8* was serially diluted at 1:5 five times (lane 2, 3, 4, 5, 6, and 7), and then the amount of RNA was compensated by total RNA isolated from Ag8.653 (that does not express  $\mu$  transcripts) for 5  $\mu$ g in each sample. The same amount of total RNA isolated from hybridomas *VXH* and *CH2XH* was also loaded on the gel and Northern blot analysis was performed as described in the legend to Figure 3A. (a) Autoradiogram (exposed for 72 hr) of the nitrocellulose blot that was hybridized with a  $C\mu$  cDNA probe. (b) The same blot was rehybridized with a GAPDH probe to control for the amount of RNA loaded onto each lane of the blot. Film was exposed for 24 hr. With equal amounts of RNA loaded onto each lane, there are still differences in the size of  $\mu$  mRNA in hybridomas *VXH* and *CH2XH* from *FH* (panel a).



**Figure 12 RT-PCR Assay to Compare the Length of Coding Region in  $\mu$  mRNAs with or without a Nonsense Codon.** 5  $\mu$ g total cellular RNA isolated by the GIT/CsCl method from each hybridoma was used for cDNA synthesis. 1/20 (0.2  $\mu$ g) of cDNA product from *FH* and 1/10 (0.5  $\mu$ g) of cDNA product from *VXH* and *CH2XH* were amplified by RT-PCR as described in section 2.8.2, and the resulting products were resolved by electrophoresis in a 1% TAE agarose gel and visualized by staining with ethidium bromide in panel a. All RT-PCR products detected by 3 sets of primers are the same as expected in three hybridomas. Panel b depicts a schematic representation showing the positions of three sets of primers that were used in RT-PCR and the expected sizes of RT-PCR product. Asterisk (\*) indicates nonspecific priming products of RT-PCR. Primer A and B are the same as described in the legend to Figure 2. Primer C is the  $V_H81X$ . Forward primer, while primer D is the  $C\mu2Bam$ . Backward primer. All the sequences are listed in section 2.2.1.2.1.

**a****b**

### 3.6 Discussion

Nonsense codons in mRNA are known to be recognized during translation in the cytoplasm. Nonsense codons have been shown to decrease the cytoplasmic steady-state level of  $\mu$  mRNA by 60 to 100 fold (Jäck *et al.*, 1989). Since metabolism of  $\mu$  mRNA with a nonsense codon is regulated by post-transcriptional mechanisms (Jäck *et al.*, 1989), this lower cytoplasmic steady-state level of  $\mu$  mRNA with a nonsense codon can result from either a nuclear or a cytoplasmic event, or both. The data presented in this chapter demonstrate that  $\mu$  mRNA with a nonsense codon is reduced in both the nucleus and the cytoplasm of plasma cells. The involvement of a nuclear process in the nonsense codon-mediated RNA degradation has been extensively discussed in Chapter I. Thus this section of the dissertation focuses on the interpretation of the results obtained in this chapter.

#### 3.6.1 Ig mRNA with a Nonsense Codon Starts to Decrease in the Nucleus of Plasma Cells

To determine the level of nuclear RNA, one needs to exclude the cytoplasmic components in the procedure of nuclear RNA isolation. Since the outer membrane of nuclei is continuous with the membrane of the endoplasmic reticulum in the cytoplasm (Arnstein and Cox, 1992), the outer membrane of nuclei should be removed with the cytoplasmic components. An ideal way to monitor the removal of cytoplasmic components to use specific markers for inner and outer nuclear membranes to stain the nuclei before and after preparation. If the outer membrane of nuclei has been exclusively removed, we would expect to find no staining of outer nuclear membrane after the

purification procedure. Although over 1,000 proteins have been reported in the nuclear pore (Forbes, 1992; Rout and Wente, 1994), our laboratory does not have these specific markers. In addition, our laboratory does not have a specific marker to detect polyribosome contamination in the nuclei preparation. Thus, I used an alternative approach to quantify the amount of cytoplasmic RNA contamination in the modified nuclear RNA isolation protocol (section 2.12.3.2 in Chapter II; Nevins, 1980; Birnie, 1978; Penman, 1966). As shown in Figure 5B and summarized in Table 3A, I found that the cytoplasmic contamination in nuclear RNA preparation was less than 0.01%, suggesting the effect of cytoplasmic RNA contamination on nuclear RNA isolation can be ignored in our current protocol. The removal of cytoplasmic components was also determined by several parameters, such as the absence of cytoplasmic tabs as revealed by the phase contrast microscopy (Figure 6), the presence of enriched rRNA precursors, the increased ratio of 28S to 18S rRNA (Figure 8a), and the decreased level of H2b mRNA (Figure 8e) in the nuclear RNA samples.

As shown in Figure 8 and summarized in Table 4, I found that the nuclear  $\mu$  mRNA levels of  $\mu$  mRNA with nonsense codons (in hybridomas *VXH* and *CH2XH*) are decreased by about 7 fold when compared to that of  $\mu$  mRNA without a nonsense codon (in hybridoma *FH*). This lower steady-state level of  $\mu$  mRNA in hybridomas *VXH* and *CH2XH* does not result from the hybridomas having defects in the expression of mRNA or protein, because hybridomas *VXH* and *CH2XH* express comparable amounts of  $\gamma$ 2b, H2b and c-myc mRNAs (Table 4 and Table 5) and  $\gamma$ 2b protein (Beck-Engeser, unpublished result). Thus, I conclude that the reduction in the level of  $\mu$  mRNA with a



nonsense codon starts in the nucleus of plasma cells.

The lower nuclear level of  $\mu$  mRNA with nonsense codons could result from 1)  $\mu$  mRNA with a nonsense codon being degraded faster in the nucleus; 2) the presence of a nonsense codon preventing the processing of precursor  $\mu$  transcripts to  $\mu$  mRNA; or, 3) both. Due to the low abundance of nuclear RNA, I did not measure the nuclear decay rate of  $\mu$  mRNA by the use of a transcriptional inhibitor. However, the second possibility is consistent with the finding that the steady-state level of nuclear precursor  $\mu$  RNA with a nonsense codon increases by at least 2 fold over that of precursor  $\mu$  transcript without a nonsense codon (Table 4). It has been reported that histone pre-mRNA is rapidly degraded if it is not productively processed (Pandey *et al.*, 1994), therefore, the effect of a nonsense codon on  $\mu$  RNA processing could be more severe than what I found. In addition, I found that the length of precursor  $\mu$  transcripts is independent of the position of a nonsense codon in the  $\mu$  gene: In both  $V_H$ .stop- and  $C\mu 2$ .stop-containing hybridomas, precursor  $\mu$  RNAs retain the large  $J_H$ - $C\mu$  intron (Figure 8c). This evidence suggests that a nonsense codon does not specifically prevent the splicing of its downstream sequences. Instead, the accumulation of precursor  $\mu$  transcripts probably results from interaction between the nonsense codon recognition system with the splicing system.

A similar phenomenon has also been reported by Cheng and Maquat (1993). They found deletion of all splice sites that reside downstream of a nonsense codon does not abrogate the nonsense codon-mediated reduction of TPI mRNA. I do not know, however, whether there is a specific sequence in the large  $J_H$ - $C\mu$  intron that is subjected to the

regulation of the nonsense codon recognition system. The inhibitory effect of a nonsense codon on the splicing of precursor RNA transcripts has also been reported in the literature (Naeger *et al.*, 1992, Lozano *et al.*, 1994). Accumulation of the precursor RNAs has also been noticed by other groups studying the expression of T cell receptor  $\beta$  gene (personal communication with Dr. Miles F. Wilkinson) and AHFR gene (Kessler *et al.*, 1993) in mammalian systems.

The presence of precursor  $\mu$  transcripts that are 300-500 bp smaller than the largest precursor  $\mu$  transcript in each hybridoma suggests that the splicing of primary  $\mu$  transcript does not occur in the 5' to 3' order. Instead, the splicing of this large intron at proximal 5' end may occur after the splicing of small introns in the constant region of the  $\mu$  gene. This is consistent with studies which show that the size of the intron and exon influence the efficiency of splicing: in eukaryotic genes that contain large exons (i.e. 300 bp in C $\mu$  exons of  $\mu$  gene), an increase in the size of an intron correlates with decreased splicing efficiency (personal communication with Dr. Susan Berget). Out of order splicing has also been reported in other systems (Beyer and Osheim, 1988; Bingham, 1993).

### 3.6.2 $\mu$ mRNA with a Nonsense Codon is Degraded Faster Than $\mu$ mRNA Without a Nonsense Codon in the Cytoplasm of Plasma Cells

The best method to measure the decay rate of a mRNA is to use metabolic labeling. However, our previous experiments failed because uridine is toxic to B cells (Jäck, unpublished data). Alternatively, I used two well established inhibitors of RNA synthesis to measure the cytoplasmic decay rates of  $\mu$  mRNA (Figure 9). Both DRB and

higher concentrations of Actinomycin C1 (over 5  $\mu\text{g/ml}$ ) were found to inhibit the phosphorylation of the C-terminal domain of the largest subunit of eukaryotic RNA polymerase II in HeLa cells exposed to heat shock, which results in inhibition of transcription in HeLa cells (Dubois *et al.*, 1994). In contrast to the studies that show nonsense codons do not influence the cytoplasmic decay rates of mRNA (see review in Chapter I), I found that the levels of  $\mu$  mRNA with nonsense codons are decreased by about 1.5 fold during the 8-hour drug treatment of Actinomycin C1, while the level of  $\mu$  mRNA without a nonsense codon remains relatively stable during this period (Table 5). In the case of DRB treatment, the half-life of  $\mu$  mRNA decreases from relatively stable in *FH* (that contains functional  $\mu$  mRNA) to 3 to 4 hr in *VXH* and *CH2XH* (that contain nonsense codons in their  $\mu$  mRNAs) during the 8 hr-treatment. Based on these data, I conclude that  $\mu$  mRNA with nonsense codons is degraded faster than that without a nonsense codon. This is consistent with the assumption that the only identified translational machinery resides in the cytoplasm of an eukaryotic cell, thus mRNA with a nonsense codon should be recognized and degraded in the cytoplasm.

In addition, I noticed the differences in the half lives of  $\mu$  mRNA when they were measured by the two transcriptional inhibitors. I proposed that the differences are probably due to the fact that Actinomycin C1 reduces the levels of cytoplasmic mRNAs more dramatically than DRB (compare  $\mu$  and GAPDH hybridizations in the Figures 9A and 9B). Thus, the lower level of GAPDH mRNA at 8 hour after Actinomycin C1 treatment is not accurate enough to serve as a loading control to normalize the level of  $\mu$  mRNA. This problem may be overcome by the use of a stable mRNA (such as 28S

rRNA or  $\beta$ -actin mRNA) as a loading control. The levels of 28S rRNA on the gel can be visibly compared in panel e of Figure 9A and 9B, where rRNAs are revealed by ethidium bromide staining.

### 3.6.3 DRB Does Not Influence the RNA Metabolism of H2b Gene

The fact that the amount of H2b mRNA left in *FH* cells did not decrease as the concentration of DRB was increased (Figure 10) suggests that the metabolism of H2b mRNA is subjected to a different regulation pathway in the presence of DRB. The DRB-specific stabilized effect of H2b mRNA would result if: a) DRB blocks the transcription of a short-lived degradation factor that is specific for histone mRNA; or b) DRB, a nucleotide analogue of adenosine, blocks the RNA binding site on H2b-specific RNA degradation factor, and thus inhibits the nuclease activity of the enzyme (personal communication with Dr. Jeff Ross). Dr. Ross' lab has recently purified a biochemically activated nuclease that is specific for histone mRNA. He is going to test whether DRB specifically blocks the histone-specific RNA degradation by using H2b mRNA +/- DRB as substrates of the nuclease activity of the purified protein. If DRB blocks the histone-specific nuclease, they should find a high level of H2b mRNA when they include DRB in the substrate, while a low level of H2b mRNA when there is no DRB in the substrate. Alternatively, c) DRB may block the translation of the H2b mRNA. It has been shown that the degradation of histone mRNA is mediated by a ribosome-associated nuclease. Translation is needed to bring the nuclease to its specific substrate on the mRNA (Graves *et al.*, 1987). Thus DRB can also exert its effect by inhibiting the translation process of

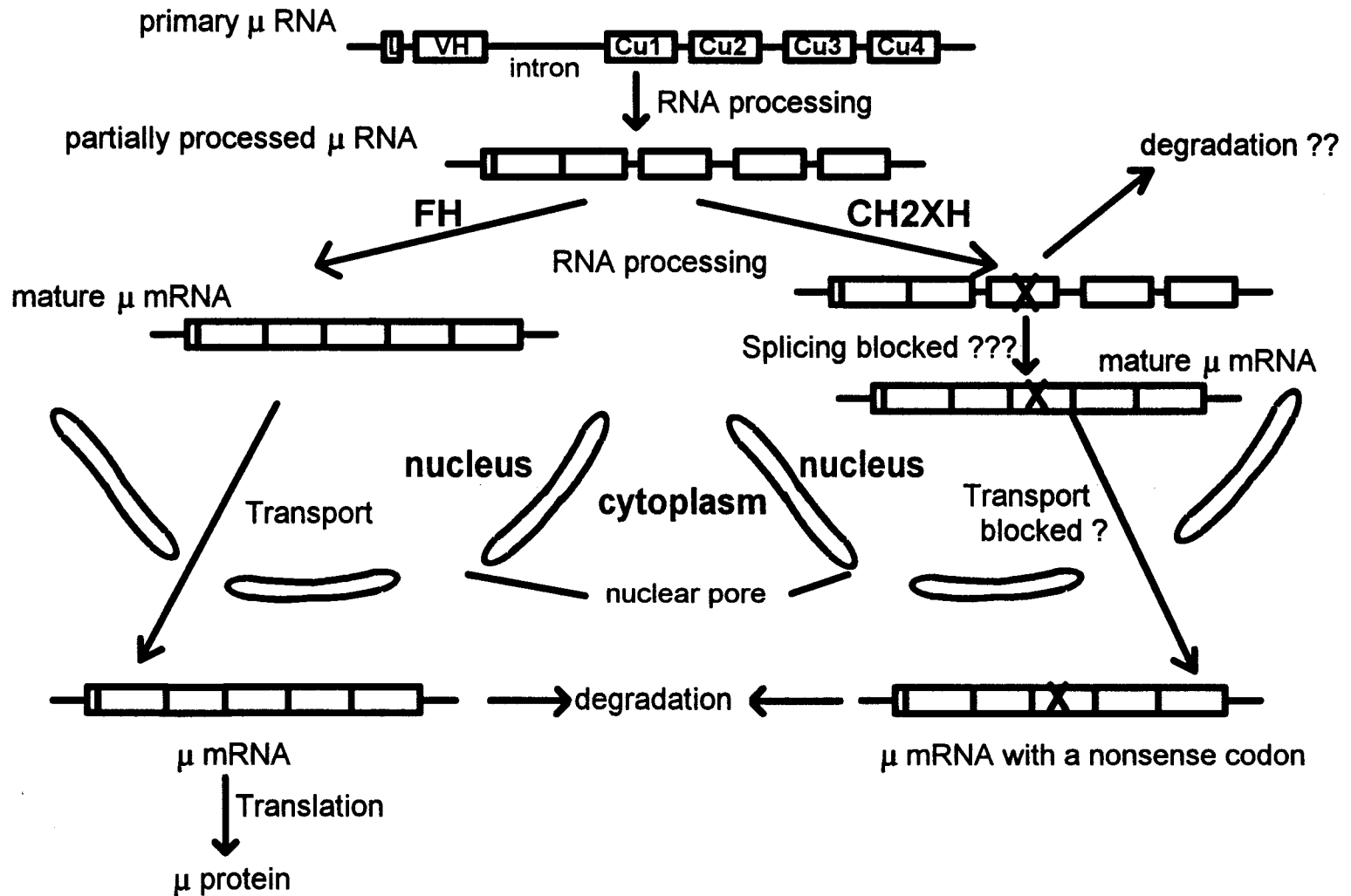
H2b mRNA. This hypothesis can be tested by an  $^{35}\text{S}$  methionine pulse-chase experiment. If DRB blocks the translation of H2b mRNA, I would expect to see a decrease in the level of  $^{35}\text{S}$  methionine-labeled H2b protein. d) DRB may not block the transcription of H2b mRNA. This hypothesis may be tested by a nuclear run-on experiment. If DRB does not block the transcription of DRB, I would expect to see the normal  $^3\text{H}$ -uridine incorporation of H2b mRNA after addition of DRB.

I have summarized the findings of this Chapter in Figure 13. Briefly, I found that the reduction of cytoplasmic level of  $\mu$  mRNA with a nonsense codon in plasma cells results from both a nuclear and a cytoplasmic event. In the nucleus, the presence of a nonsense codon inhibits the splicing of the largest  $\text{J}_\text{H}\text{-C}\mu$  intron in precursor  $\mu$  RNA. In the cytoplasm, degradation is attributed to the lower cytoplasmic level of  $\mu$  mRNA with nonsense codons. This is the first report that has shown that both nuclear and cytoplasmic events are involved in the nonsense codon-mediated mRNA degradation. This could be a very unique phenomenon for Ig mRNA. Thus, B cells have more than one mechanism to eliminate nonproductive Ig mRNAs, which may contribute to the potent efficiency of humoral immune response.

**Figure 13 A Schematic Representation of  $\mu$  RNA Metabolism in Plasma Cells.**

Two different splicing pathways for functional  $\mu$  RNA (left) or  $\mu$  RNA with a nonsense codon (right) in plasma cells. The genomic organization of the murine  $\mu$  gene is presented at the top. Exons are represented by open boxes, and introns by solid lines. X designates the presence of a nonsense codon. For  $\mu$  transcript with a nonsense codon (i.e., a functional  $\mu$  RNA), the presence of a nonsense codon prevents the splicing of the largest  $J_H$ - $C\mu$  intron in primary transcript, which might contribute to the lower nuclear level of  $\mu$  mRNA. Lower amounts of  $\mu$  mRNA escapes to the cytoplasm, where it is subjected to rapid cytoplasmic degradation. The effect of a nonsense codon on either nuclear degradation or nucleus-to-cytoplasm export of  $\mu$  mRNA has not been determined.

# $\mu$ mRNA Metabolism in B Lineage Cells



CHAPTER IV  
TEST OF A MODEL TO EXPLAIN THE MECHANISM BY WHICH  
IG  $\mu$  mRNA WITH A NONSENSE CODON  
IS DECREASED IN THE NUCLEUS OF PLASMA CELLS

4.1 Introduction

In Chapter III, I found that  $\mu$  mRNA with a nonsense codon is decreased in both the nucleus and the cytoplasm of plasma cells. The presence of a nonsense codon prevents the splicing of the large  $J_H-C\mu$  intron. However, I have not elucidated how a nonsense codon can signal the reduction of  $\mu$  mRNA in the nucleus. Several models have been proposed to explain the mechanism of the nonsense codon-mediated mRNA degradation (see Chapter I). The main objective of this chapter is to determine whether the modified translational translocation model (Figure 14) is the mechanism by which a nonsense codon triggers the reduction of  $\mu$  mRNA in the nucleus.

Based on the assumption that cytoplasmic translational machinery is the only identified factor that can recognize a nonsense codon, Urlaub *et al.* (1989) proposed a translational translocation model. I have modified Urlaub's model to accommodate our secretory  $\mu$  protein. As a secretory protein,  $\mu$  protein is first synthesized as a precursor bearing an N-terminal signal peptide (also called leader peptide) (Kuby, 1994). Shortly after its synthesis, the signal peptide binds to the signal recognition particle (SRP) in the



cytoplasm. The SRP also interacts with the ribosome in which the nascent peptide resides, thus pausing the  $\mu$  protein translation in the free polysome fraction. There are many SRP-receptors and signal sequence receptors on the surface of endoplasmic reticulum (ER). The binding of the  $\mu$  mRNA-ribosome-bound SRP to its receptor targets the  $\mu$  mRNA-ribosome complex to the surface of ER. This targeting releases the translational pausing effect of SRP, thus allowing  $\mu$  protein translation to continue efficiently on the surface of ER (Arnstein and Cox, 1992). Protein translation on the surface of ER not only facilitates the splicing of the 3' part of the RNA molecule in the nucleus, but also pulls the  $\mu$  mRNA into the cytoplasm. If translation is prematurely terminated by a nonsense codon, the splicing of the 3' part of RNA in the nucleus is inhibited. In addition, ribosomes fall off the RNA, thus the ribosomes cannot facilitate the export of RNA to the cytoplasm. The 'trapped' unspliced RNA in the nucleus is degraded, which leads to the reduction of nuclear  $\mu$  RNA and subsequently cytoplasmic RNA.

Once the mature  $\mu$  mRNA is in the cytoplasm, its steady-state level is regulated by a cytoplasmic mRNA degradation event. This is consistent with my finding that  $\mu$  mRNA with nonsense codons have a shorter half-life than that of  $\mu$  mRNA without a nonsense codon. Mason *et al.* (1988) have shown that the change of  $\mu$  mRNA cytoplasmic location from the ER-membrane bound fraction to the free polysome fraction decreases its stability by about 6 fold. Additionally, protein translation on the surface of ER might increase the stability of  $\mu$  mRNA, presumably by protecting the instability sequences downstream of the nonsense codon from attack by cytoplasmic degradation

factors.

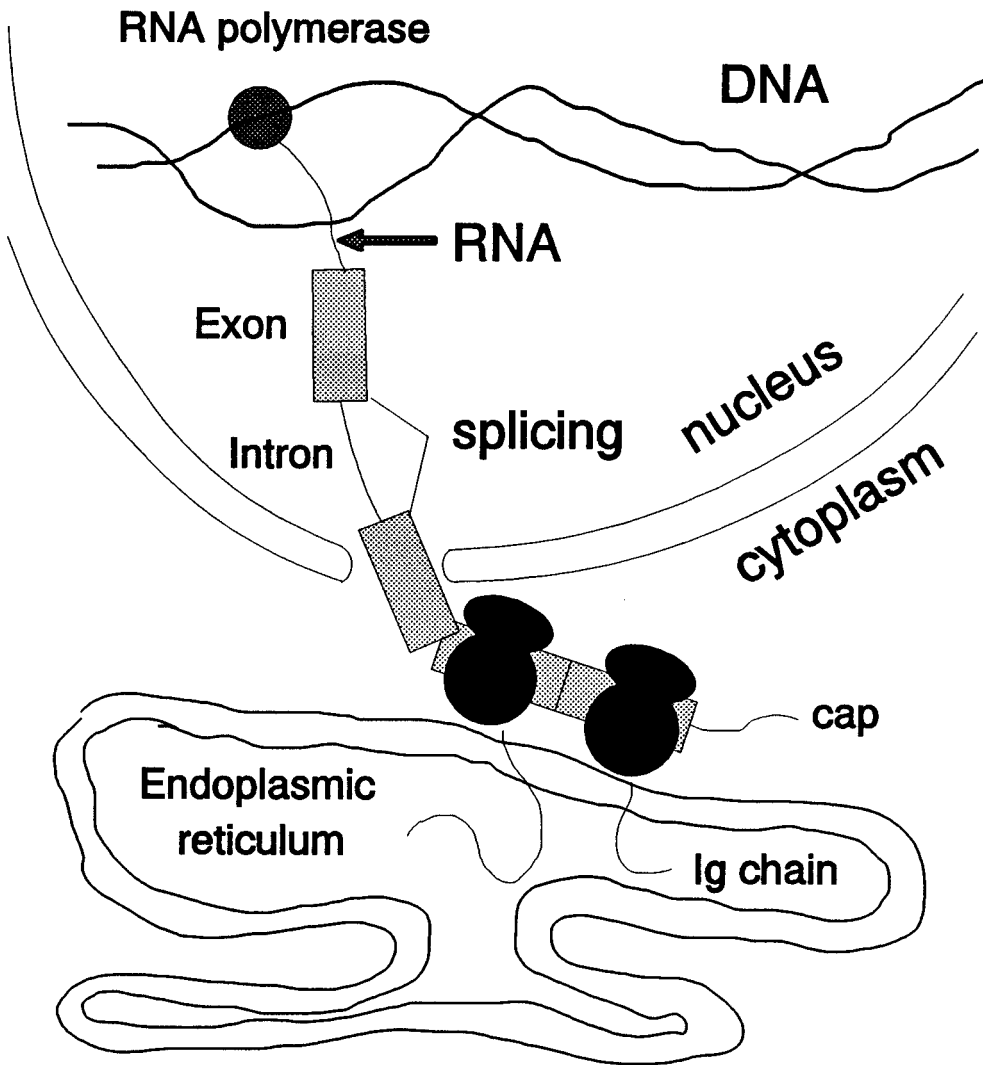
There are several predictions from our model. If a nonsense codon decreases the steady-state level of  $\mu$  mRNA by inhibiting the nuclear splicing of downstream sequences, then:

- 1) when a nonsense codon is present in different exons of a  $\mu$  gene, the size of partially spliced  $\mu$  transcripts should correlate with the position of a nonsense codon;
- 2) when I introduce a nonsense codon in the last exon, the steady-state level of  $\mu$  mRNA should not be affected since no downstream splicing is required for RNA processing;
- 3) when I replace the genomic sequences downstream of the nonsense codon with their corresponding cDNA sequences, the steady-state level of  $\mu$  mRNA should be restored to its wild-type level since no downstream splicing is required for RNA processing;
- 4) the presence of a nonsense codon should not influence the steady-state level of  $\mu$  mRNA when it is derived from a cDNA clone since no intron splicing is required for  $\mu$  mRNA expression.

The first prediction is challenged by my finding that precursor  $\mu$  transcripts in hybridoma *CH2XH* still contain the large  $J_H-C\mu$  intron that resides upstream of the nonsense codon (see Chapter III). In this chapter, I have tested the other predictions by analyzing the RNA expression of functionally rearranged wild-type or *in vitro* modified  $\mu$  genes that have been stably introduced into terminally differentiated B lymphocytes.

Figure 14 **A Modified Translational Translocation Model.** I have modified Urlaub's model to accommodate our secretory  $\mu$  protein. Ribosomes begin to translate a  $\mu$  RNA as it emerges from a nuclear pore and before the completion of its 3' processing. Protein translation on the surface of ER not only facilitates the splicing of the 3' part of the RNA molecule in the nucleus, but also pulls the  $\mu$  mRNA into the cytoplasm. If translation is prematurely terminated by a nonsense codon, nuclear splicing of the 3' part of the RNA is inhibited. Ribosomes then fall off the RNA, and the ribosomes cannot facilitate the export of RNA to the cytoplasm. The 'trapped' unspliced RNA in the nucleus is degraded, which leads to the reduction of nuclear  $\mu$  RNA and subsequently cytoplasmic RNA.

# A Model To Explain How mRNA With A Nonsense Codon Is Degraded



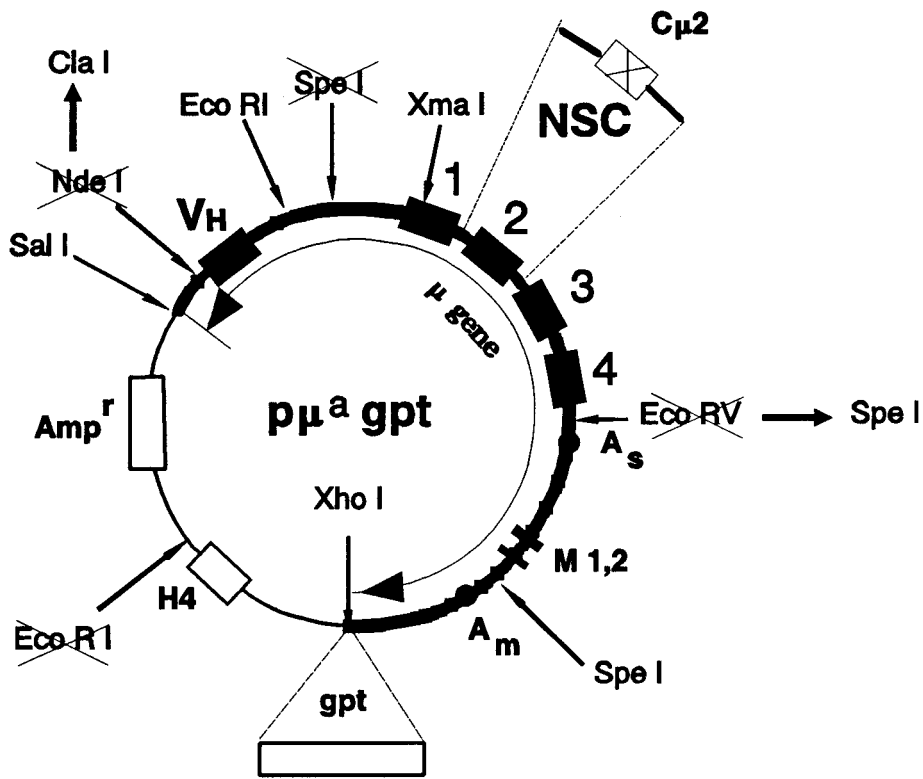
## 4.2 Results



### 4.2.1 Construction of Plasmids

All the constructs used in this study are generated in a  $p\mu^*$  based expression vector (Figure 15). The functionally rearranged murine  $\mu$  gene isolated from the hybridoma 17.2.25 contains the following sequences starting from the 5' end: a short leader exon, an intron, a joined VDJ ( $V_H$ ) exon, a large  $J_H-C\mu$  intron, and a series of constant gene exons of "a" allotype in genomic configuration (Loh *et al.*, 1983; Grosschedl and Baltimore, 1984; Grosschedl *et al.*, 1985). The insertion of *E. coli* enzyme, guanosylphosphoribosyl transferase (*gpt*), into the expression vector allows the selection of stable transfectants in the media containing xanthine and mycophenolic acid (MPA). The expression of *gpt* mRNA was used as an internal control for the copy number of active transcripts of the plasmid. Several restriction endonuclease sites have been engineered into the  $p\mu^*gpt\Delta M$  vector for the purpose of convenient cloning.

#### 4.2.1.1 Deletion of the Membrane Exons in the $p\mu^*gpt$ Plasmid

The membrane exons in the  $\mu$  gene were deleted to eliminate the effect of alternative splicing on the stability of  $\mu$  mRNA (Peterson, 1994). The plasmid  $p\mu^*gpt$  was linearized with *EcoRV* that cut between  $C\mu 4$  and membrane exons. After dephosphorylation treatment with CIP, the plasmid was re-ligated in the presence of a *Spe I* linker. Thus, the membrane exons were within a *Spe I* fragment of 0.92 kb, which was subsequently deleted by *Spe I* digestion and religation of the modified plasmid. The resulting plasmid is designed as  $p\mu^*gpt\Delta M$ .

Figure 15 A Schematic Representation of the Plasmid  $p\mu^a gpt\Delta M$ .

- |   |                                     |
|---|-------------------------------------|
|  | Ig introns, promoter and enhancer   |
|  | Ig exons                            |
| 1, 2, 3, 4  | C $\mu$ exons                       |
| A <sub>m</sub> , A <sub>s</sub>   | Poly(A) signal                      |
| M   | membrane domain                     |
| <b>gpt</b>  | guanosyl phosphoribosyl transferase |
| H4  | histone 4                           |
| NSC   | nonsense codon                      |

#### 4.2.1.2 cDNA Replacement and Deletion of Downstream Sequences of the Nonsense Linker in the $\mu^{\text{gpt}}\Delta\text{M}$ Plasmid

To study the effect of a nonsense codon on the splicing of downstream sequences, I replaced genomic sequences downstream of a nonsense codon with their corresponding cDNA sequences. A 3.316-kb *XbaI-SpeI* fragment that includes sequences in  $C_{\mu}$  exons was isolated from the  $\mu^{\text{gpt}}\Delta\text{M}$  vector and subcloned into pGEM9zf(-). The subcloned plasmid was then linearized with *BamHI* enzyme that cut in the middle of  $C_{\mu 2}$  exon, and the *BamHI* ends were blunted with Klenow enzyme (Pharmacia). A *NheI*-containing amber stop linker [5'-pd(CTAGCTAGCTAG)-3', Pharmacia, Lot # 2067220011] that includes three amber nonsense codons in each open reading frame was cloned into the Klenow blunted-*BamHI* site in the middle of  $C_{\mu 2}$  exon. The plasmids were screened for the presence of amber stop linker by *NheI* digestion. Then the 3.4-kb *EcoRI-SpeI* fragments without or with a stop linker were cloned back to the  $\mu^{\text{gpt}}\Delta\text{M}$  vector, resulting in the deletion of a 3.512-kb *EcoRI-XbaI* fragment in the large  $V_{\text{H}}-C_{\mu}$  intron (construct A and B in Figure 16a).

The 1.244-kb *BamHI-NheI* fragment that includes genomic sequences from the  $C_{\mu 2}$  to  $C_{\mu 4}$  exon was replaced by its corresponding 0.862-kb cDNA sequence from plasmid 5.1 (Reth and Alt, 1984) in the *XbaI-SpeI* subclone. The introduction of the *NheI*-amber stop linker into the  $C_{\mu 2}$  exon and the subsequent cloning procedure are the same as described above (construct G and H in Figure 16a). To make construct J and L (in Figure 16a), a 0.86-kb *NheI* fragment that contains the sequences downstream of the stop linker was deleted or was cloned back in opposite orientation. The accuracy of cloning was confirmed by several restriction enzyme digestions (Figure 16b).

#### 4.2.1.3 Introduction of a Nonsense Linker into Four Exons of Constant Region in the $p\mu^{\text{gpt}}\Delta\text{M}$ Plasmid

To determine whether the position of a nonsense codon influences the steady-state level of  $\mu$  mRNA in plasma cells, I generated DNA constructs containing wild-type and modified  $\mu$  genes with a nonsense linker at different exons of the  $\mu$  gene (Figure 17). The subclone plasmid that contains the 3.316-kb *XbaI-SpeI* fragment of  $C\mu$  exons in genomic configuration (as described in section 4.2.1.2) was linearized with *SmaI*, *BglIII*, *BstXI*, or *ApaI*, respectively. The 3'-overhangs of *ApaI* or *BstXI* were blunted with T4 DNA polymerase, and the 5'-overhangs of *BglIII* was blunted with Klenow enzyme. After dephosphorylation treatment with CIP, each plasmid was ligated in the presence of a *NheI*-containing amber stop linker. The 3.328-kb *XbaI-SpeI* fragments of  $C\mu$  exons that contain nonsense codons in different  $C\mu$  exons were subsequently cloned back to the  $p\mu^{\text{gpt}}\Delta\text{M}$  vector (Figure 17a). The presence of the *NheI*-containing nonsense linker at the proper positions was confirmed by *NheI* digestion (Figure 17b).

#### 4.2.1.4 Generation of a $P_{\text{cmv}}\text{-}\mu$ cDNA Clone With or Without a Nonsense Linker

To determine whether the presence of a nonsense codon influences the splicing of precursor  $\mu$  transcript, I generated a  $\mu$  cDNA clone with or without a nonsense codon. Since  $\mu$  cDNA clone does not express efficiently under the authentic IgH promoter, I replaced the IgH promoter with the human cytomegalovirus immediate early promoter (pCMV). A  $\mu_s$  cDNA sequence, which was cloned from 991 hybridoma cells (Balb/c) into the pCR<sup>TM</sup> II vector, was cut out as 1.9 kb of *EcoRI-NheI* fragment and cloned into *EcoRI/XbaI* sites in pUHD10-1.gpt expression vector by a two-step ligation as described

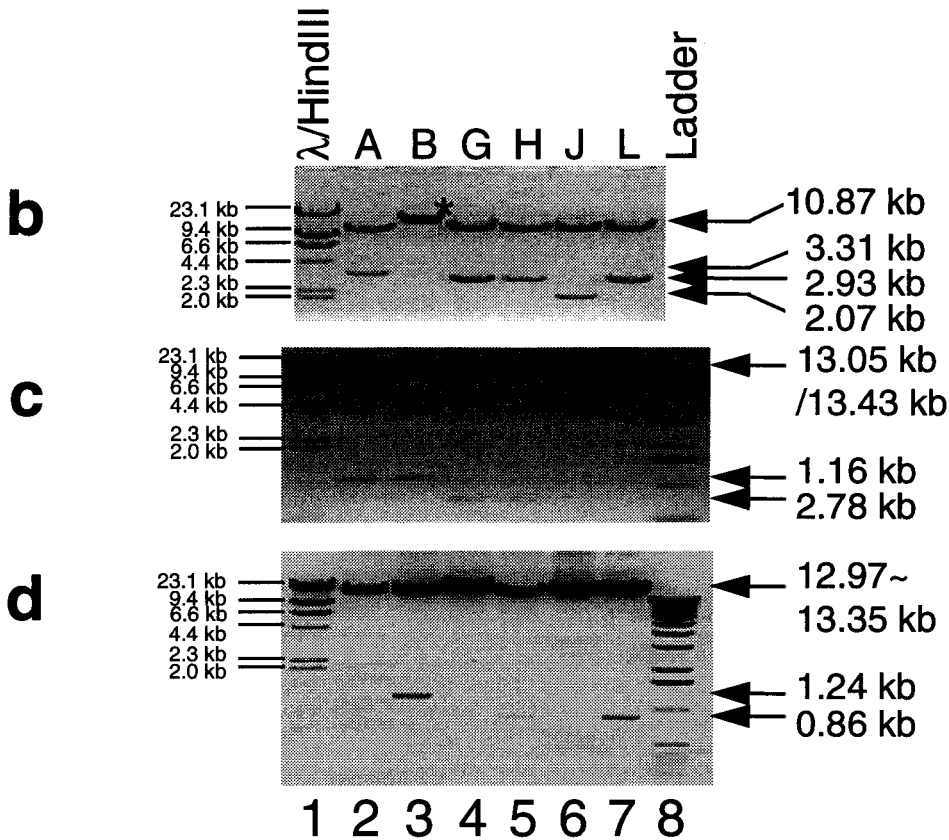
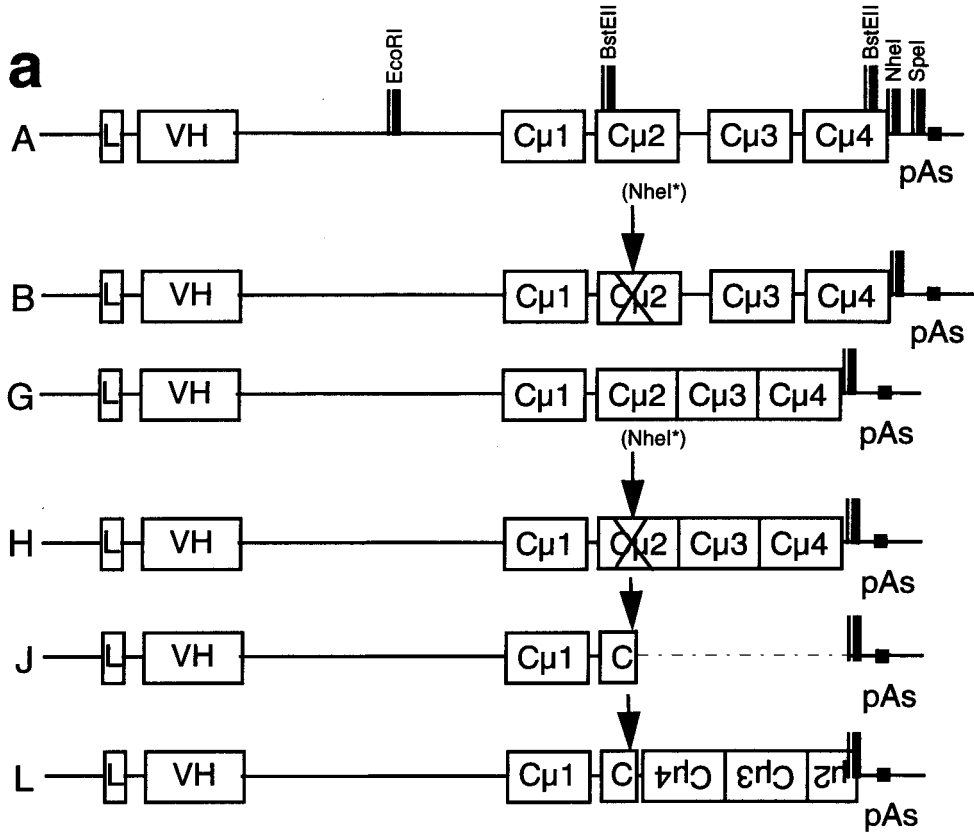


in Chapter II (Construct M in Figure 22a). The parent pUHD10-1 vector contains a 746-bp fragment of pCMV (Deuschle *et al.*, 1989). A *Bst*EII site in  $C\mu 2$  exon of  $\mu_s$  cDNA was destroyed by Klenow treatment and cloned into a *Nhe*I-containing amber stop linker [5'-pd(CTAGCTAGCTAG)-3', Pharmacia, Lot # 2067220011] (construct N in Figure 22a).

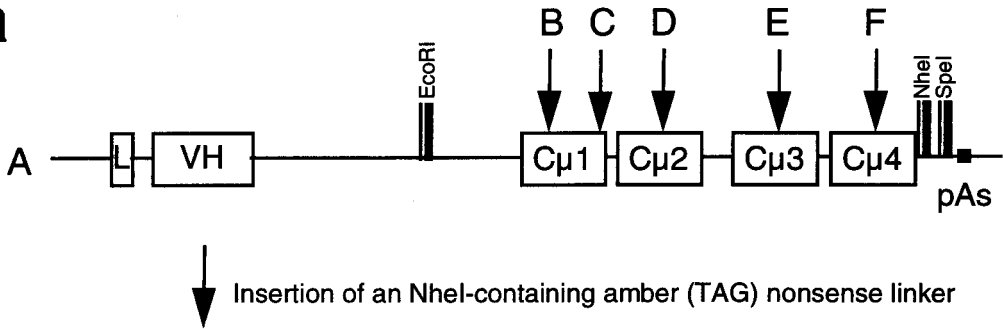
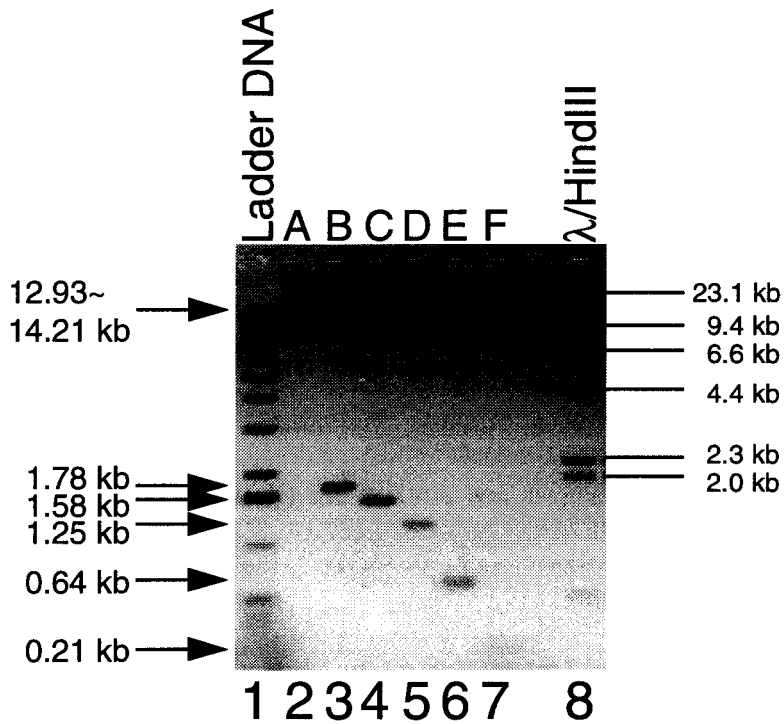
#### 4.2.1.5 Generation of Stable Transfectants Containing Modified $\mu$ Genes

Plasmid DNAs containing modified functional rearranged  $\mu$  genes were introduced into a mouse plasmacytoma cell line *J558L* ( $\mu$ - $\lambda$ +) by electroporation. The cells were maintained in MPA-containing growth media to select for the expression of *gpt*. The expression of  $\mu$  gene was screened by cytoplasmic immunofluorescence (CIF) using goat anti-IgM antibody:  $\mu$  protein was detected in stable transfectants containing constructs A, C, F, G and J (data not shown). Further experiments were carried out using pools that were generated from 30-33 independent clones.

**Figure 16 Restriction Analysis of DNA Constructs Containing Wild-Type and Modified  $\mu$  Genes.** (a) Schematic representations of wild-type and modified  $\mu$  gene constructs, showing a nonsense linker (arrow) in the middle of the  $C\mu 2$  exon and the cDNA replacement of genomic sequences downstream of the nonsense codon. Double lines depict the positions of the restriction endonuclease sites. Photographs of ethidium bromide-stained 1.0% agarose gels are shown in panels b to d. All plasmids were diluted and quantitated to the same concentration for further experiments. 1  $\mu$ g DNA of each construct was digested with 0.2-0.5 units of enzyme and the digestion reaction was performed according to the manufacturer's instructions. DNA standards used to determine the size of DNA fragments: 1 kb DNA ladder (lane 1) and  $\lambda$ /*Hind*III (lane 8). In panel b, the integrity of the constant region of  $\mu$  gene was confirmed by *Eco*RI-*Spe*I digestion; In panel c, the accuracy of cDNA replacement in the constant region of  $\mu$  gene was confirmed by *Bst*EII digestion; and, in panel d, the presence of *Nhe*I-containing nonsense linker at the proper positions was confirmed by *Nhe*I digestion. All the digests had the predicted sizes as indicated on the right. The fragment (\*) in lane 3 was not digested in panel b, but yielded expected products in an independent digestion.



**Figure 17 Restriction Analysis of DNA Constructs Containing Wild-Type and Modified  $\mu$  Genes Containing a Nonsense Codon at Different Positions of the Constant Region of  $\mu$  Gene.** (a) Schematic representations of wild-type and modified  $\mu$  gene constructs, showing the nonsense linker (arrows) in different exons of the  $\mu$  gene. Double lines depict the positions of restriction endonuclease sites. (b) A photograph of an ethidium bromide-stained 1.0% agarose gel. All plasmids were diluted and quantified to the same concentration for further experiments. 1  $\mu$ g DNA of each construct was digested with 0.2-0.5 units of *NheI* and the digestion reaction was performed according to the manufacturer's instructions. The presence of the *NheI*-containing nonsense linker at the proper positions was confirmed by *NheI* digestion. The resulting digests have the predicted sizes as indicated at left. The integrity of the constant region of  $\mu$  gene was confirmed by the *EcoRI-SpeI* digestion (data not shown). DNA standards used to determine the size of DNA fragments: 1 kb DNA ladder (lane 1) and  $\lambda$ /*HindIII* (lane 8).

**a****b**

#### 4.2.2 Positional Effect of a Nonsense Codon on the Steady-State Level of $\mu$ mRNA.

Total RNA in stable transfectants was isolated by the GIT/CsCl method and analyzed by Northern blot analysis using a  $C\mu$  probe. Results of two independent experiments with similar findings are shown in Figures 18A and 18B. In Figure 18A, the relative steady-state level of  $\mu$  mRNA ( $[\mu]$ ) was calculated by dividing the hybridization signal from  $\mu$  mRNA by the signal of gpt mRNA (panel c). I found that the levels of  $\mu$  mRNA with nonsense codons in the middle of  $C\mu 1$ ,  $C\mu 2$ , and  $C\mu 3$  exons were decreased by at least 5 fold (lane 3, 5, and 6, respectively, in Figure 18A) when compared to control level (lane 2 in Figure 18A). In contrast, the level of  $\mu$  mRNA with a nonsense codon in the middle of  $C\mu 4$  exon (lane 7 in Figure 18A) was comparable to control  $\mu$  mRNA (lane 2 in Figure 18A). These data are consistent with the translational translocation model. However, the level of  $\mu$  mRNA with a nonsense codon at the end of  $C\mu 1$  exon (construct C, lane 4 in Figure 18A) was about 80% of total  $[\mu]$  detected in  $\mu$  mRNA without a nonsense codon (construct A, lane 2 in Figure 18A). The relatively stable level of  $\mu$  mRNA in stable transfectants containing construct C might result from: a) a cloning or transfection error; b) the mRNA has skipped the exon that contains a nonsense codon (i.e.,  $C\mu 1$  exon in this case); or c) the translational translocation model is not the mechanism by which  $\mu$  mRNA with a nonsense codon is degraded. This is because the translational machinery in the cytoplasm should recognize the nonsense codon and send out a degradation signal no matter where it is in the open reading frame.

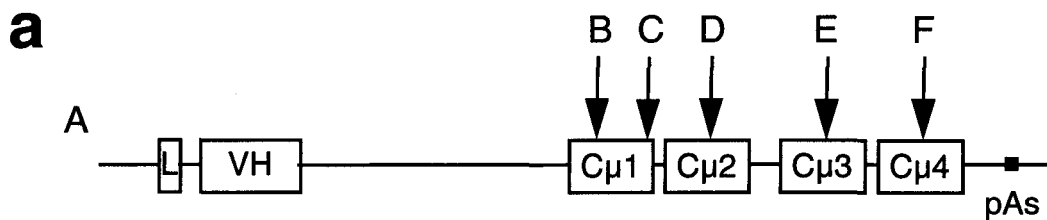
To distinguish among these possibilities, I performed immunoprecipitations using goat anti-IgM antibody. As shown in Figure 19, the presence of the nonsense codon at

F of  $\mu$  gene decreases the coding region of  $\mu$  mRNA by 142 nt, which results in the truncated protein being about 47 amino acids shorter (that correlates to 5.2 KD deletion in molecular mass) than the complete  $\mu$  chain (lane 9 in Figure 19). For C-containing transfectants, the 1013 kb nucleotide sequence downstream of the nonsense codon correlates with 338 amino acids shorter in the truncated protein of 32 KD (lane 6 in Figure 19). Consistent with the lower levels of  $\mu$  mRNA expression (Figure 18A and 18B), there were no detectable  $\mu$  proteins in lysates isolated from stable transfectants containing constructs B, D and E (lane 5, 7 and 8, respectively, in Figure 19). Thus, I conclude that the size of truncated proteins are consistent with the expected products predicted from the positions of the nonsense codon. These data ruled out the possibility of a cloning or transfection error, or exon skipping. However, these truncated proteins were not secreted into the supernatant (lane 12 and 15, respectively).

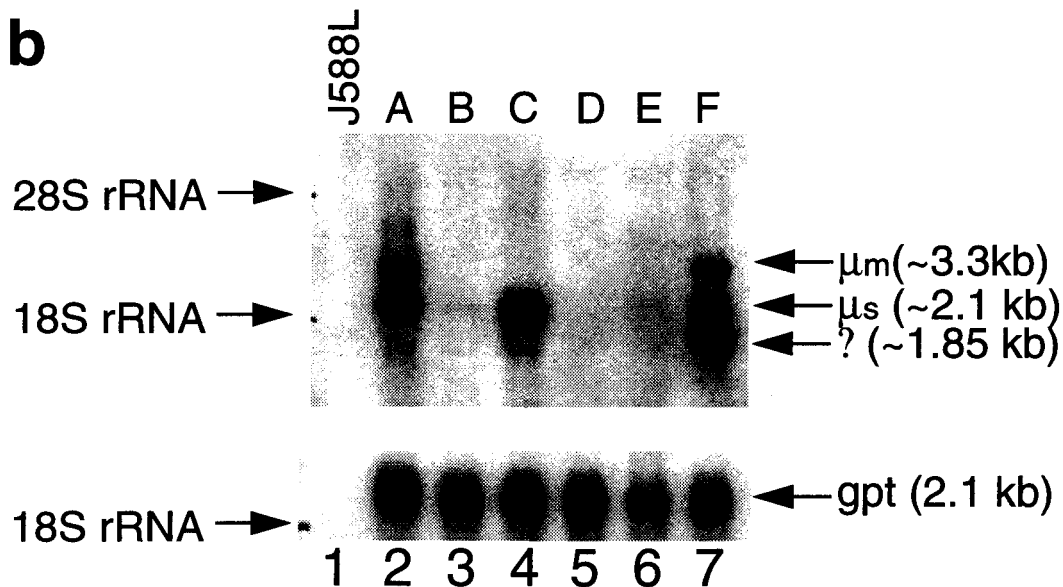
The multiple bands of  $\mu$  mRNA in lanes 2 and 7 in Figure 18A were not reproducible, as shown in lanes 3 and 4 in Figure 18B. The different sizes of  $\mu$  mRNA might result from the alternative use of either a membrane or a secreted poly A site. This may result from the presence of two polyadenylation sites in the plasmid  $p\mu^*gpt\Delta M$  (Figure 15), although the membrane exons have been deleted. The distance between the two poly A sites is about 350 bp, which may account for the difference in size of multiple bands I found in Figure 18A. Alternatively, the differences in the size of  $\mu$  mRNA might result from the presence of a nonsense codon. This is unlikely because the multiple bands were also found in stable transfectants containing functional  $\mu$  gene (lane 2

**Figure 18A Analysis of  $\mu$  mRNA Expression in *J558L* Transfectants Containing a Nonsense Codon at the Different Positions of the Constant Region in the Gene.** (a) Schematic representations of wild-type and modified  $\mu$  gene constructs, showing the nonsense linker (arrows) at different positions of  $C\mu$  exons. (b) A representative autoradiogram of the nitrocellulose blot hybridized with a  $C\mu$  cDNA probe (as shown in Figure 1). Total RNA (10  $\mu$ g) from pooled *J558L* transfected cells was isolated by the GIT/CsCl method and subjected to Northern blot analysis as described in the legend to Figure 3A. The same blot was rehybridized with a gpt probe to control for the loading of RNA. (c) The radioactivity of the bands was determined by a betascope blot analyzer, and relative amounts of  $\mu$  mRNA (indicated sizes of  $\mu$  mRNA were scanned in each lane) were calculated by dividing the  $\mu$  signal by the gpt signal. The presence of a nonsense codon in the middle of  $C\mu 1$  (construct B, 17%),  $C\mu 2$  (construct D, 15%), and  $C\mu 3$  (construct E, 20%) decreases the [ $\mu_s$ ] by at least 5 fold when compared to the control [ $\mu$ ] (construct A, setting to 100%). The presence of a nonsense codon at the end of the  $C\mu 1$  exon (construct C, 135%) and in the middle of the  $C\mu 4$  exon (construct F, 83%) did not decrease the [ $\mu_s$ ] when compared to the control. Lane 1, non-transfected *J558L* cells were used as a negative control. Arrows on the left indicate the positions of ribosomal RNAs; on the right indicate the positions of  $\mu$  and gpt mRNAs.





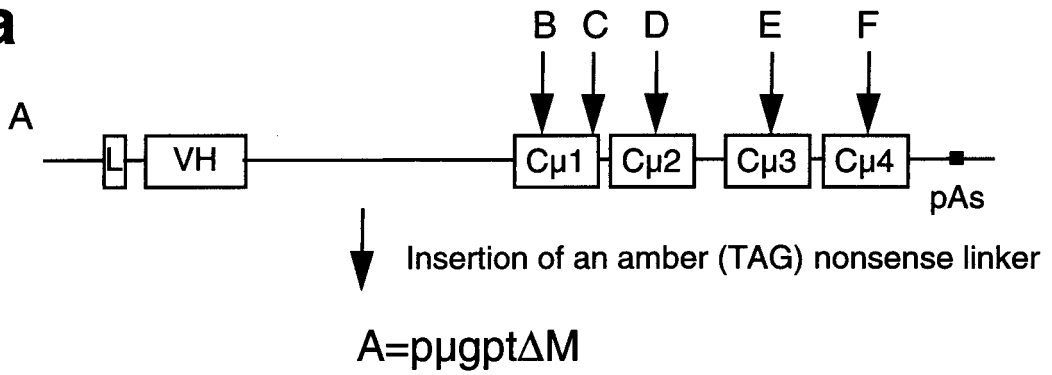
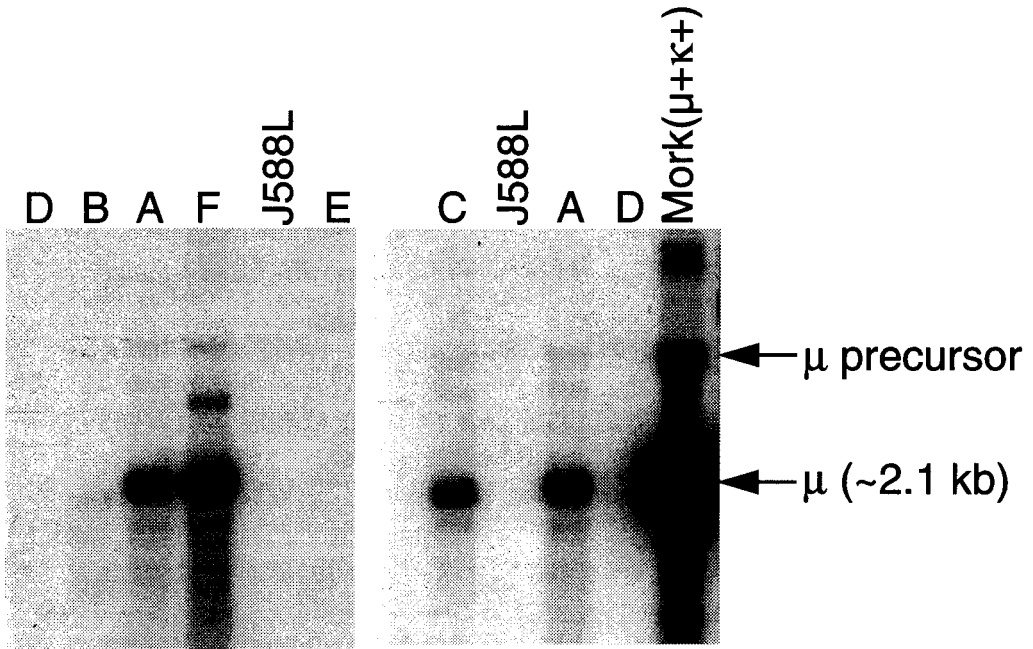
↓ Insertion of an amber (TAG) nonsense linker



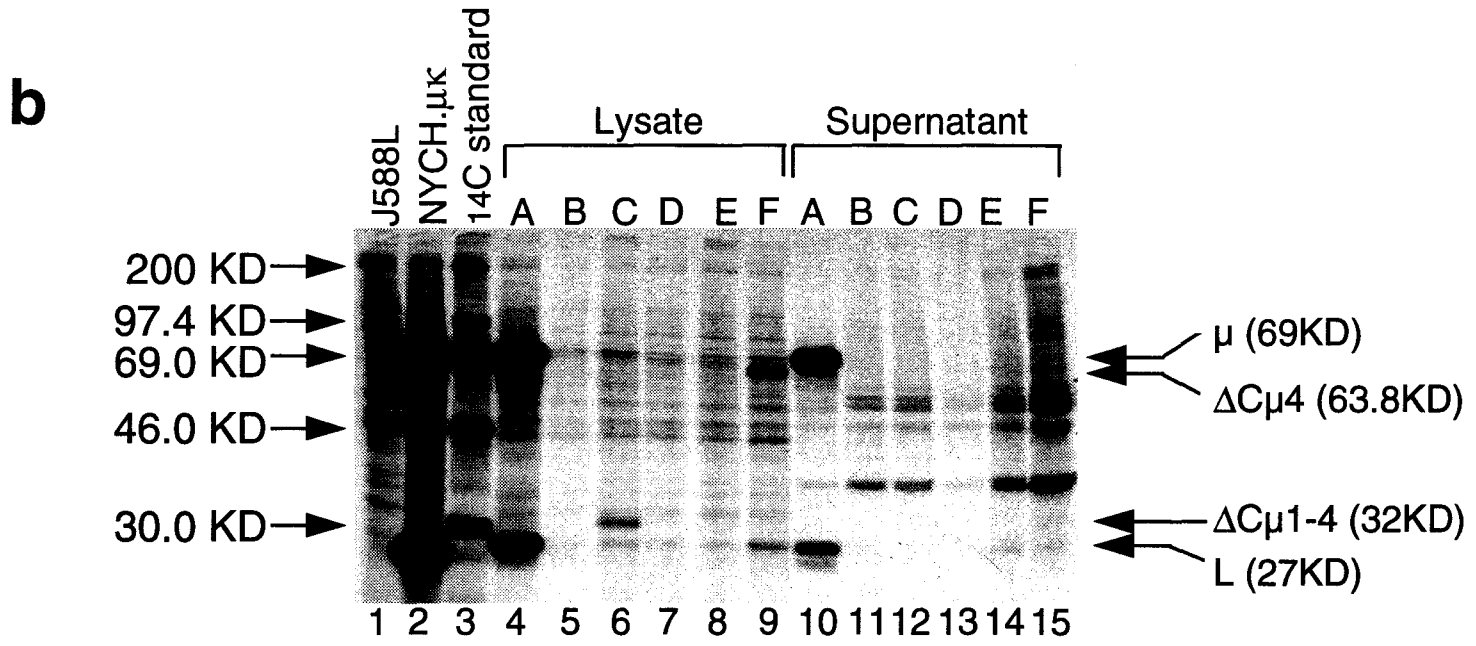
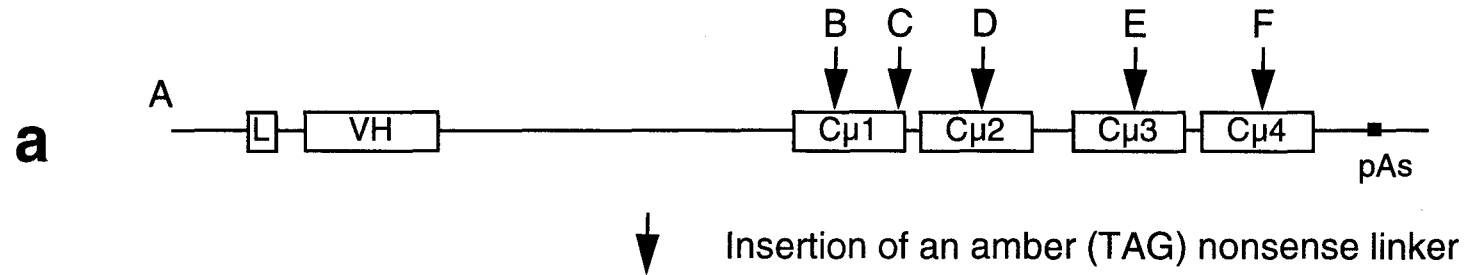
**c**

[ $\mu_m$ ]	0.59	0.52
[ $\mu_s$ ]	0.82 0.14 1.11 0.12 0.17 0.68	
[other band]		1.15
total [ $\mu$ ]	1.41	2.35

**Figure 18B Analysis of  $\mu$  mRNA Expression in *J558L* Transfectants Containing a Nonsense Codon at the Different Positions of the Constant Region in the Gene.** (a) Schematic representations of wild-type and modified  $\mu$  gene constructs, showing the nonsense linker (arrows) at different positions in  $C\mu$  exons. (b) A representative autoradiogram of the nitrocellulose blot hybridized with a  $C\mu$  cDNA probe (as shown in Figure 1). Total RNA (10  $\mu$ g) from pooled transfected *J558L* cells was isolated by the GIT/CsCl method and subjected to Northern blot analysis as described in the legend to Figure 3A. The same blot was rehybridized with a *gpt* probe to control for the loading of RNA. Lanes 5 and 8, nontransfected *J558L* cells were used as a negative control. Arrows on the right indicate the positions of precursor  $\mu$  RNA and  $\mu$  mRNA. The hybridization signals in this Figure were not quantitated.

**a****b****c**

**Figure 19 Analysis of Intracellular and Secreted  $\mu$  Heavy Chain Expression in *J558L* Transfectants Containing a Nonsense Codon at the Different Positions of the Constant Region in the Gene. (a) Schematic representations of wild-type and modified  $\mu$  genes, showing the nonsense linker (arrows) at different exons in  $\mu$  gene. (b) A fluorograph of an immunoprecipitation experiment. [ $^{35}\text{S}$ ]-methionine biometabolically labeled cell extracts and supernatant of *J558L* transfectants were incubated with goat antisera against mouse IgM, followed by *S. aureus*. Solubilized proteins were analyzed by SDS-PAGE on a 10% acrylamide gel, and labeled proteins were detected by fluorography. Lane 1, *J558L* plasmacytoma cells; lane 2, NYCH. $\mu\kappa$  cells that express  $\mu$  and  $\kappa$  chains; lanes 4 to 15, different pools of *J558L* cells transfected with wild-type and modified  $\mu$  genes as depicted in a. The protein with a molecular weight (MW) of 32 KD (lane 6) was identified as  $\Delta\text{C}\mu_{1-4}$ , because it has the predicted MW of a nonsense codon at C site in panel a. For the same reason, a protein of 63.8 KD has been identified as  $\Delta\text{C}\mu_4$ . All these truncated proteins are not secreted outside the cell (lane 11 and 15, respectively).**



in panel b of Figure 18A. Thus the presence of multiple bands that hybridized to a  $\mu$  cDNA probe is probably not due to the presence of a nonsense codon, and it may result from use of an alternative poly A site.

#### 4.2.3 cDNA Replacement of Sequences Downstream of a Nonsense Codon Does Not Restore its Steady-State Level of Ig $\mu$ mRNA to Its Wild-type

Another approach to test whether a nonsense codon decreases the steady-state level of  $\mu$  mRNA by inhibiting the splicing of downstream sequences is to replace the genomic sequences downstream of the nonsense codon with their corresponding cDNA sequences, and analyze its effect on the steady-state level of  $\mu$  mRNA.

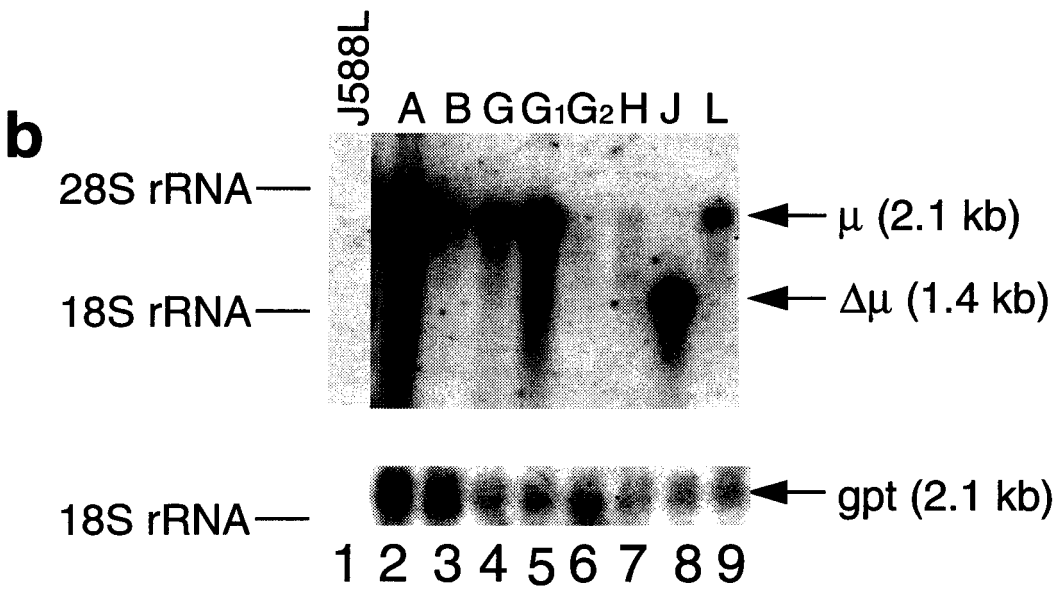
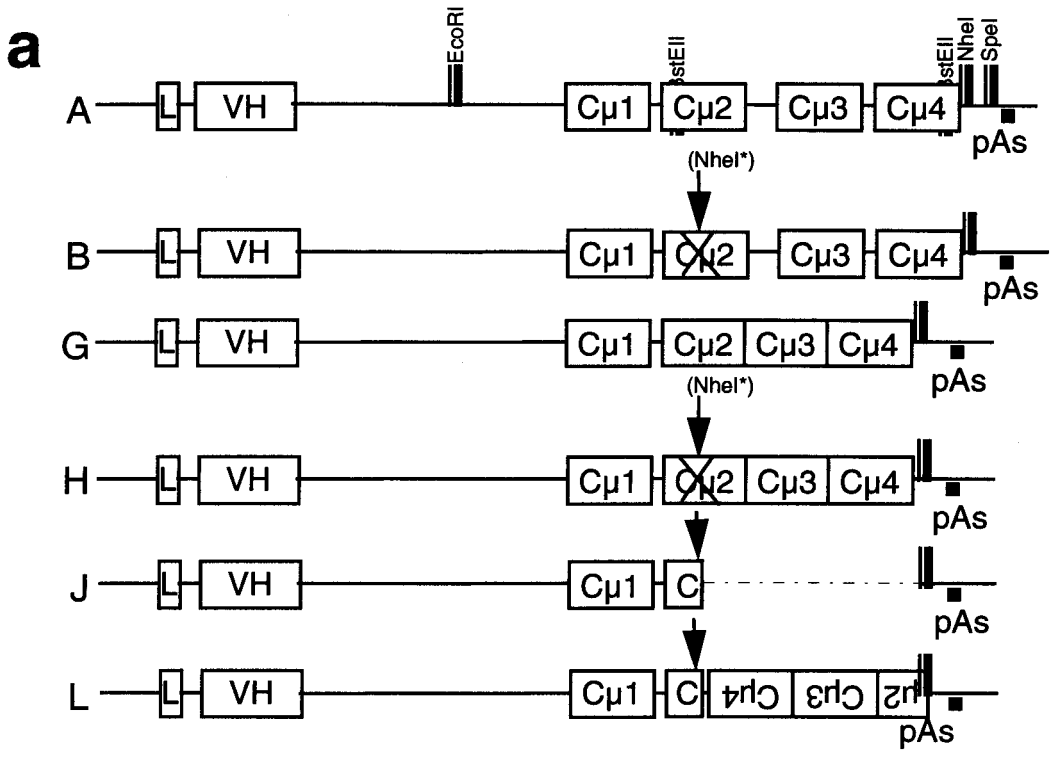
Total RNA in stable transfectants was isolated by the GIT/CsCl method and analyzed by Northern blot analysis using a  $C\mu$  probe (panel b in Figure 20A and 20B). The relative steady-state level of  $\mu$  mRNA was calculated by dividing the hybridization signal from  $\mu$  mRNA by the signal of gpt mRNA (panel b of Figure 20A and 20B), and are summarized in panel c.  $G_1$  and  $G_2$  represent RNA isolated from stable transfectants that were generated by two independent constructs from the same cloning process (i.e., the genomic sequences downstream of the nonsense codon had been replaced by their corresponding cDNA sequences). G represents RNA isolated from the stable transfectant that was generated by mixing equal amount of  $G_1$  and  $G_2$ . The undetectable level of  $\mu$  mRNA in  $G_2$  (lane 6 in Figure 20A and lane 4 in Figure 20B) might result from an unnoticed mutation in its DNA construct. The levels of  $\mu$  mRNA ( $[\mu]$ ) in the transfectants of construct G and  $G_1$  (lane 4 and 5 in Figure 20A, respectively) were 2 to 4 times lower than that of wild-type (lane 2). This might result from either another cloning or

transfection error, or small introns between  $C_{\mu 2-3}$  and/or  $C_{\mu 3-4}$  are required for good expression of  $\mu$  mRNA (See detailed discussion below).

The level of  $\mu$  mRNA in the transfectants of construct H (cDNA replacement with a nonsense linker in the middle of  $C_{\mu 2}$  exons) was at least 20 fold lower (lane 7 in Figure 20A and lane 5 in Figure 20B) when compared to the control (lane 2 in Figure 20A and 20B). This result can be explained in two ways. One is that there is a cloning error. This possibility was excluded by the result of the immunoprecipitation, in which I found truncated  $\mu$  protein in the lysate of H transfectants (lane 6 and 9, respectively, Figure 21) was 40 KD. Their sizes were consistent with the expected products predicted from the positions of the nonsense codon (that is, a deletion of 790 nucleotides correlating with the loss of 263 amino acids). These data also ruled out the possibility of a cloning or transfection error, or exon skipping. Since I have repeated these experiments twice, it is unlikely that the same error has been repeated. The other possibility is that this result also argues against the translational translocation model.

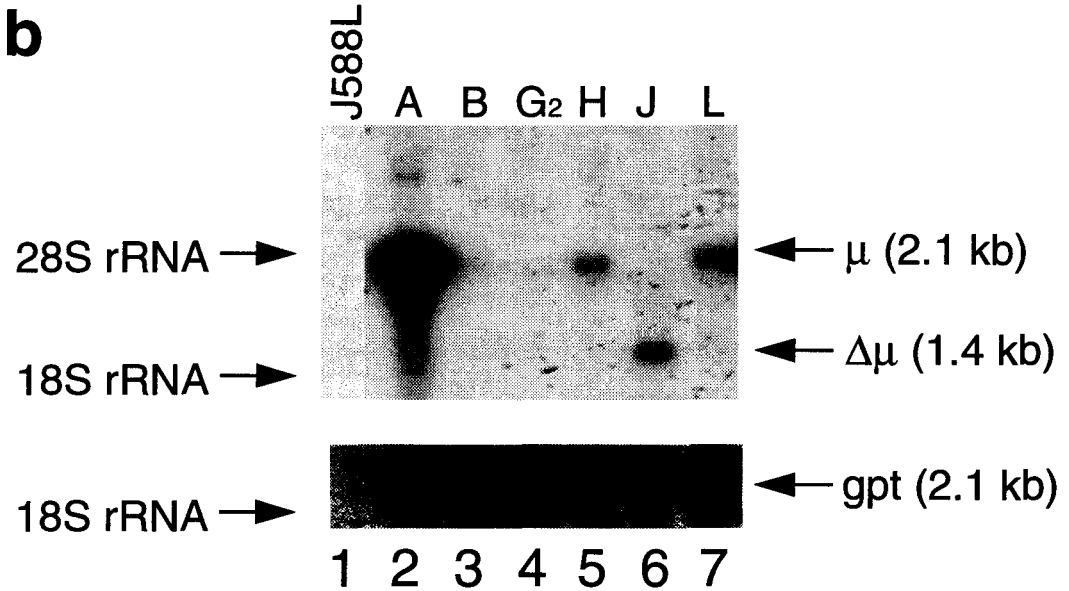
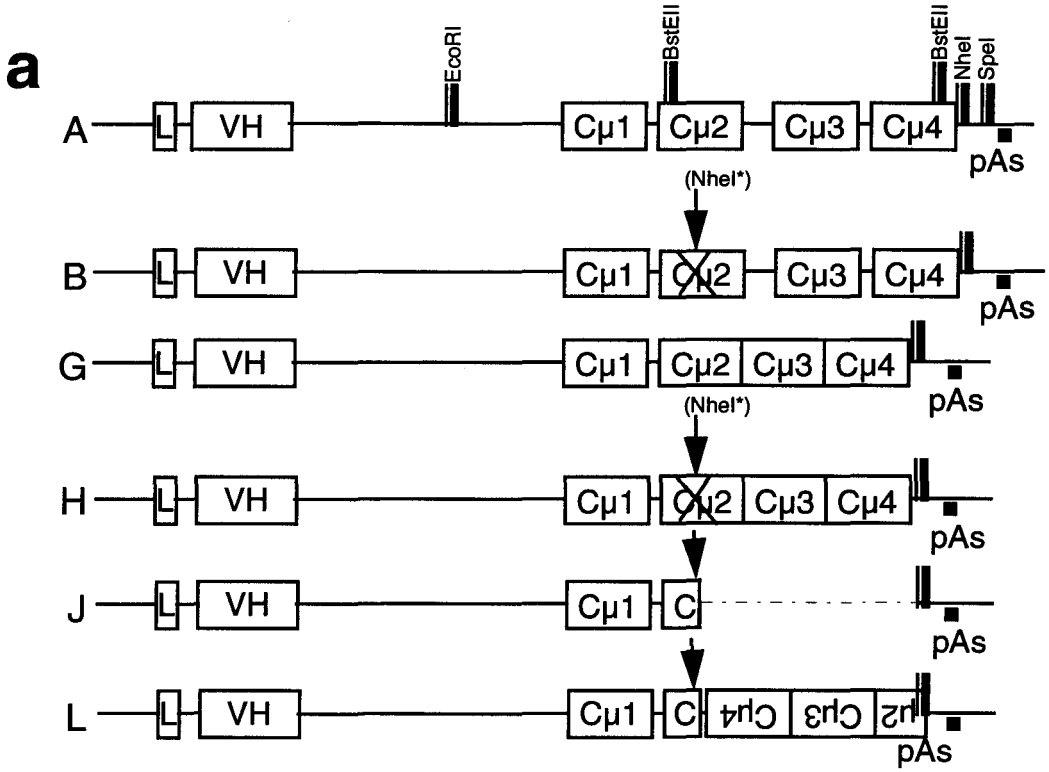
**Figure 20A Analysis of  $\mu$  mRNA Expression in *J558L* Transfectants Containing Modified  $\mu$  Genes.** (a) Schematic representations of wild-type and modified  $\mu$  genes, showing a nonsense linker (arrow) in the middle of the  $C\mu 2$  exon and the cDNA replacement of genomic sequences downstream of the nonsense codon. (b) Northern blotting of  $\mu$  mRNAs. Total RNA (10  $\mu$ g) from *J558L* cells stably transfected with various  $\mu$  genes was isolated by the GIT/CsCl method and subjected to Northern blot analysis as described in the legend to Figure 3A. Nontransfected *J558L* cells were used as a negative control (lane 1).  $G_1$  and  $G_2$  represent RNA isolated from stable transfectants that were generated by two independent constructs of the same cloning process.  $G$  represents RNA isolated from a stable transfectant that was generated by mixing equal amounts of  $G_1$  and  $G_2$ . The presence of a nonsense codon in the middle of  $C\mu 2$  exon (lane 3) decreases the  $[\mu]$  by about 30 fold when compared to the control  $[\mu]$  (lane 2). The levels of  $\mu$  mRNA ( $[\mu]$ ) were 2 to 4 fold lower in the transfectants containing construct  $G$  and  $G_1$  (lane 4 and 5, respectively); 4 fold lower in the transfectants containing construct  $J$  (lane 8); and 50 fold lower in transfectants containing construct  $L$  (lane 9), than that of wild-type control (lane 2). The  $[\mu]$  in transfectants containing constructs  $G_2$  and  $H$  was below the detectable limit ( $\leq 0.1\%$  of the  $[\mu]$  in transfectants containing construct  $A$ ).





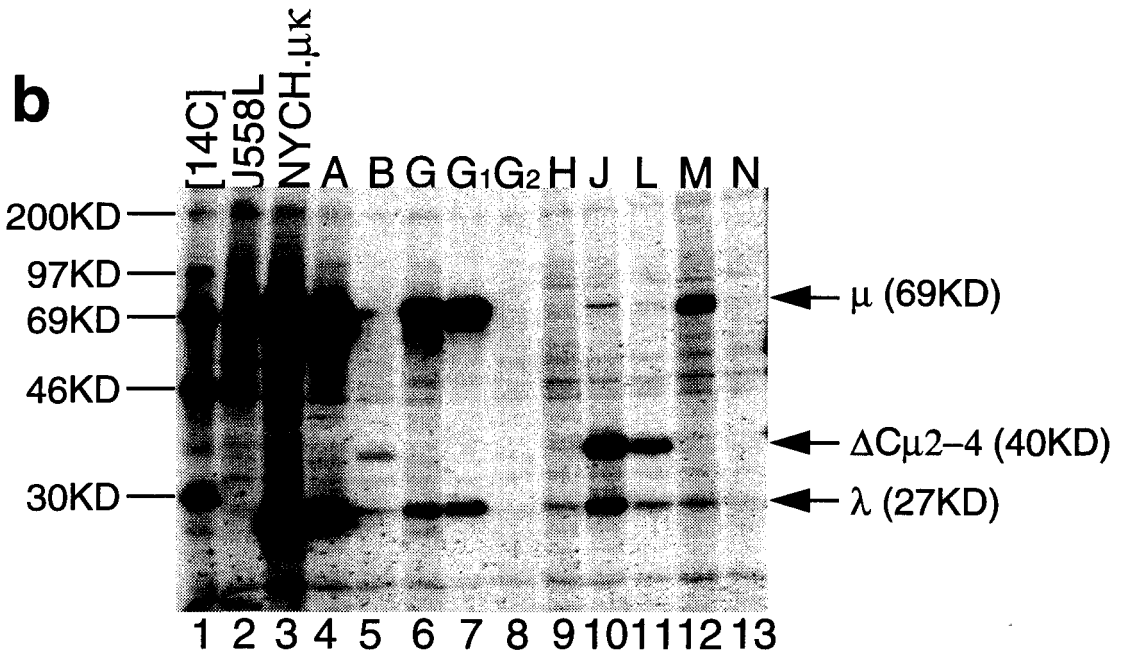
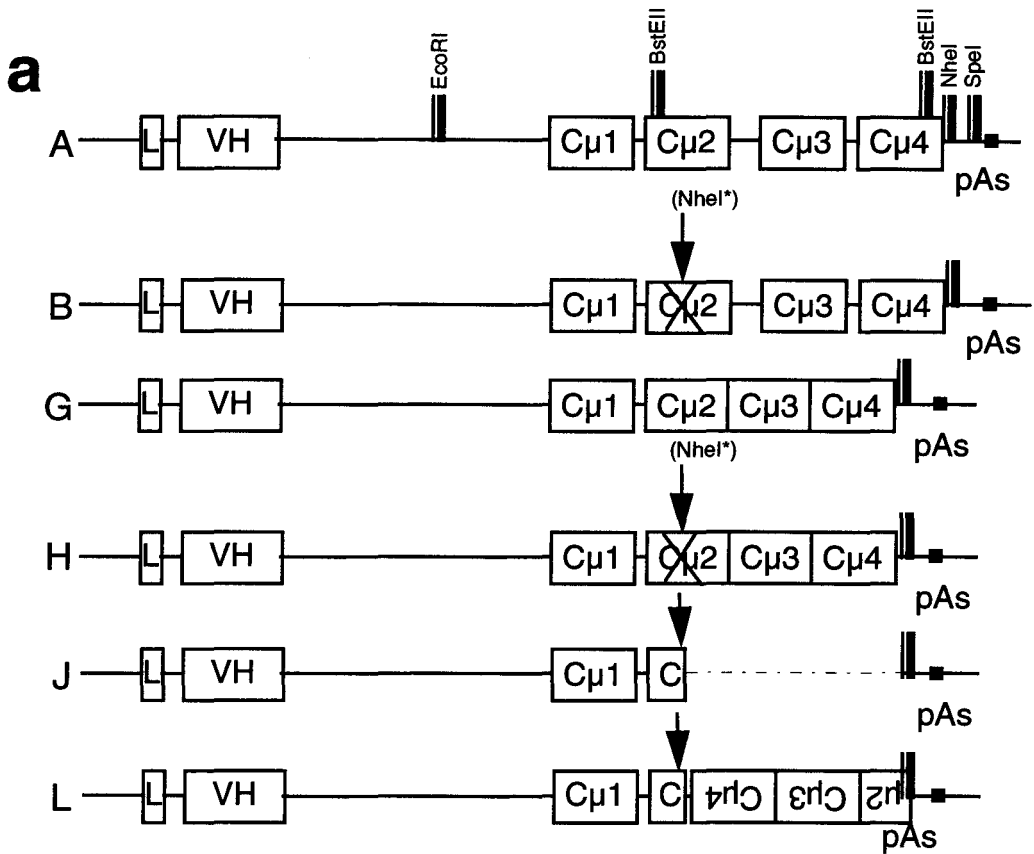
**c**      %[μ]:    100 2.9 23 56 <0.1 25 2.0

**Figure 20B Analysis of  $\mu$  mRNA Expression in *J558L* Transfectants Containing Modified  $\mu$  Genes.** (a) Schematic representations of wild-type and modified  $\mu$  genes, showing a nonsense linker (arrow) in the middle of the  $C\mu 2$  exon and the cDNA replacement of genomic sequences downstream of the nonsense codon. (b) Northern blotting of  $\mu$  mRNAs. Total RNA (10  $\mu$ g) from transfected *J558L* cells was isolated by the GIT/CsCl method and subjected to Northern blot analysis as described in the legend to Figure 3A (upper panel). The same blot was rehybridized with a *gpt* probe to control for the loading of RNA (lower panel). (c) The relative steady-state level of  $\mu$  mRNA was calculated by dividing the hybridization signal from  $\mu$  mRNA by the signal to *gpt* mRNA on the same lane. Lane 1, non-transfected *J558L* cells were used as a negative control. Arrows on the left indicate the positions of ribosomal RNAs; on the right indicate the positions of precursor  $\mu$  RNA,  $\mu$  mRNA and *gpt* mRNA.



**c**      %[μ]:            100 5.3 2.3 6.1 18 8.7

**Figure 21 Analysis of Intracellular  $\mu$  Heavy Chain Expression in *J558L* Transfectants Containing Modified  $\mu$  Genes.** (a) Schematic representations of the wild-type and modified  $\mu$  genes, showing a nonsense linker (arrow) in the middle of the  $C\mu 2$  exon and the cDNA replacement of genomic sequences downstream of the nonsense codon. (b) A fluorograph of an immunoprecipitation. [ $^{35}\text{S}$ ]-methionine biometabolically labeled cell extracts of *J558L* transfectants were first incubated with goat antisera against mouse IgM, followed by *S. aureus*. Solubilized proteins were analyzed by SDS-PAGE on a 10% acrylamide gel, and labeled proteins were detected by fluorography. The protein with a MW of 40 KD (lane 5, 10 and 11) was identified as  $\Delta C\mu 2-4$ , because it has the predicted MW of a nonsense codon in the middle of  $C\mu 2$ . Lane 1, *J558L* plasmacytoma cells; lane 2, NYCH. $\mu\kappa$  cells that expresses  $\mu$  and  $\kappa$  chains; lanes 4 to 15, different pools of *J558L* cells transfected with wild-type and modified  $\mu$  genes as depicted in a. M and N are RNA isolated from cell lines containing  $\mu$  cDNA under the control of Pcmv (see panel a in Figure 22 for illustration and section 4.2.4 for discussion).

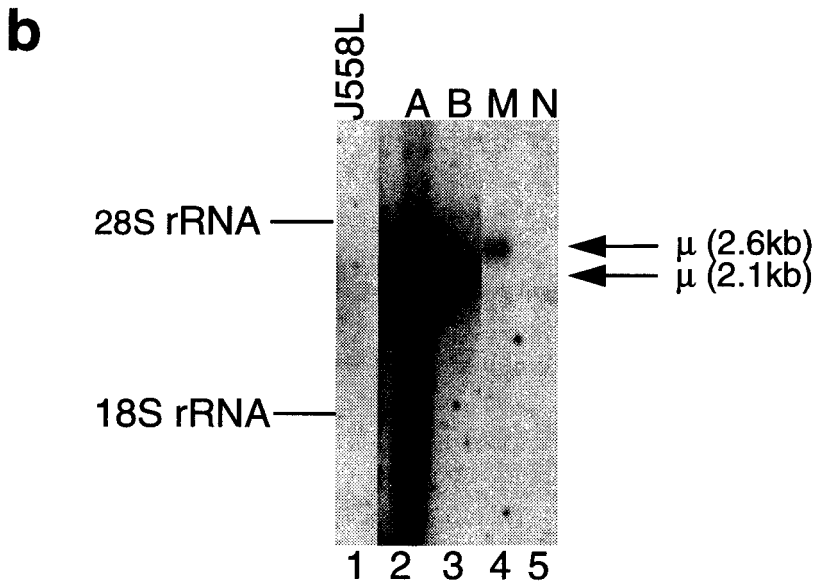
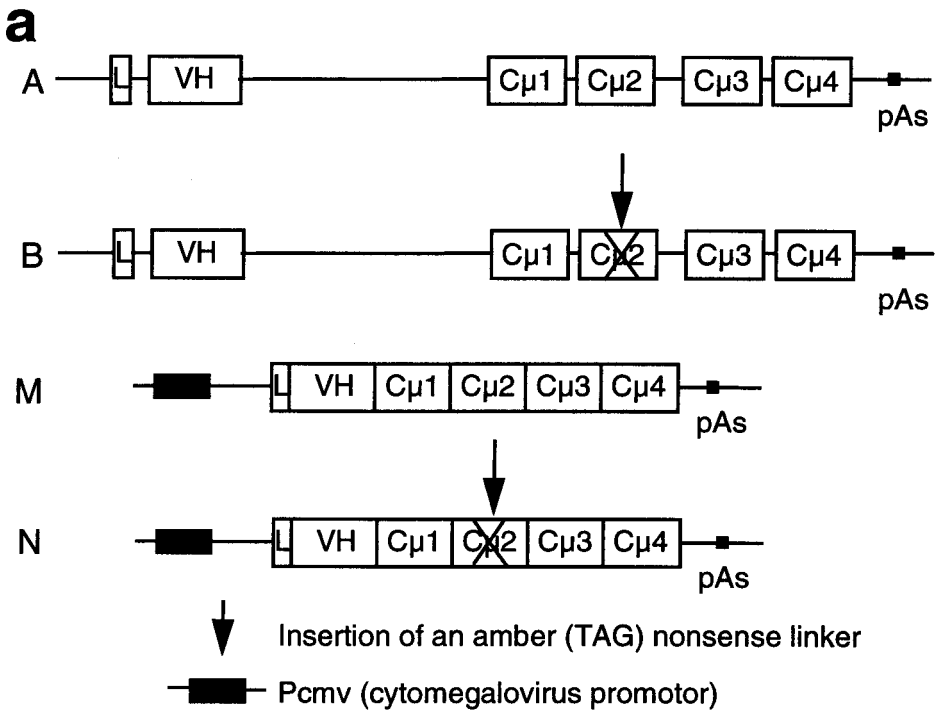


#### 4.2.4 Removal of Intron Sequences from Ig $\mu$ Gene Does Not Protect Its mRNA from Nonsense Codon-Mediated RNA Degradation.

To determine whether a nonsense codon affects the steady-state level of  $\mu$  mRNA by interfering with its splicing process, I cloned a  $\mu$  cDNA clone with or without a nonsense codon in the middle of the  $C\mu 2$  exon into a cytomegalovirus promoter (pCMV)-based expression vector and analyzed the steady-state level of  $\mu$  mRNA in stably transfected cells.

While the level of  $\mu$  mRNA derived from a cDNA clone under the Pcmv (lane 4 in Figure 22) was only 5% of the level of genomic  $\mu$  gene under the IgH promoter (lane 2 in Figure 22), the level of  $\mu$  mRNA derived from the  $\mu$  cDNA clone with a nonsense codon was undetectable (lane 5 in Figure 22). If these results are reproducible, they suggest that the removal of introns from the  $\mu$  gene cannot abrogate the effect of a nonsense codon on the  $\mu$  mRNA level. Thus, these data argue against the effect of a nonsense codon on splicing, at least as the only mechanism, in  $\mu$  mRNA metabolism. However, the low level of total  $\mu$  mRNA with a nonsense codon derived from a Pcmv may result from either the nuclear-cytoplasmic transport of  $\mu$  mRNA being blocked, or the mature  $\mu$  mRNA with a nonsense codon being subjected to the effect of other nuclear or cytoplasmic degradation events. The effect of cytoplasmic RNA degradation is supported by my previous finding that additional cytoplasmic degradation contributes to the low steady-state level of  $\mu$  mRNA with a nonsense codon (see Chapter III).

Figure 22 **Expression of  $\mu$  mRNA Transcribed from Pcmv- $\mu$  cDNA with or without a Nonsense Codon in J558L Transfectants.** (a) Schematic representations of  $\mu$  mRNA transcribed from Pcmv-cDNA with or without a nonsense codon, showing a nonsense linker (arrow) in the middle of the C $\mu$ 2 exon. (b) Northern blotting of  $\mu$  mRNAs. Total RNA (10  $\mu$ g) from J558L cells stably transfected with various  $\mu$  genes was isolated by the GIT/CsCl method and subjected to Northern blot analysis as described in Materials and Methods and in the legend to Figure 3A. Nontransfected J558L cells were used as a negative control (lane 1). Lanes in this figure are pasted together from the same RNA agarose gel in Figure 20A. The autoradiogram of gpt hybridization is not shown here. The larger size of  $\mu$  mRNA in lane 4 results from the size of Pcmv is about 0.5-kb bigger than that of PIg (Deuschle *et al.*, 1989; Grosschedl and Baltimore, 1985).



**c**

%[ $\mu$ ]	1	2	3	4	5
	100	2.9	0.5	<0.1	<0.1



### 4.3 Discussion

#### 4.3.1 A Nonsense Codon Does Not Affect the Steady-State Level of $\mu$ mRNA by Preventing the Splicing of Its Downstream Sequences

The level of  $\mu$  mRNA with a nonsense codon at the end of the  $C_{\mu 1}$  exon (construct C) when compared to its wild-type counterpart (construct A) strongly argues against the translational translocation model (Figure 18A and 18B). This is strengthened by the finding that neither a cDNA replacement of downstream sequences to the nonsense codon (Figure 20A and 20B) nor cDNA clone with a nonsense codon expressed under a Pcmv (Figure 22) restored the level of  $\mu$  mRNA to its wild-type counterpart. Together with the data in Chapter III, in which I found long precursor  $\mu$  transcripts in hybridomas *VXH* and *CH2XH* that contain nonsense codons in their  $\mu$  genes, I suggest that degradation of  $\mu$  mRNA with a nonsense codon involves more complicated mechanisms rather than simply the cytoplasmic translational machinery sending out signals to inhibit the nuclear splicing process. An alternative explanation for the finding that a nonsense codon affects splicing of  $\mu$  RNA is via nuclear scanning rather than cytoplasmic recognition: The nonsense codon is recognized by a nuclear degradation factor before, or at the time of, RNA splicing. Since the spliceosome or other nuclear RNA binding protein are bound to the RNA transcript in the nucleus (Green, 1991; Dreyfuss *et al.*, 1992), they might sequester the nonsense codon from recognition by a nuclear scanning system. However, I could not rule out the possibility of recognition being independent of RNA splicing and somehow interacting with the splicing process (see discussion in Chapter III). This hypothesis needs to be further tested.

Consistent with my finding in Chapter III that the presence of a nonsense codon

reduces  $\mu$  mRNA level by increasing the cytoplasmic turnover rate, I found that the level of  $\mu$  mRNA derived from a  $\mu$  cDNA with a nonsense codon in the middle of  $C_{\mu 2}$  exon under the control of Pcmv was undetectable when compared to that of its wild-type counterpart. This suggests that an additional cytoplasmic event degrades  $\mu$  mRNAs with nonsense codons even if they can escape the nuclear degradation event. However, this cytoplasmic degradation factor probably has a very short half-life or it only acts as a secondary surveillance after the nuclear degradation event (see discussion in Chapter III). Alternatively, the presence of a nonsense codon may also prevent the nucleus-cytoplasm transport of  $\mu$  mRNA. It might be important for B cells to have more than one surveillance pathway to eliminate the Ig mRNA with nonsense codons, and thus ensure an effective humoral immune response.

#### 4.3.2 Introns Are Required for Effective Expression of $\mu$ Gene

The difference between the  $\mu$  mRNA steady-state levels of construct G and A was unexpected (Figure 20), and might argue that small introns between  $C_{\mu 2-3}$  and  $C_{\mu 3-4}$  are required for effective expression of  $\mu$  mRNA. This is consistent with a study which showed that an intron is required for optimal expression of cytoplasmic  $\mu$  mRNA (Neuberger and Williams, 1988). This intron requirement is not specific for a particular intron, but has a cumulative effect, i.e. as long as an intron is present in the expression vector, the steady-state level of cytoplasmic  $\mu$  mRNA is increased; and the more introns that are present in the expression vector, the higher the steady-state level of cytoplasmic  $\mu$  mRNA. Cooperation between introns has been reported to increase both the specificity

and the efficiency of splicing (Neel *et al.*, 1993). On the other hand, this intron requirement has also been shown to be promoter-dependent: An intron is required in the case of Ig or  $\beta$ -globin promoters, but not in the case of cytomegalovirus or heat-shock promoters (Neuberger and Williams, 1988). Furthermore, this intron requirement is also cell-type independent since it is also needed in fibroblast transfectants (Neuberger and Williams, 1988).

Intron requirement has also been shown to be necessary for effective expression of other eukaryotic genes (Reviewed by Liu, 1994), such as human, mouse and rabbit  $\beta$ -globin (Hamer and Leder, 1979; Buchman *et al.*, 1988; Collis *et al.*, 1990), mouse dihydrofolate reductase (Gasser *et al.*, 1982; Buchman *et al.*, 1988), human triosephosphate isomerase (Nesic *et al.*, 1993 and 1994), SV40 late transcripts (Ryu and Mertz, 1989), human purine nucleoside phosphorylase (Jonsson *et al.*, 1992), mouse thymidylase synthase (Deng *et al.*, 1989), and maize alcohol dehydrogenase-1 (Callis *et al.*, 1987; Ryu and Mertz, 1989). In contrast, many cellular and viral genes do not contain introns, and introns are not needed for effective expression from most cDNA clones. I do not know what features of a gene determine the intron requirement of effective production of cytoplasmic mRNA. However, it is very interesting to find that at least four of the genes (Ig,  $\beta$ -globin, and dihydrofolate reductase, TPI) degrade their nonsense codon-containing mRNAs via a unique nuclear mechanism, i.e. RNA processing and/or transport. Thus, I speculate that the intron requirement for effective gene expression might be a common feature for genes that are subjected to nonsense codon-mediated mRNA degradation via a nuclear process.

It has been shown that for most genes, the presence of introns does not significantly influence their transcriptional rates (Hamer and Leder, 1979; Ryu and Mertz, 1989; Ryu and Mertz, 1989; Collis *et al.*, 1990); rather, their presence has very dramatic post-transcriptional effects on mRNA metabolism, including stabilization of primary transcripts within the nucleus, excision of introns, polyadenylation, and transport of mature mRNA to the cytoplasm (Hamer and Leder, 1979; Buchman and Berg, 1988; Ryu and Mertz, 1989; Collis *et al.*, 1990; Huang and Gorman, 1990). When an intron cannot provide the function required for efficient precursor RNA processing, its own excision occurs inefficiently (Ryu *et al.*, 1994).

The mechanism of intron requirement in gene expression is only speculative. Introns might influence post-transcriptional processes via their sequences associating with appropriate ribonucleoprotein (Dreyfuss *et al.*, 1992; Jarmolowski *et al.*, 1992). For example, their promoter dependence might result from different promoters being transcribed at different locations in the nucleus via specific transcriptional factors. I propose that for certain promoters, such as CMV and heat shock, transcripts are synthesized near the nuclear pore and can be readily exported. However, in the case of Ig and  $\beta$ -globin promoters, they might transcribe their primary mRNAs far from the nuclear pore, which makes their RNA export difficult. In these cases, factors that bind to introns might not only help to stabilize or splice the RNA, but also help to locate the RNAs on a track towards the nuclear pore and facilitate RNA export. If small introns such as intron 4 and/or 5 of  $\mu$  gene in construct G are missing, even if there is no nonsense codon,  $\mu$  transcript is degraded in the nucleus because it could not be

transported outside the nucleus. This also argues against the importance of the pulling effect of translation proposed by the translational translocation model (Urlaub *et al.*, 1989). The similar results from construct H, J and K might result from a scanning system that recognizing the nonsense linker as the authentic termination codon and the downstream sequences as different lengths of 3' untranslated region. Since there are no introns downstream to hold the RNA in the nucleus,  $\mu$  transcripts might be easily exported. This is supported by the finding that the use of different RNA polymerase II promoters influences the cytoplasmic stability of  $\beta$ -globin mRNA (Enssle *et al.*, 1993). This possibility argues against the use of other promoters with or without cDNA clones in the study of nonsense codon-mediated mRNA degradation of the genes that require intron for efficient expression.

#### 4.4 Proposed Further Experiments

##### 4.4.1 For the Result of Positional Effect of a Nonsense Codon

I showed that the presence of a nonsense codon at the end of  $C\mu 1$  exon did not decrease the  $\mu$  mRNA level when compared to that of its wild-type counterpart. To test whether this results from RNA binding protein sequestering (e.g. spliceosome) the nonsense codon at the end of an exon, one can introduce a nonsense codon at the beginning or the end of the  $C\mu 2$  exon, and repeat all the experiments. According to the current central dogma of splicing, both the 5' end and 3' end of an exon participate in the formation of a spliceosome (see reviews in Green, 1991; Lamond, 1993). If the spliceosome sequesters the recognition of nonsense codons by nuclear degradation factor,

one should find that the amount of  $\mu$  mRNA is comparable to that of its wild-type counterpart when the nonsense codon is present at either end of the  $C\mu 2$  exon. However, the final proof might come from the characterized degradation factor or splicing factor that is bound to the  $\mu$  mRNA from the construct C-containing transfectant. The other obstacle is that we also do not have a way to dissect the nuclear and cytoplasmic compartments. Further plans depend on the results of these experiments.

#### 4.4.2 For the Result of cDNA Replacement on $\mu$ mRNA Expression

To better control for the copy numbers between different transfectants, one might perform a nuclear run-on experiment to measure the transcriptional rate of  $\mu$  gene in construct A, G and H.

To rule out the possibility of unnoticed mutations in the H DNA construct that might affect our results, I have generated eight other independent clones. It would be unlikely that independent clones have the same unnoticed phenotype as observed before.

#### 4.4.3 For the Effect of a Nonsense Codon in $\mu$ mRNA Derived from Pcmv- $\mu$ cDNA

Since  $\mu$  gene expression in mammalian cells is promoter-dependent and intron-dependent, the use of a Pcmv to express the  $\mu$  gene from its corresponding cDNA clone might not reflect the  $\mu$  gene expression from its genomic sequence under the Ig promoter. Thus, one should be more cautious in interpreting data that are obtained from the use of a cDNA clone.

To better understand whether the use of a Pcmv to express  $\mu$  gene represents *in vivo*  $\mu$  gene expression, one can quantify the levels of nuclear  $\mu$  mRNA and cytoplasmic  $\mu$  mRNA by Northern blot analysis as described in Chapter III:

	<u><math>\mu</math> mRNA (WT):</u>	<u>cDNA</u>	<u>cDNA + a stop</u>
<u>Expected results:</u>			
	Total RNA	1X	decreased
Result A	Nuclear RNA	1X	decreased
	Cytoplasmic RNA	1X	decreased
Result B	Nuclear RNA	1X	1X
	Cytoplasmic RNA	1X	decreased

Result A suggests that the nuclear degradation event is independent of the splicing process. Result B might result from either the presence of additional cytoplasmic degradation machinery that can degrade mature  $\mu$  mRNA, or the blockage of nuclear-cytoplasm transport of  $\mu$  mRNA derived from the Pcmv-cDNA clone.

To determine whether  $\mu$  cDNA clone with a nonsense codon is degraded faster than its wild-type counterpart, one could use the Actinomycin C or DRB method as described in Chapter II and III. But one obstacle is that the amount of  $\mu$  cDNA expressed under the Pcmv is only 0.5% of the corresponding genomic  $\mu$  gene expressed from Ig promoter. Thus, one would probably start with too little  $\mu$  mRNA.

## SUMMARY

In summary, I have demonstrated that the presence of a nonsense codon reduces  $\mu$  mRNA levels in both the nucleus and the cytoplasm of plasma cells. In the nucleus, the presence of a nonsense codon prevents the splicing of the largest  $J_H-C\mu$  intron in precursor RNA. In the cytoplasm, the presence of a nonsense codon reduces  $\mu$  mRNA level by increasing the rate of  $\mu$  mRNA turnover. Thus, there are distinct cytoplasmic and nuclear mechanisms for the reduction of  $\mu$  mRNA with nonsense codons. The probability of producing nonproductive Ig mRNAs in the process of generating tremendous Ig diversity is higher than most of other mRNAs; therefore, the existence of at least two mechanisms to prevent the translation of nonproductive Ig mRNAs might be unique to B cells. However, the mechanism is much more complicated than one can imagine! To date, no model has been proposed that accounts for all the results emerging in the field. I think the main obstacle yet to be resolved is to determine whether the recognition of a nonsense codon occurs only in the cytoplasm, or only in the nucleus, or in both.



## REFERENCES

- Alt, F.W., Rosenberg, N., Casanova, R.J., Thomas, E. and Baltimore, D. (1982a) *Nature* **296**, 325-331.
- Alt, F.W., Rosenberg, N., Enea, V., Siden, E., Thomas, E. and Baltimore, D. (1982b) *J. Mol. Cell Biol.* **2**, 386-400.
- Alt, F.W., Yancopoulos, G.D., Blackwell, T.K., Wood, C., Thomas, E., Boss, M., Coffman, R., Rosenberg, N., Tonegawa, S. and Baltimore, D. (1984) *EMBO J.* **3**, 1209-1219.
- Altenburger, W., Steinmetz, M. and Zachau, H.G. (1980) *Nature* **287**, 603-607.
- Arnstein, H.R.V. and Cox, R.A. (1992) In: Protein synthesis, Oxford University Press, p89-91.
- Atkinson, M.J., Michnick, D.A., Paige, C.J. and Wu, G.E. (1991) *J. Immunol.* **146**, 2805-2812.
- Atwater, J.A., Wisdom, R. and Verma, I.M. (1990) *Ann. Rev. Genet.* **24**, 519-541.
- Aviv, H., Voloch, Z., Bastos, R. and Levy, S. (1976) *Cell* **8**, 495-503.
- Barker, G.F. and Beemon, K. (1991) *Mol. Cell. Biol.* **11**, 2760-2768.
- Baserga, S.J. and Benz Jr., E.J. (1992) *Proc. Natl. Acad. Sci. USA* **89**, 2935-2939.
- Baumann, B., Potash, M.J. and Köhler, G. (1985) *EMBO J.* **4**, 351-359.
- Belasco, J.G. and Brawerman, G. (1993) "Control of Messenger RNA Stability", eds: Academic Press, San Diego, USA.
- Belgrader, P., Cheng, J. and Maquat, L.E. (1993) *Proc. Natl. Acad. Sci. USA* **90**, 482-486.
- Belgrader, P. and Maquat, L.E. (1994) *Mol. Cell. Biol.* **14**, 6326-6336.

- Belgrader, P., Cheng, J., Zhou, X., Stephenson, L.S. and Maquat, L.E. (1994) *Mol. Cell. Biol.* **14**, 8219-8228.
- Birnie, G.D. (1978) *Methods Cell Biol.* **17**, 13-26.
- Bornemann, K.D., Brewer, J.W., Beck-Engesser, G.B., Corley, R.B., Haas, I.G. and Jäck, H.-M. (1995) *Proc. Natl. Acad. Sci. USA*, in press.
- Bothwell, A.L.M., Paskind, M., Reth, M., Imanishi-Kari, T., Rajewsky, K. and Baltimore, D. (1981) *Cell* **24**, 625-637.
- Buchman, A.R. and Berg, P. (1988) *Mol. Cell. Biol.* **8**, 4395-4405.
- Burrows, P.D., Beck-Engesser, G.B. and Wabl, M.R. (1983) *Nature* **306**, 243-246.
- Burrows, P.D., Beck, G.B. and Wabl, M.R. (1981) *Proc. Natl. Acad. Sci. USA* **78**, 564-568.
- Beyer, A.L. and Osheim, Y.N. (1990) *Genes and Dev.* **2**, 754-765.
- Bingham, P.M. (1993) *J. Cell. Biol.* **121**, 729-743.
- Callis, J., Fromm, M. and Walbot, V. (1987) *Genes and Dev.* **1**, 1183-1200.
- Chasin, L.A., Urlaub, G., Mitchell, P., Ciudad, C., Barth, J., Carothers, A.M., Steigerwalt, R. and Grunberger, D. (1990) *Prog. in Clin. & Biol. Res.* **340A**, 295-304.
- Cheng, J., Fogel-Petrovic, M. and Maquat, L.E. (1990) *Mol. Cell Biol.* **10**, 5215-5225.
- Cheng, J. and Maquat L.E. (1993) *Mol. Cell. Biol.* **13**, 1892-1902.
- Cheng, J., Belgrader, P., Zhou, X., Stephenson, L.S. and Maquat, L.E. (1994) *Mol. Cell. Biol.* **14**, 6317-6325.
- Chodosh, L.A., Fire, A., Sumuels, M., and Sharp, P.A. (1989) *J. Biol. Chem.* **264**, 2250-2257.
- Chomczynski, P. and Sacchi, N. (1987) *Anal. Biochem.* **162**, 156-159.
- Cleveland, D.W. (1988) *Trends. Biochem. Sci.* **13**, 339-343.
- Collis, P., Antoniou, M. and Grosveld, F. (1990) *EMBO J.* **9**, 233-240.
- Connor, A., Wiersma, E. and Shulman, M.J. (1994) *J. Biol. Chem.* **269**, 25178-25184.

- Cox, A. and Emtage, J.S. (1989) *Nucleic Acids Res.* **17**, 10439-10454.
- Daar, I.Q. and Maquat, L.E. (1988) *Mol. Cell. Biol.* **8**, 802-813.
- Dani, C., Blanchard, J.M., Piechaczyk, M., El Sabroury, S., Marty, L. and Jeanteur, P. (1984a) *Proc. Natl. Acad. Sci. USA* **81**, 7046-7050.
- Dani, C., Piechaczyk, M., Audigier, U., El Sabroury, S., Cathala, G., Marty, L., Fort, P., Blanchard, J.M. and Jeanteur, P. (1984b) *Eur. J. Biochem.* **145**, 299-304.
- Decker, C.J. and Parker, R. (1994) *TIBS* **19**, 336-340.
- Deng, T., Li, Y., Jolliff, K., and Johnson, L.F. (1989) *Mol. Cell. Biol.* **9**, 4079-4082.
- Deuschle, U., Pepperkok, R., Wang, F., Giordano, T.J., McAllister, W.T., Ansorge, W. and Bujard, H. (1989) *Proc. Natl. Acad. Sci. USA* **86**, 5400-5404.
- Diatz, H.C., Valle, D., Francomano, C.A., Kendzior, Jr., R.J., Pyeritz, R.E. and Cutting, G.R. (1993) *Science* **259**, 680-683.
- Dubois, M.F., Bellier, S., Seo, S.J. and Bensaude, O. (1994) *J. Cell. Physiol.* **158**, 417-426.
- Dreyfuss, G., Matunis, M.J., Pinol-Roma, S. and Burd, C.G. (1992) *Annu. Rev. Biochem.* **62**, 289-321.
- Eckner, R., Ellmeier, W. and Birnstiel, M.L. (1991) *EMBO J.* **10**, 3513-3522.
- Ehretsmann, C.P., Carpousis, A.J. and Krisch, H.M. (1992) *FASEB J.* **6**, 3186-3192.
- Enssle, J., Kugler, W., Hentze, M.W. and Kulozik, A.E. (1993) *Proc. Natl. Acad. Sci. USA* **90**, 10091-10095.
- Favaloro, J., Treisman, R. and Kamen, R. (1980) *Methods Enzymol.* **65**, 718-749.
- Forbes, D.J. (1992) *Annu. Rev. Cell Biol.* **8**, 495-527.
- Fort, P., Marty, L., Piechaczyk, M., El Sabrouy, S., Dani, C., Jeanteur, P. and Blanchard, J.M. (1985) *Nucleic Acids Res.* **13**, 1431-1442.
- Gallwitz, D. (1975) *Nature* **257**, 247-248.
- Gasser, C.S., Simonsen, C.C., Schilling, J.W. and Schimke, R.T. (1982) *Proc. Natl. Acad. Sci. USA* **79**, 6522-6566.

- Genovese, C. and Milcarek, C. (1990) *Mol. Immunol.* **27**, 733-743.
- Genovese, C., Harrold, S. and Milcarek, C. (1991) *Somatic Cell & Mol. Genet.* **17**, 69-81.
- Gerster, T., Picard D. and Schaffner, W. (1986) *Cell* **45**, 45-52.
- Grandy, D.K., Engel, J.D. and Dodgson, J.B. (1982) *J. Biol. Chem.* **257**, 8577-8580.
- Graves, R.A., Pandey, N.B., Chodchoy, N. and Marzloff, W.F. (1987) *Cell* **48**, 615-626.
- Green, M.R. (1991) *Annu. Rev. Cell Biol.* **7**, 559-599.
- Greenberg, M.E. and Ziff, E.B. (1984) *Nature* **311**, 433-438.
- Grosschedl, R., Weaver, D., Baltimore, D. and Costantini, F. (1984) *Cell* **38**, 647-658.
- Grosschedl, R. and Baltimore, D. (1985a) *Cell* **41**, 885-897.
- Grosschedl, R., Costantini, F. and Baltimore, D. (1985b) Tissue-specific expression of Ig genes in transgenic mice and cultured cells. In: Banbury Report 20 (Cold Spring Harbor, New York: Cold Spring Harbor Laboratory, 187-196.
- Gruss, P., Lai, C. J., Dhar, R. and Houry, G. (1979) *Proc. Natl. Acad. Sci. USA* **76**, 4317-4321.
- Hamer, D.H. and Leder, P. (1979) *Cell* **17**, 737-747.
- Herrick, D., Parker, R. and Jacobson, A. (1990) *Mol. Cell. Biol.* **10**, 2269-2284.
- Herrick, D.J. and Ross, J. (1994) *Mol. Cell. Biol.* **14**, 2119-2128.
- Holtzman, E., Smith, I., and Penman, S. (1966) *J. Mol. Biol.* **17**, 131-135.
- Honjo, T. (1983) *Annu. Rev. Immunol.* **1**, 499-528.
- Huang, M.T. and Gorman, C.M. (1990) *Nucleic Acids Res.* **18**, 937-947.
- Humphries, R.K., Ley, T.J., Anagnou, N.P., Baur, A.W. and Nienhuis, A.W. (1984) *Blood* **64**, 23-32.
- Jäck, H.-M. and Wabl, M. (1987) *Proc. Natl. Acad. Sci. USA* **84**, 4934-4938.

- Jäck, H.-M. (1988) Expression der Gene für die schweren Immunoglobulinketten in verschiedenen B-Zell-Differenzierungsstadien. Ph.D. Dissertation, Eberhard-Karls-Universität Tübingen, Tübingen, Germany.
- Jäck, H.-M. and Wabl, M. (1988) *EMBO J.* **7**, 1041-1046.
- Jäck, H.-M., Berg, J. and Wabl, M. (1989) *Eur. J. Immunol.* **19**, 843-847.
- Jäck, H.-M., Beck-Engeser, G., Sloan, B., Wong, M.L. and Wabl, M. (1992) *Proc. Natl. Acad. Sci. USA* **89**, 11688-11691.
- Jackson, R.J. (1993) *Cell* **74**, 9-14.
- Jarmolowski, A., Boelens, W.C., Izaurralde, E. and Mattaj, I.W. (1992) *J. Cell. Biol.* **124**, 627-635.
- Jonsson, J.J., Foresman, M.D., Wilson, N., and McIvor, R.S. (1992) *Nucleic Acids Res.* **20**, 3191-3198.
- Kearney, J.F., Radbruch, A., Liesegang, B. and Rajewsky, K. (1979) *J. Immunol.* **123**, 1548-1550.
- Kedzierski, W. and Porter, J. (1991) *BioTechniques* **10**, 210-214.
- Kelly, K., Cochran, B.H., Stiles, C.D. and Leder, P. (1983) *Cell* **35**, 603-610.
- Kelly, D.E. and Perry, R.P. (1986) *Nucleic Acids Res.* **14**, 5431-5447.
- Kessler, S.W. (1975) *J. Immunol.* **115**, 1617-1624.
- Khalili, K. and Weinmann, R. (1984) *J. Mol. Biol.* **180**, 1007-1021.
- Krowczynska, A., Yenofsky, R. and Brawerman, G. (1985) *J. Mol. Biol.* **181**, 231-239.
- Kuby, J. (1994) Chapter 8. Organization and expression of immunoglobulin genes, p175-208, *in: Immunology*, 2nd ed. W.H. Freeman and Company, New York, USA.
- Kuehl, W.M. (1977) *Curr. Topics Microbiol. Immunol.* **76**, 1-47.
- Laemmli, U.K. (1970) *Nature* **227**, 680-685.
- Lamond, A.I. (1993) *Curr. Biol.* **3**, 62-65.
- Leeds, P., Peltz, S.W., Jacobson, A. and Culbertson, M.R. (1991) *Genes Dev.* **5**, 2303-

2314.

- Leeds, P., Wood, J.M., Lee, B.-S. and Culbertson, M.R. (1992) *Mol. Cell. Biol.* **12**, 2165-2177.
- Legrain, P. and Rosbash, M. (1989) *Cell* **57**, 573-583.
- Lim, S.K., Sigmung, C.D., Gross, K.W. and Maquat, L.E. (1992) *Mol. Cell. Biol.* **12**, 1149-1161.
- Liu, X. (1994) Effects of intron and exon sequence elements on intron-dependent and intron-independent gene expression. Ph.D. Thesis, University of Wisconsin, Madison, Wisconsin.
- Loh, D.Y., Bothwell, A.L.M., White-Scharf, M.E., Imanishi-Kari, T. and Baltimore, D. (1983) *Cell* **33**, 85-93.
- Losson, R. and Lacroute, F. (1979) *Proc. Natl. Acad. Sci. USA* **76**, 5134-5137.
- Lozano, F., Maertzdorf, B., Pannel, R. and Milstein, C. (1994) *EMBO J.* **13**, 4617-4622.
- Malim, M.H., Hauber, J., Le, S-Y., Maizel, J.V. and Cullen, B.R. (1989) *Nature* **338**, 254-257.
- Mason, J.O., Williams, G.T. and Neuberger, M.S. (1988) *Genes Dev.* **2**, 1003-1011.
- Maquat, L.E., Kinniburgh, A.J., Rachmilewitz, E.A. and Ross, J. (1981) *Cell* **27**, 543-553.
- Maquat, L.E. (1991) *Curr. Opin. Cell Biol.* **3**, 1004-1012.
- Marzluff, W.F. and Pandey, N.B. (1988) *Trends Biochem. Sci.* **13**, 49-52.
- Meo, T., Johnson, J.P., Beechey, C.V., Andrews, S.J., Peters, J. and Searle, A.G. (1980) *Proc. Natl. Acad. Sci. USA* **77**, 550-553.
- Morrison, S.L. and Scharff, M.D. (1981) *Rev. Immunol.* **3**, 1-22.
- Muhlrad, D. and Parker, R. (1994) *Nature* **370**, 578-581.
- Mulligan, R.C. and Berg, P. (1981) *Proc. Natl. Acad. Sci. USA* **78**, 2072-2076.
- Naeger, L.K., Schoborg, R.V., Zhao, Q., Tullis, G.E. and Pintel, D.J. (1992) *Genes*

*Dev.*, **6**, 1107-1119.

Neel, H., Weil, D., Giansante, C. and Dautry, F. (1993) *Genes Dev.* **7**, 2194-2205.

Nesic, D., Cheng, J. and Maquat, L.E. (1993) *Mol. Cell. Biol.* **13**, 3359-3369.

Nesic, D. and Maquat, L.E. (1994) *Genes Dev.* **8**, 363-375.

Nevins, J.R. (1980) *Methods in Enz.* **65**, 768-774.

Neuberger, M.S. and Williams, G.T. (1988) *Nucleic Acids Res.* **16**, 6713-6724.

Oi, V.T., Bryan, V.M., Herzenberg, L.A. and Herzenberg, L.A. (1980) *J. Exp. Med.* **151**, 1260-1274.

Okada, A. and Alt, F.W. (1994) *Seminar in Immunol.* **6**, 185-196.

Old, R.W. and Woodland, H.R. (1984) *Cell* **38**, 624-626.

Pachter, J.S. (1992) *Crit. Rev. Euk. Gene Exp.* **2**, 1-18.

Pandey, N.B., Williams, A.S., Sun, J.-H., Brown, V.D., Bond, U. and Marzluff, W.F. (1994) *Mol. Cell. Biol.* **14**, 1709-1720.

Parker, R. and Jacobson, A. (1990) *Proc. Natl. Acad. Sci. USA* **87**, 2780-2784.

Peltz, S.W., Brown, A.H. and Jacobson A. (1993) *Genes Dev.* **7**, 1737-1754.

Pelletier, J. and Sonenberg, N. (1988) *Nature* **334**, 302-305.

Perry, R.P. and Kelly, D.E. (1970) *J. Cell. Physiol.* **76**, 127-140.

Perry, R.P. and Kelly, D.E. (1979) *Cell* **18**, 1333-1339.

Penman, S. (1966) *J. Mol. Biol.* **17**, 117-130.

Peterson, M.L. (1994) A processing and the expression of immunoglobulin genes, p. 321-342. In: E.C. Snow (ed.), *Handbook of B and T lymphocytes*. Academic Press, San Diego, California.

Pulak, R. and Anderson, P. (1993) *Genes Dev.* **7**, 1885-1897.

Qian L., Theodor, L., Carter, M.S., Vu, M.N., Sasaki, A.W. and Wilkinson, M.F. (1993) *Mol. Cell. Biol.* **13**, 1686-1696.

- Pulak, R. and Anderson, P. (1993) *Genes Dev.* **7**, 1885-1897.
- Reth, M.G. and Alt, F.W. (1984) *Nature* **312**, 418-423.
- Richter, J.D. (1991) *Bioessays* **13**, 179-183.
- Rogers, J., Choi, E., Souza, L., Carter, C., Word, C., Kuehl, M., Eisenberg, D. and Wall, R. (1981) *Cell*, **26**, 19-27.
- Ross, J. (1989) *Sci. Am.* **260**, 48-55.
- Rout, M.P. and Went, S.R. (1994) *Trends Cell Biol.* **4**, 357-365.
- Ryu, W.-S., Gelembiuk, G., Liu, X., and Mertz, J.E. (1994) (manuscript in preparation).
- Ryu, W.S. and Mertz, J.E. (1989) *J. Virol.* **63**, 4386-4394.
- Sachs, A.B. (1993) *Cell* **74**, 413-421.
- Sambrook, J., Fritsch, E.F. and Maniatis, T. (1989) *Molecular Cloning: a laboratory manual*, 2nd ed. Cold Spring Harbor Laboratory Press, Cold Spring Harbor, N.Y.
- Schibler, U., Marcu, K.B. and Perry, R.P. (1978) *Cell* **15**, 1495-1509.
- Shen-Ong, G.L.C., Keath, E.J., Piccoli, S.P. and Cole, M.D. (1982) *Cell* **31**, 443-452.
- Simpson, S.B. and Stoltzfus, C.M. (1994) *Mol. Cell. Biol.* **14**, 1835-1844.
- Sommerville, J. (1986) *Trends Biochem. Sci.* **11**, 438-442.
- Southern, P.J. and Berg, P. (1982) *J. Mol. App. Genetics* **1**, 327-341.
- Sun, J., Pilch, D.R. and Marzluff, W.F. (1992) *Nucleic Acid. Res.* **20**, 6057-6066.
- Takeshita, K., Forget, B.G., Scarpa, A. and Benz, E.J. (1984) *Blood* **64**, 13-22.
- Tokunaga, K., Taniguchi, H., Shimizu, M. and Sakiyama, S. (1986) *Nucleic Acid. Res.* **14**, 2829.
- Tonegawa, S. (1983) *Nature* **302**, 575-581.
- Tonegawa, S. (1985) *Sci. Am* **253**, 122-142.



- Tucker, P.W., Marcu, K.B., Newell, N., Richards, J. and Blattner, F.R. (1979) *Science* **206**, 1303-1306.
- Urlaub, G., Mitchell, P.J., Ciudad, C.J. and Chasin, L.A. (1989) *Mol. Cell. Biol.* **9**, 2868-2880.
- Wabl, M.R., Beck-Engeser, G.B. and Burrows, P.D. (1984) *Proc. Natl. Acad. Sci. USA* **81**, 867-870.
- Wabl, M.R., Burrows, P.D., von Gabain, A. and Steinberg, C. (1985) *Proc. Natl. Acad. Sci. USA* **82**, 479-482.
- Wall, R. and Kuehl, M. (1983) *Ann. Rev. Immunol.* **1**, 394-422.
- Wilhelm, J.E. and Vale, R.D. (1993) *J. Cell Biol.* **123**, 269-274.
- Wilkinson, M.F. (1988) *Nucleic Acid. Res.* **16**, 10934.
- Zandomeni, R., Bunick, D., Ackerman, S., Mittleman, B. and Weissmann, R. (1983) *J. Mol. Biol.* **167**, 561-574.

## VITA

The author, Tianhong Li, was born in Beijing, People's Republic of China on April 28, 1965 to Biqian Ye and Yichang Li.

Her secondary education was completed in July, 1983 at the Middle School Attached to Qinghua University. In September, 1983, Ms. Li entered the School of Medicine, Beijing Medical University, and received an M.D. in July, 1989. Ms. Li began her graduate studies in the Department of Microbiology and Immunology, Loyola University Chicago, in August, 1989. She joined the laboratory of Hans-Martin Jäck, Ph.D., in February, 1991. Ms. Li was the recipient of the Graduate School Assistantship from August, 1989 to July, 1993. In the academic year of 1993-1994, Ms. Li was awarded a University Dissertation Fellowship.

Ms. Li has accepted a position as a postdoctoral fellow in the laboratory of David A. Dichek, M.D., at the Gladstone Institute of Cardiovascular Disease, University of California at San Francisco, San Francisco, California. She will move on to study the direct *in vivo* gene transfer into the blood vessel wall.

## APPROVAL SHEET

The dissertation submitted by Tianhong Li has been read and approved by the following committee:

Dr. Hans-Martin Jäck, Ph.D., Director  
Assistant Professor, Department of Microbiology and Immunology  
Loyola University of Chicago

Dr. Sally A. Amero, Ph.D.  
Assistant Professor, Department of Molecular and Cellular Biochemistry  
Loyola University of Chicago

Dr. Thomas M. Gallagher, Ph.D.  
Assistant Professor, Department of Microbiology and Immunology  
Loyola University of Chicago

Dr. Phong T. Le, Ph.D.  
Assistant Professor, Department of Cell Biology, Neurobiology and Anatomy  
Loyola University of Chicago

Dr. Alan J. Wolfe, Ph.D.  
Assistant Professor, Department of Microbiology and Immunology  
Loyola University of Chicago

The final copies have been examined by the director of the dissertation and the signature which appears below verifies the fact that any necessary changes have been incorporated and that the dissertation is now given the final approval by the Committee with reference to content and form.

This dissertation is, therefore, accepted in partial fulfillment of the requirements for the degree of Doctor of Philosophy.

5/25/95

Date

Hans-Martin Jäck  
Director's Signature